
**TOPICAL REPORT: A TEN
STEP PROTOCOL AND PLAN
FOR CCS SITE
CHARACTERIZATION, BASED
ON AN ANALYSIS OF THE
ROCKY MOUNTAIN REGION,
USA**

Type of Report: Topical Report

Reporting Period Start Date: December 8, 2009

Reporting Period End Date: September 30, 2013

Principal Authors of this report:

Brian McPherson, University of Utah

Vince Matthews, Colorado Geological Survey

Date Report was Issued: December 31, 2013

DOE Award Number DE-FE0001812

Submitting Organization:

University of Utah

Department of Civil and Environmental Engineering

Salt Lake City, Utah 84112 USA

DISCLAIMER

This report was prepared as an account of work sponsored by an agency of the United States Government. Neither the United States Government nor any agency thereof, nor any of their employees, makes any warranty, express or implied, or assumes any legal liability or responsibility for the accuracy, completeness, or usefulness of any information, apparatus, product, or process disclosed, or represents that its use would not infringe privately owned rights. Reference herein to any specific commercial product, process, or service by trade name, trademark, manufacturer, or otherwise does not necessarily constitute or imply its endorsement, recommendation, or favoring by the United States Government or any agency thereof. The views and opinions of authors expressed herein do not necessarily reflect those of the United States Government or any agency thereof.

Abstract

This report expresses a Ten-Step Protocol for CO₂ Storage Site Characterization, the final outcome of an extensive Site Characterization analysis of the Rocky Mountain region, USA. These ten steps include: (1) regional assessment and data gathering; (2) identification and analysis of appropriate local sites for characterization; (3) public engagement; (4) geologic and geophysical analysis of local site(s); (5) stratigraphic well drilling and coring; (6) core analysis and interpretation with other data; (7) database assembly and static model development; (8) storage capacity assessment; (9) simulation and uncertainty assessment; (10) risk assessment. While the results detailed here are primarily germane to the Rocky Mountain region, the intent of this protocol is to be portable or generally applicable for CO₂ storage site characterization.

Table of Contents

Abstract 3

Executive Summary 5

Narrative 7

1. Regional Assessment and Data Gathering 7

2. Identification and analysis of appropriate local sites 8

 NEW MEXICO 19

 ARIZONA 20

3. Public engagement: outreach, planning and permitting 21

4. Geologic and geophysical studies at local characterization site 26

5. Stratigraphic well drilling and coring 42

Pre-Drilling Activity 42

Pre-Drilling Risk Mitigation 44

Discussion and Key Learning’s 45

Conclusion 52

6. Core analysis and interpretation with other geological and geophysical data 53

Core Sampling and Inventory 53

Plug Acquisition 53

Core Slabbing 56

Core Analysis 58

Total Organic Carbon (TOC) 59

X-Ray Diffraction (XRD) 59

Spectral Core Gamma (SCG) 60

Fracture Analysis 60

Porosity and Permeability 60

Noble Gas Tracers 63

Capillary Pressure 63

Relative Permeability 67

7. Database assembly and static model development 73

8. Capacity assessment 81

9. Simulation and uncertainty assessment 91

10. Final risk assessment 99

Conclusions 118

References 119

Executive Summary

This report expresses a Ten-Step Protocol for CO₂ Storage Site Characterization, the final outcome of an extensive Site Characterization analysis of the Rocky Mountain region, USA. These ten steps include:

(1) Regional assessment and data gathering: The four state geological surveys of Arizona, Colorado, New Mexico, and Utah conducted regional geologic assessments of three of the most promising sedimentary units for sequestering CO₂ in the Colorado Plateau physiographic province. The maps and interpretations are important contributions because they were a coordinated effort to use the same techniques and interpretations across state boundaries, which is rarely done;

(2) Identification and analysis of appropriate local sites for characterization: a local candidate CCS site was identified in each of the states of Arizona, Colorado, New Mexico and Utah. Such site-specific characterization analyses were performed as part of the “Characterization of Most Promising Sequestration Formations in the Rocky Mountain Region” (RMCCS) project. The primary objective of these local-scale analyses was to provide a basis for regional-scale characterization efforts within each state of the RMCCS region;

(3) Public engagement: a concerted outreach effort is necessary for any CCS project, inasmuch as public acceptance is necessary before a project can proceed. For the RMCCS project in particular, public outreach took a variety of forms from informal meetings with stakeholders, to public meetings with print and radio media in attendance. A website provided up-to-date information to the public. Public informational meetings were held both before and after drilling of the project’s characterization well;

(4) Geologic and geophysical analysis of local site(s): local-scale studies included structural contour maps, net sand and porosity maps, geothermal data, and salinity data, and eventually simulation models for assessing storage capacity potential and other key aspects required for a CCS project to proceed;

(5) Stratigraphic well drilling and coring: a characterization well is an essential aspect following site selection, and such a well could be utilized for injection or monitoring during later stages of a CCS project. For the RMCCS project in particular, a stratigraphic characterization well was drilled to 9750’ depth in the Sand Wash Basin, Colorado near the town of Craig;

(6) Core analysis and interpretation with other data: an effective characterization well plan would involve core acquisition and analysis. For the RMCCS project in particular, cores were taken from the Dakota, and Entrada formations. Because drilling exceeded budgeted costs, the Weber Formation was never reached. A number of key lessons were learned about drilling a well of this nature;

(7) Database assembly and static model development: effective characterization requires effective cataloguing of data and excellent data access, which can be achieved through state-of-the-art database and simulation methods. For the RMCCS project in particular, a geocellular model of the area surrounding the drilled well was developed to simulate potential injection and storage of CO₂ in the Craig, Colorado area. The data used in constructing the model included information from the stratigraphic characterization well, more than 1,000 surface measurements, 2700 geophysical well logs, 15,000 formation tops, all available core data, 78 miles of 2-D seismic lines, and published geologic studies. The seismic lines were all processed to the same standard;

(8) Storage capacity assessment: state-of-the-art methods for capacity resource potential are necessary for evaluating and comparing potential CCS sites to other candidates; for the RMCCS project in particular, sequestration capacities were modeled based on local and regional studies, resulting in forecasted capacity for the three most promising candidate storage formations; these formations in aggregate could provide between 12.9 and 136.8 billion metric tons of CO₂ storage, providing likely more than 150 years of sequestration potential at current rates of emission;

(9) Simulation and uncertainty assessment: effective reservoir simulation is necessary for evaluating storage capacity, likely migration pathways, monitoring design, and other factors. Of particular importance is the application of simulation and associated uncertainty quantification for risk assessment. For the RMCCS project in particular, a new workflow was developed for uncertainty assessment; the approach is based on random “pseudo wells” placed in a geocellular model that allowed the derivation of the minimum number of characterization wells necessary to quantify the capacity of an area like the Sand Wash Basin. This analysis clearly showed that the appropriate density of characterization data/well is dependent on the character of the geologic formations, even within the same basin;

(10) Risk assessment: perhaps the most critical aspect of a CCS project is risk assessment, inasmuch as a project cannot proceed unless risks are insignificant; this report details an effective risk assessment approach for candidate CCS sites.

While this ten-point characterization plan is based on analysis of the Rocky Mountain region, the intent of this protocol is to be portable or generally applicable for CO₂ storage site characterization associated with any region.

Narrative

1. Regional Assessment and Data Gathering

The first step in any geologic sequestration project involves regional assessment and data gathering. For this project, the State Geologists from Arizona, New Mexico, Utah, and Colorado met and conducted a preliminary regional assessment. They agreed that the Colorado Plateau presented an excellent opportunity to conduct a broad scale, regional study of the potential for carbon capture and sequestration. The Dakota, Entrada, and Weber were formations (and their equivalents) that were widespread throughout the Plateau and generally had good permeability and porosity.

Prior to the initial meeting, each geological survey was asked to select one or more areas that might be suitable for a pilot project to characterize the three formations. Several criteria were necessary for a successful site to propose. First, a site must be found where the landowner is willing to allow for a characterization well to be drilled. Second, the site must have structural and stratigraphic characteristics that would make it suitable for long-term sequestration of CO₂. It would be preferable if the site had a preliminary estimate of CCS capacity. And third, the site should have potential for attracting industry partnership and investment.

Colorado brought a site located near Craig, Colorado to the initial meeting. The site had all three formations present and the appearance of large structural closure near the margin of the Plateau. The site was located on Colorado state lands. The Colorado State Land Board (a sibling agency of the Colorado Geological Survey) is in the Colorado Department of Natural Resources providing the opportunity for a close working relationship. The Craig Power station, a coal-fired electric generating station was located on the structure. Shell and Tri-state Generation and Transmission indicated a possible interest in joining the project. The location was situated near a coal plant with significant emissions, near several gas processing plants with emissions, and near a potential oil-shale operation that would generate new emissions. It was also considered to be an attractive site for new cement plant operations or any other industry that might need to control emissions. The site had also had a preliminary estimate of storage capacity under Phase II of the Southwest Partnership for Carbon Sequestration.

Each of the other states also brought potential sites within their boundaries. However, none of these sites ultimately were able to meet all of the necessary criteria. And, all agreed that the Colorado site was the only one that would have any chance of moving forward.

Because of the long, and excellent, relationship that the Colorado Geological Survey had experienced with Dr. Brian McPherson and the Southwest Partnership for Carbon Sequestration, Dr. McPherson and his team at the University of Utah was invited to join in the proposal to DOE. Additionally, he brought Schlumberger Carbon Services into the partnership.

Each state geological survey was to investigate those basins on the Plateau where the three formations (or their equivalents) were present at depths sufficient for injection and storage of CO₂. For Colorado that included the Sand Wash, Piceance, San Juan, and Paradox Basins; for Utah the basin selected was the Uinta; for New Mexico, the San Juan Basin; and for Arizona, the Black Mesa Basin. Formations analyzed were Dakota, Entrada, Weber, Hermosa, Cedar Mesa, De Chelly, and Leadville.

Data that were gathered for the analyses were derived from subsurface well logs (digital where available), regional literature, and existing core descriptions. Data used in the analyses included salinity, porosity, depth, thickness, and temperature.

Well log data were analyzed, interpreted, correlated, and incorporated into various interpretive software programs available to each survey (Petra and ArcGIS). Structural contour

maps on the tops of the potential formations were prepared by each survey. Isopach maps of the potential formations in the Colorado Plateau were also prepared by each survey. The data were exported in ARC for inclusion in NATCARB V. Ultimately the data were incorporated into Petrel for modeling capacity.

2. Identification and analysis of appropriate local sites

The geology of the Colorado Plateau, located in the Southwestern United States, contains several deep saline formations that are suitable for geological carbon sequestration. These formations occur below 3000' depth, are capped by seals and their salinity is generally higher than 10,000 mg/l. Three ubiquitous reservoirs within the four-state region of AZ, CO, NM and UT are the Cretaceous Dakota Formation, the Jurassic Entrada Formation and the Permian Weber Formation, mainly occurring in the northern sedimentary basins of the Colorado Plateau Region the main emphasis of this study. Additional formations studied at the regional scale in the Four Corners area on the southern end of the Colorado Basin, were the Hermosa Group, the stratigraphic equivalent of the Weber in the NM San Juan Basin, the DeChelly Formation in AZ, CO and UT, the Cedar Mesa Formation in AZ, and the Leadville Formation in NM.

The Geological Surveys of the four states in which the Colorado Plateau Region is located, AZ, CO, NM and UT, were tasked to improve the regional geologic assessment of the listed formations. That was accomplished by generating structure and thickness contour maps for each of the formations for which they were responsible. These maps were not just based on interpolating well-derived data, but also incorporated additional available information and studies. Each of the partnering geologists contributed in-depth, sedimentary-basin expertise during the compilation of the regional geology. In addition to digital contour maps, the surveys also provided regional porosity data and geothermal gradient values.

Besides the regional assessment carried out on the deep saline formations occurring across the state boundaries, each of the four states were asked to prepare a site-specific study. For Colorado this site was the Sand Wash Basin (Figure 2.1), the main location of the detailed site characterization efforts. Utah looked at several sites and found two with potential, willing outside-cooperating partners: Woodside Dome site near Green River Utah and the Bonanza site,— both in the Uinta Basin (Figure 2.1). Several potential storage sites were identified in the San Juan Basin (Figure 2.1) also, but no outside cooperating partners were available. The regional assessment for Arizona indicated the best storage site occurs near the Navajo Generating Station (Figure 2.1) but because of lack of detailed well data at that site, this site requires more in-depth study, comparable to the Craig-site, before a final determination about the suitability of the site can be made. The site specific storage capacity estimates are included in this report as well.

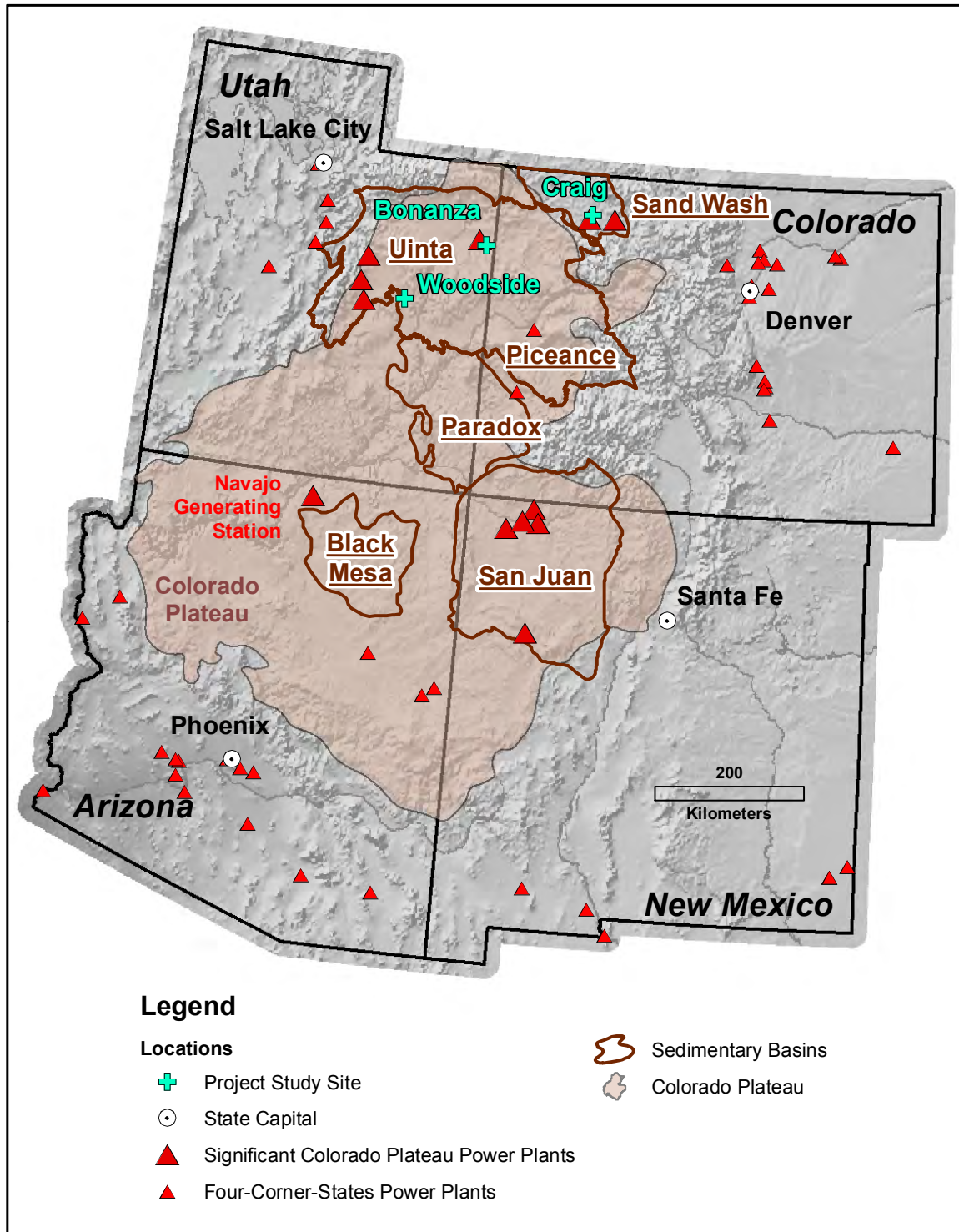


Figure 2.1: Colorado Plateau carbon emission sources in relation and potential site-specific geological sequestration reservoir candidates.

UTAH

Geologic, oil and gas field, and structure contour maps of the Uinta Basin were used to identify nonproducing structures, abandoned oil and gas fields, and areas with potential

stratigraphic traps for the Weber, Entrada, and Dakota Sandstones. A table of potential CO₂ storage sites was compiled. Data added to the table included the area of each site which was defined using geologic maps; the depth, thickness, and porosity were defined from published reports or from a representative well log. Reservoir pressure and temperature were calculated from standard pressure and geothermal gradients for the area. Storage capacity was determined two ways: (1) using CO₂ density from a chart published by Hardage and Sava (May 2009), and (2) calculating CO₂ density from an ideal gas law equation. The storage capacity equation used was: area (ft²) * thickness (ft) * porosity * CO₂ density (lbs/ft³) * 0.04 (efficiency) = lbs (lbs/2204 = lbs/metric ton).

Minimum site qualifications were:

- (1) must have at least one of the three primary targets (Weber, Entrada, or Dakota),
- (2) potential reservoirs must be at least 2500-ft (760-m) drill depth [this was later changed to minimum 3000-ft (1000-m) drill depth],
- (3) must have minimum storage capacity of 30 million metric tonnes (MMT)
- (4) must contain saline water with 10,000 total dissolved solids (TDS) or more, and
- (5) must be within the Colorado Plateau.

Table 2.1 shows the sites, the basic reservoir parameters, and the storage calculations. We also included land ownership, current status of land usage, and relevant infrastructure. Some of the sites did not meet the minimum qualifications and are designed with an X in the ranking column. Copies of Table 2.1 (without rankings) were given to four UGS geologists who were asked to rank the sites following instructions below Table 2.1. The rankings in column 1 of the table are based on the input from the geologists.

Topical Report: DOE-FE0001812

December, 2013

Table 2.1. Preliminary site evaluation for CO₂ storage capacity in the Uinta Basin. Each site must have at least one of the three primary reservoirs—Weber, Entrada, and Dakota.

| Rank | Location | Area | Depth (ft): Kd Je Pw other | Thickness (ft): Kd Je Pw other | Porosity (%) | Status | Land | Resource: Power plant Coal Rail | Pressure (psi) Calc. @ 0.45psi/ft | Temp (°F) Calc. @ 60+1°F/ 100 ft | Storage Estimate MMT- Chart | Storage Estimate MMT- Equation |
|------|--|---|--|--|---|---|----------------------------|--|---|--|--|--|
| 1 | Bonanza 9S-10S 24E-25E | 100 sq mi 528,000 acres. Potentially much larger 2,790,000,000 ft ² | Kd 11,000 Je 12,000 Jn 12,250 Pw 13,800 | Kd 80 Je 150 Jn 600 IPw 200 | Kd 15 Je 12 Jn 10 Pw 10 | Gas wells Tw – Kd. Natural Buttes area. Very active gas drilling | BLM, SITLA | Within 6 mi. of Bonanza Power Plant. Remote location. | Kd 5000 Je 5400 Jn 5500 Pw 6200 | Kd 170 Je 180 Jn 180 Pw 200 | Kd 25.5 Je 41.0 Jn 136.7 Pw 40.5 TOTAL 243.6 MMT | Kd 30.2 Je 45.3 Jn 151.9 Pw 50.3 TOTAL 277.7 MMT |
| X | Cisco Dome 19S-20S 21E-22E | 24 sq mi 13,440 acres 669,000,000 ft ² | Kd TS Je 2822 Jn 3500 Pw NA | Je 400 Jn 300 | Je 18 Jn 12 | Prod Kd - Jm Je abd Jn non- productive | BLM | 75 mi. from Castle Dale. Next to undeveloped coal, rail and freeway access. | Je 1300 Jn 1600 | Je 90 Jn 95 | Je 37.6 Jn 18.8 TOTAL 56.4 MMT | Je 6.4 Jn 13.7 TOTAL 20.1 |
| X | Gordon Creek 14S 7E- 8E | 13 sq mi. 68,640 acres 362,000,000 ft ² | Kd 4025 Je 6400 Jn 8400 Pwr 11,150 | Kd 50 Je 270 Jn 350 Pwr 500 | Kd 6 Je silt & sh 2-4 Jn 16 Pwr 0-4 | Kf prod. SWP site | mix | High Plateau 20 mi from Castle Dale. SWP demo site. | Kd 1800 Je 2900 Jn 3800 Pwr 5000 | Kd 100 Je 125 Jn 140 Pwr 170 | Kd 0.9 Je 1.7 Jn 18.4 Pwr 2.8 TOTAL 23.7 MMT | Kd 0.8 Je 1.7 Jn 18.3 Pwr 3.3 TOTAL 24.1 |
| X | Green River south Little Grand Fault 21S 17E | 12 sq mi 63,360 acres 335,000,000 ft ² | Kd-Jn TS Pwr 3000 Mm 10,000 | Pwr 260 Mm 400+ | Pwr 6-16 Mm 2-6 | Non- productive | BLM, military, SITLA | Next to I-70 and rail line 36 mi from Castle Dale; 20 mi from undeveloped coal. | Pwr 1400 Mm 4500 | Pwr 90 Mm 160 | Pwr 5.4 Mm 4.4 TOTAL 9.8 MMT | Pwr 3.2 Mm 4.8 TOTAL 8.0 MMT |
| 3 | Last Chance Anticline 26S 7E | 24 sq mi 126,720 acres 669,000,000 ft ² | Kd-Jn TS Pwr 3050 Mm 4600 | Pwr 150 Mm 900 | Pwr 14 (30 ft) Mm 16 | SI gas wells; Moenkopi | BLM, SITLA, part WSA | 90 mi south of Castle Dale. Remote location. | Pwr 1400 Mm 2000 | Pwr 90 Mm 105 | Pwr 2.2 Mm 80.4 TOTAL 82.6 MMT | Pwr 1.3 Mm 80.4 TOTAL 81.7 MMT |
| 4 | Peters Point 12S-3S 15E-17E | 30 sq mi. 158,400 acres 836,000,000 ft ² | Kd 13,000 Je 13,970 Jn 14,578 Pw 16,088 | Kd 30 Je 80 Jn 50 IPw 320 Mm 600 | Kd 10 Je 6 Jn 8 Pw 6 Mm 6 | Tertiary- Jn. Very active field | BLM - BBC lease. | Remote location 40 mi from Castle Dale. | Kd 5900 Je 6300 Jn 6500 Pw 7200 Mm 7500 | Kd 190 Je 200 Jn 200 Pw 220 Mm 230 | Kd 2.0 Je 2.9 Jn 2.9 Pw 14.6 Mm 27.3 TOTAL 49.6 MMT | Kd 2.3 Je 3.6 Jn 3.1 Pw 14.6 Mm 27.3 TOTAL 50.9 |

| | | | | | | | | | | | | |
|---|---|--|---|-------------------|--------------------|--------------------|--|---|---------------------|---------------------|---|--|
| | | | Mm 16,615 | | | | | | | | | |
| X | Summit SRS 19S 11E- 12E & all SRS | 1300 sq mi. 6,864,000 acres 36,250,000,000 ft ² | Pwr outcrops Mm 4100 | Mm 700 | Mm 2-10 | Non- productive | Location is SITLA. Potential is BLM with lots of WSA | 20 mi from Castle Dale. Good access. | Mm 1800 | Mm 100 | Mm 847.0 TOTAL 847.0 MMT | Mm 716.2 TOTAL 716.2 MMT |
| 2 | Woodside Dome 19S 13E- 14E | 40 sq mi. 126,720 acres 1,115,000,000 ft ² | Kd NA Je - Jn TS Pwr 3000 Mm 6400 | Pwr 450 Mm 700 | Pwr 6-8 Mm 2-10 | SI well BBC | BLM | 30 mi from Castle Dale. Good access. | Pwr 1300 Mm 2900 | Pwr 95 Mm 120 | Pwr 26.1 Mm 27.2 TOTAL 53.3 MMT | Pwr 9.9 Mm 28.0 TOTAL 37.9 MMT |

Kd = Dakota Sandstone, Je = Entrada Sandstone, Jn = Navajo Sandstone, IPw = Weber Sandstone, Pwr = White Rim Sandstone, Mm = Madison (Redwall, Leadville, Deseret), Kf = Ferron Sandstone of the Mancos Shale, Jm = Morrison Formation, Tw = Wasatch Formation, WSA = Wilderness Study Area, BLM = Bureau of Land Management, SITLA = School and Institutional Trust Lands Administration, mi = miles, Sq mi = square miles, ft² = square feet (calculated from sq miles), psi = pounds per square inch, F = Fahrenheit, NA = not applicable (usually absent), prod = producing, SI = shut in well, BBC = Bill Barrett Corporation, SRS = San Rafael Swell, MMT = million metric tonnes.

Storage estimate chart versus equation. Storage is calculated area * height (thickness)* porosity * density of CO₂ * efficiency (using 0.04). Density of CO₂ can be very difficult to determine. The chart was published in the AAPG Explorer but without a reference. The equation is based on ideal gas law. The big difference comes at lower pressure when near the triple point of gas, liquid, and super critical. The only significant difference in storage capacity using the two methods is at Cisco Dome.

The top two sites were the Bonanza and Woodside locations (Figures 2.1 & 2.2). Bonanza was ranked number 1 because the area is similar to the RMCCS Craig, Colorado test site. Bonanza has all three primary targets, is closest to the Craig test site, and has very similar stratigraphy. The location is next to the Bonanza coal-fired power plant. The Dakota reservoir is gas productive and may have to be eliminated from near-term consideration. There is not a well-defined trap in the Bonanza site but structural and fault traps are present updip (southeast) of the site on the Douglas Creek Arch in Colorado. A stratigraphic trap may exist for both the Dakota and Weber reservoirs within the Bonanza area, but more data is needed. The storage area is potentially much larger than what was evaluated in Table 2.1.

Woodside Dome was ranked number 2. The Dakota Sandstone crops out along the flanks of Woodside Dome and the Entrada Sandstone is too shallow for consideration. But the White Rim Sandstone (Weber equivalent) along with the deeper Redwall Limestone combined, may have sufficient storage capacity. Woodside Dome has easy access, is a well-defined anticline on the surface, and is near newly developed coal. It is close enough that a CO₂ pipeline could be constructed from the power plants in the Castle Valley area to the west.

Last Chance Anticline was ranked number 3. The potential reservoirs are the White Rim Sandstone and the Mississippian Redwall Limestone. Most of the potential storage capacity is in the Redwall which is not one of the primary target reservoirs. The location is very remote but has a well-defined structure.

Peters Point was ranked number 4. Peters Point has numerous potential reservoirs but most of the storage capacity is in the Redwall Limestone. Peters Point is a very active gas field with production from the Navajo, Dakota Sandstone, Mesaverde Group, and Wasatch Formation. The natural gas drilling and production would be a significant impediment to any near-term CO₂ storage.

Cisco Dome was eliminated from consideration due to the water quality (6800 TDS in the Entrada Sandstone determined after the initial rankings). Cisco Dome was initially ranked 1 or 2 by most of the geologists due to excellent reservoir quality, well-defined structure and easy access near undeveloped coal. The temperature and pressure data are near the phase shift from gas to super critical. As a result, Cisco Dome has more than 30 MMT or less than 30 MMT of storage capacity depending on how the CO₂ density is derived.

Gordon Creek was eliminated because (1) the storage capacity was less than 30 MMT and (2) this field had been scheduled to be extensively studied by another project. Green River South was eliminated because the storage capacity was less than 30 MMT. Summit SRS (San Rafael Swell) was eliminated because it lacked any potential in the three target reservoirs. The area has potential in the Redwall but the White Rim Sandstone was dropped from consideration because the formation crops out near the crest of the SRS.

Evaluation of the Bonanza Site

The Bonanza site in eastern Uinta Basin is in T. 8 S. to 10 S., and Range 23 E. to 25 E., Uintah County, Utah (figure 2.2). The Bonanza coal-fired power plant lies within the down dip portion of the site. Several wells have penetrated the Dakota Sandstone in the northwest portion of the site but only one well has penetrated the deeper Entrada and Weber Sandstones. The Bonanza site is a down dip extension of the Hells Hole field (Moretti Jr., and others, 1992). The parameters used to calculate the CO₂ storage capacity are shown in Table 2.2, the calculated storage volumes are shown in Table 2.3.

The preliminary calculation (Table 2.1) used 4% efficiency and resulted in 243.6 to 277.7 MMT total storage capacity. The preliminary calculation included the storage capacity of the Navajo Sandstone which was not evaluated in the final analysis. Subtracting out the storage capacity of the Navajo the preliminary total capacity for the Bonanza site was 106.9 to 125.8 MMT. The final CO₂ storage capacity for the Dakota, Entrada, and Weber reservoirs at the Bonanza Site at 4% efficiency is 232 MMT, significantly more than the preliminary calculation. Additional storage capacity exists in the Castlegate Sandstone of the Cretaceous Mesaverde Group and Jurassic-Triassic Navajo (Nugget) Sandstone. The Dakota Sandstone has the least storage capacity of the reservoirs evaluated. The thin lenticular sandstone beds in the Dakota provide good stratigraphic traps but very little storage capacity. The Entrada Sandstone has the most storage capacity. The Entrada is laterally continuous thick eolian sandstone with good porosity. The lateral continuity of the Entrada means it is less likely to have local stratigraphic traps and needs fault closure or structural closure for a trap. The Weber Sandstone has large storage capacity but with limited well data we used the gross formation thickness as the reservoir thickness. The Weber interfingers with the arkosic red beds of the Maroon Formation in the Bonanza site. As a result, the actual reservoir thickness and therefore storage capacity of the Weber may be much less than what we calculated.

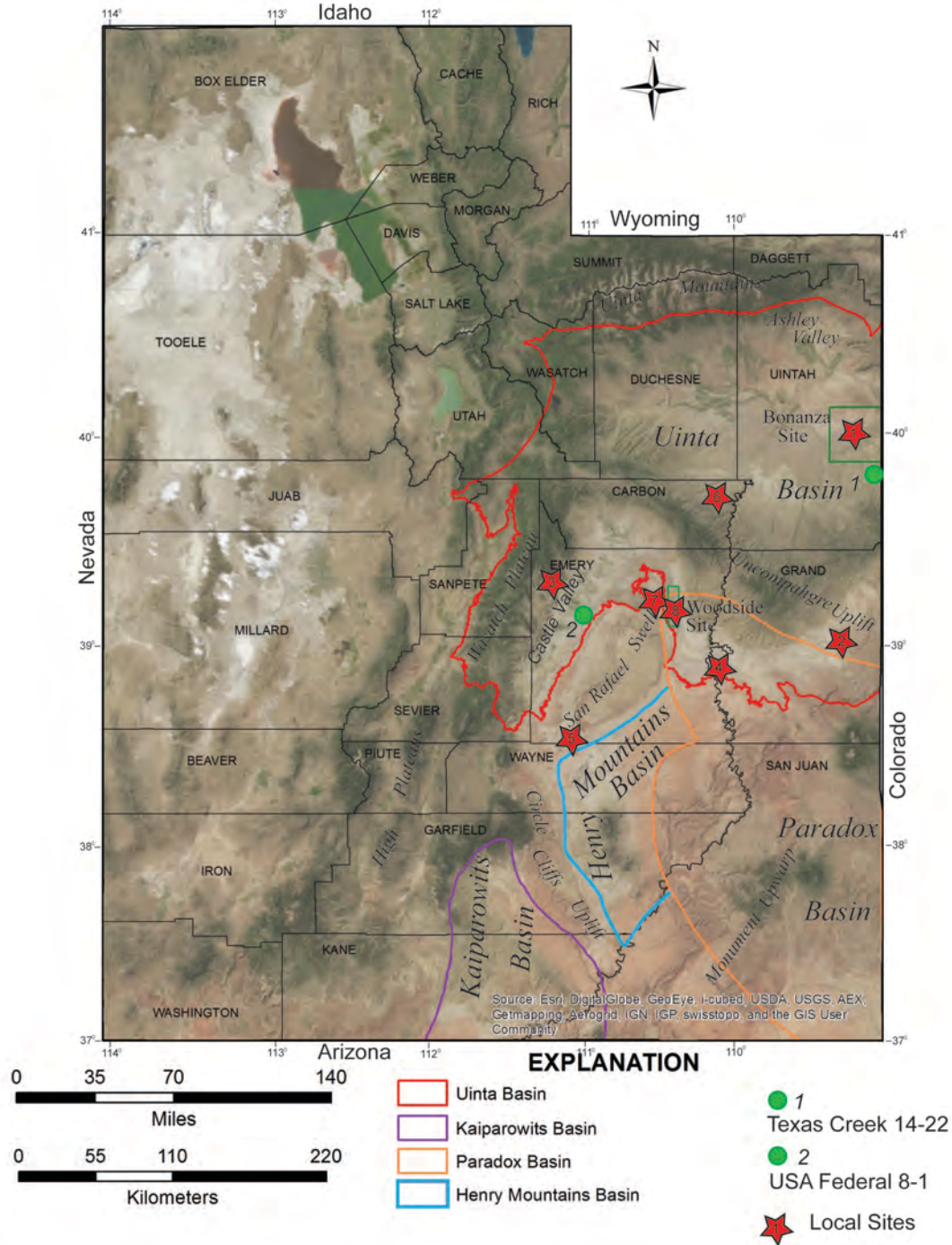
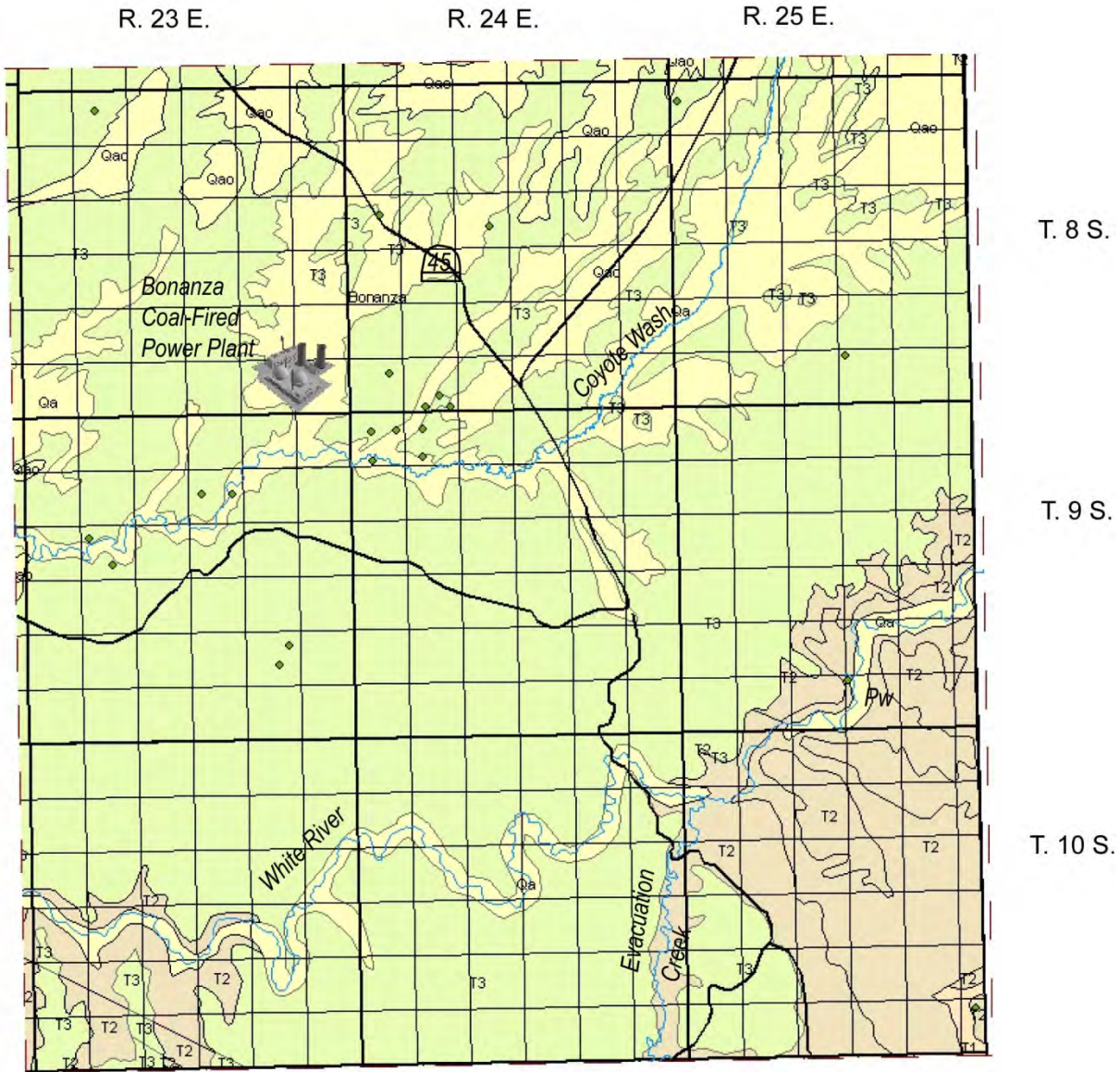
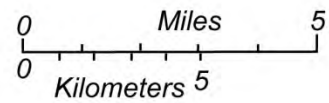


Figure 2.2. Map of Utah showing basins and uplifts of the Colorado Plateau. Local sites evaluated as potential storage sites (see table 1), 1 = Bonanza, 2 = Cisco Dome, 3 = Gordon Creek, 4 = Green River South, 5 = Last Chance, 6 = Peters Point, 7 = Summit, and 8 = Woodside. The Bonanza and Woodside sites (rectangular outlines) were selected for detail characterization. Wells (green circles) 1 has a Weber Sandstone (?) core and 2 has a White Rim core.



Bonanza site, Uintah County, Utah



EXPLANATION

- Qa and Qao Quaternary
- T3 Uinta Formation
- T2 Green River Formation
- Wells that penetrated the Dakota Sandstone



Figure 2.3. Geologic map of the Bonanza site from Hintze and others (2000). Structure contours are on the top of Dakota Sandstone from Roberts (2003); contour interval is 500 feet (150 m), mean sea level datum. Pw shows the location of the one well in the Bonanza site that penetrated the Entrada and Weber Sandstones.

Table 2.2. Parameters used to calculate the CO₂ storage capacity of the Dakota, Entrada, and Weber reservoirs at the Bonanza site. ft = feet, m = meters, km² = kilometers squared, F = degrees Fahrenheit, C = degrees Celsius, D = depth, psi = pounds per square inch, and kPal = kiloPascals.

| | Area | Average Depth | Average Reservoir Thickness | Average Porosity | Temperature Gradient | Pressure Gradient |
|----------------|---|---------------------|-----------------------------|------------------|-----------------------------------|----------------------------|
| Dakota | 328 miles ² 850 km ² | 12,122 ft 3695 m | 20 ft 6 m | 12% | 55 °F + (0.015*D) 0.03 °C/m | 0.45 psi/ft 10.2 kPal/m |
| Entrada | 326 miles ² 845 km ² | 13,016 ft 3967 m | 94 ft 29 m | 16% | 55 °F + (0.015*D) 0.03 °C/m | 0.45 psi/ft 10.2 kPal/m |
| Weber | 328 miles ² 850 km ² | 14,604 ft 4451 m | 186 ft 57 m | 7% | 55 °F + (0.015*D) 0.03 °C/m | 0.45 psi/ft 10.2 kPal/m |

Table 2.3. CO₂ storage capacity of the Dakota, Entrada, and Weber reservoirs at the Bonanza site using three different efficiency factors.

| CO ₂ Storage Capacity in Million Metric Tonnes | | | |
|---|--------------------|--------------|---------------|
| | Efficiency Factors | | |
| | 0.5% | 2.0% | 5.4% |
| Dakota | 2.29 | 8.97 | 24.21 |
| Entrada | 14.22 | 55.78 | 150.59 |
| Weber | 13.07 | 51.25 | 138.38 |
| TOTAL | 29.58 | 116.0 | 313.18 |

Evaluation of the Woodside Dome Site

Woodside Dome is a doubly-plunging anticline on the east flank of the San Rafael Swell (Figure 2.4). The Jurassic Curtis Formation is exposed on the crest of the structure. The Dakota Sandstone has been eroded off of the crest of the anticline and the Entrada Sandstone is too shallow (less than 3000 feet [1000 m]) to be considered for CO₂ storage. The Permian Black Box Dolomite, White Rim Sandstone, and Redwall Limestone contain 12.6 MMT (at 2% E) of CO₂ storage capacity in 13.5 square miles (35 km²). Structural closure is controlled by a blind reverse fault which oil operators have indicated is visible on seismic, but the amount of displacement and extent of the fault is unknown to us. We evaluated the capacity with a very conservative fault that has minor displacement and minor length. A more extensive fault could greatly increase closure and, as a result, increase the storage capacity at Woodside.

Table 2.4 shows the parameters used to calculate the CO₂ storage capacity at Woodside. Table 2.5 gives the storage capacity for the Redwall Limestone, White Rim Sandstone, and Black Box Dolomite at Woodside using three different efficiency factors. Table 2.6 compares the preliminary parameters and storage capacity, and the final parameters and storage capacity at 4% efficiency, for the Redwall and White Rim. The area is the parameter that has the greatest effect on the difference between the preliminary and final storage calculation for the White Rim reservoir. The area and thickness were both significantly reduced in the final evaluation of the Redwall reservoir.

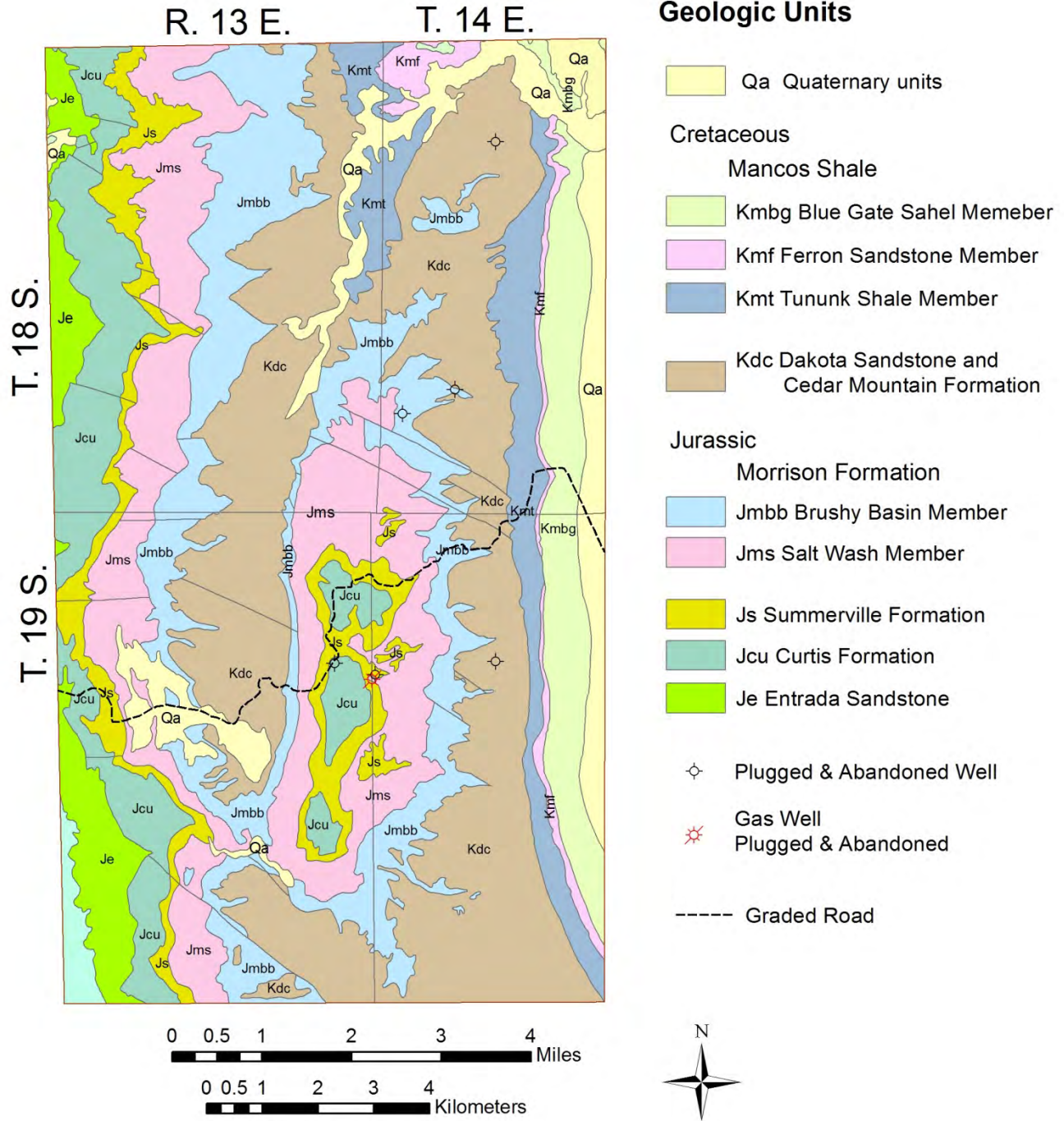


Figure 2.4. Geologic map of the Woodside Dome site from Witkind (2004). The crest of the anticline is the Jurassic Curtis Formation (Jcu), the flank is the Dakota and Cedar Mountain Formations undifferentiated (Kdc). Modified from Witkind (2004).

The preliminary area was based on the full extent of the anticline mapped on the surface. The final area is based on subsurface cross sections and structure contour mapping of the White Rim Sandstone and Redwall Limestone. Closure at the level of the two reservoirs is controlled by a blind reverse fault. We do not have seismic data over Woodside to accurately determine the displacement and extent of the fault so we took a very conservative approach to mapping the closure. Acquisition of seismic data to map the displacement and extent of the fault could result in greater area of closure and therefore larger storage capacity.

Table 2.4. Parameters used to calculate the CO₂ storage capacity of the Redwall Limestone, White Rim Sandstone, and Black Box Dolomite at Woodside. ft = feet, m = meters, D = depth, km² = kilometers squared, F = degrees Fahrenheit, C = degrees Celsius, psi = pounds per square inch, and kPal = kiloPascals.

| | Area | Average Depth | Reservoir Thickness | Average Porosity | Temperature | Pressure |
|------------------|---|-------------------|---------------------|------------------|-----------------------------------|---------------------------|
| Redwall | 16.6 miles ² 43 km ² | 6749 ft 2058 m | 345 ft 105 m | 5% | 55° F + (0.013*D) 0.03° C/m | 0.42 psi/ft 9.5 kPal/m |
| White Rim | 11.9 miles ² 31 km ² | 3445 ft 1050 m | 420 ft 128 m | 15% | 55° F + (0.012*D) 0.04° C/m | 0.42 psi/ft 9.5 kPal/m |
| Black Box | 13.5 miles ² 35 km ² | 3422 ft 1043 m | 75 ft 23 m | 16% | 55° F + (0.012*D) 0.04° C/m | 0.42 psi/ft 9.5 kPal/m |

Table 2.5. CO₂ storage capacity of the Redwall, White Rim, and Black Box reservoirs at the Woodside Site using three different efficiency factors.

| CO₂ Storage Capacity | | | |
|--|--------------------|-------------|-------------|
| | Efficiency Factors | | |
| | 0.5% | 2.0% | 5.4% |
| Redwall | 0.8 | 3.2 | 8.8 |
| White Rim | 2.0 | 7.9 | 21.4 |
| Black Box | 0.4 | 1.5 | 4.1 |
| Total | 3.2 | 12.6 | 34.3 |

Table 2.6. Comparison of the preliminary parameters (from table 1) and final (in parenthesis) parameters and resulting storage capacity calculations at an efficiency factor of 5.4%. Black Box Dolomite was not evaluated in the preliminary calculations.

| | Area (miles ²) | Thickness (feet) | Porosity (%) | Temperature (°F) | Pressure (psi) | Capacity (MMT) 4% |
|------------------|----------------------------|------------------|----------------|------------------|----------------|---------------------|
| Redwall | 40 (16.6) | 700 (345) | 0.04 (0.05) | 120 (141) | 2900 (2835) | 27.2-28 (6.5) |
| White Rim | 40 (11.9) | 450 (420) | 0.07 (0.15) | 95 (98) | 1300 (1447) | 9.9-26.1 (15.9) |
| Total | | | | | | 37.1-54.1 (22.4) |

NEW MEXICO

The search for reservoirs with appropriate properties for sequestration, including

- accompanying tight seals that occur between 3,000 and 13,000 feet
- total dissolved solids of greater than 10,000 µg/l and
- apparent capacity in excess of 500K barrels of oil equivalent (BOEs)

is straightforward in New Mexico because of its long history of oil and gas production in the San Juan Basin (Figure 2.5). The tremendous size of many of the fields in this basin is sufficient to render them prospective sequestration targets. In addition, many deep saline aquifers also provide additional sequestration opportunities. Several large power plants in the area could take advantage of the many identified sequestration reservoirs.

Within the San Juan Basin, several horizons were selected as possible sequestration targets: the Dakota Group, Entrada Formation, Hermosa Group (equivalent to the Weber) and the Leadville Limestone. They are locally thick, porous and deep enough to be possible CO₂ sequestration targets. Associated seals for each of the units are in place in all areas, but ultimately, the thick sequence of shales and siltstones of the Mancos Shale is an excellent upper seal for all the units in the basin.

Within the San Juan Basin area, primary CO₂ point emissions were identified. These include the San Juan Generating Plant, Four Corners Generating Plant, Escalante Generating Plant, San Juan Gas Plant, Lybrook Gas Plant and the Giant Refinery. Of these sites, the San Juan and Four Corners Generating Plants were considered the most likely candidates for a CO₂ sequestration project because the units of interest were deep enough and thick enough to meet all of the criteria for injection.

For the primary RMCCS local site analysis, the main issues that ruled out a New Mexico site early in the selection process included:

- The lack of a partner (a source of CO₂) willing to work with the group. Both Tri-State Energy in New Mexico and PNM Resources, the operators of the two selected power plants, were contacted and declined involvement.
- The San Juan Basin is an area with complex land ownership issues. The area is a patchwork of private, state and federal lands that included both public and Indian lands. The nature of the permits and ownership issues would have made a site selection a long and uncertain affair.

These issues are not insurmountable for possible future projects, but far more upfront time will be required for site selection and permitting in the San Juan Basin than the selected Craig Well site. In most areas of the San Juan basin, agreements would probably require Federal, Tribal, State and private landholders involvement in the site selection process.

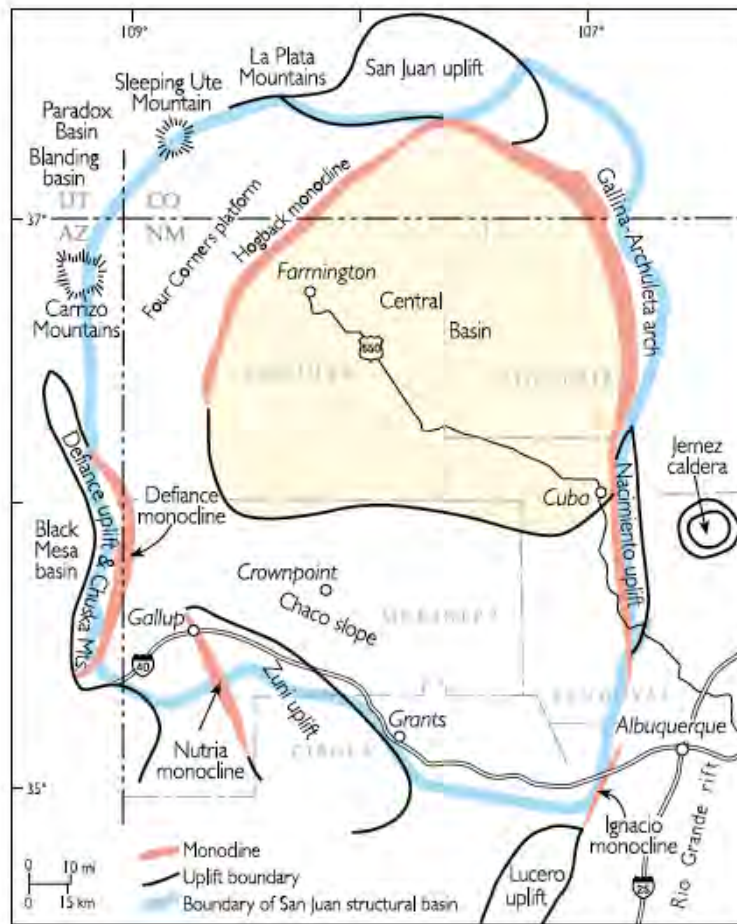


Figure 2.5: The San Juan Basin of Colorado and New Mexico which was evaluated by the Colorado Geological Survey and the New Mexico Bureau of Geology and Mineral Resources.

ARIZONA

Northeastern Arizona encompasses the southwestern part of the Colorado Plateau (Figure 2.6), an area of gently dipping to slightly tilted Paleozoic and Mesozoic strata that includes porous and permeable sandstone units. The Lower Permian Cedar Mesa Sandstone was identified for study as a potential target for CO₂ sequestration. The Cedar Mesa Sandstone is overlain by the impermeable Organ Rock Formation, which forms a seal. The salinity of groundwater in the Cedar Mesa Sandstone is unknown, and must be determined before CO₂ can be sequestered. Well logs for 755 drill holes were used to evaluate the extent, depth, and thickness of subsurface formations. The ESRI® ArcMap™ GIS software was then used to calculate the volume of the Cedar Mesa Sandstone in all areas where the top of the unit is below 3000 feet (915 meters) depth. Well logs were used to evaluate porosity, which were then used to calculate the amount of pore space at least theoretically available for CO₂ storage (the effective porosity). The Arizona Geological Survey calculates between 30 km³ and 80 km³ of pore space in the Cedar Mesa Sandstone. The net fraction of pore-space accessible to CO₂ injection is estimated to be approximately 0.5% to 5%. For context, application of this storage efficiency to the Cedar Mesa Sandstone indicates that 0.15 km³ to 4.3 km³ of pore space is accessible to injected CO₂, and that 0.114 to 3.24 billion tons of CO₂ could be sequestered in this pore space at a density of approximately 750 kg/m³.

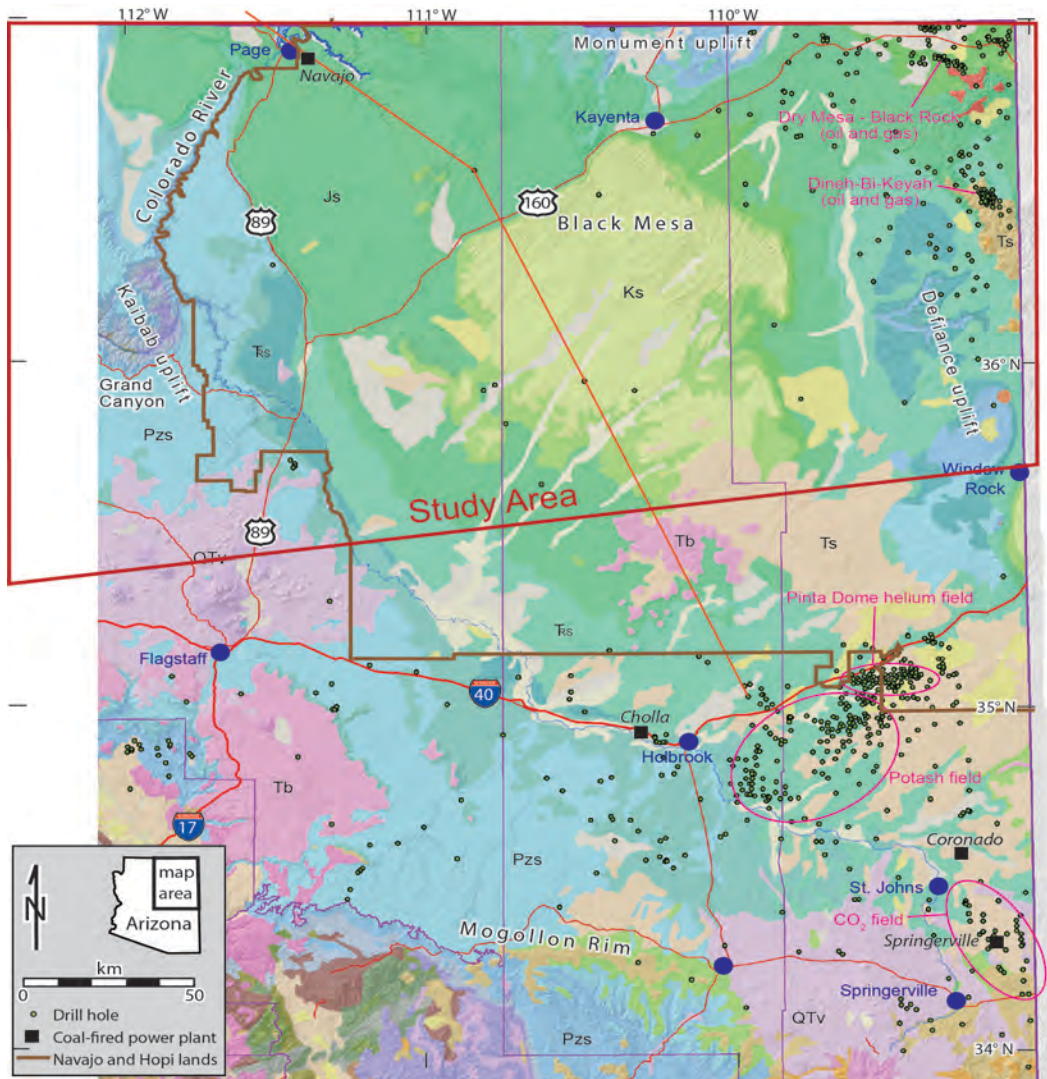


Figure 2.6: Area of northeastern Arizona where the Arizona Geological Survey studied the Cedar Mesa sandstone for its sequestration potential.

3. Public engagement: outreach, planning and permitting

The Rocky Mountain Carbon Capture and Sequestration (RMCCS) project team identified public engagement as an essential and necessary component of the projects’ success. The process of public engagement involved contact and outreach to a broad spectrum of organizations and individuals at the local and regional level. Landowners, mineral rights owners, industry, state and local government/regulatory agencies, private citizens and the print/radio/television news media were all a part of the public engagement process. Each of the contacts was purposeful and necessary to inform members of the public about the project activity, promote an understanding of the technology, address fears and concerns, secure permissions and access, obtain permits, seek funding and in-kind contributions and to generate good will toward the research, development and potential future subsurface storage of carbon dioxide. Many of the public engagement efforts were required steps in the process. As a result, many of the RMCCS team members were involved in the public engagement process.

PLANNING

The Colorado Geological Survey (CGS) took the lead in the overall planning efforts for the project. There were several key stakeholders that needed to be contacted and many of these were in the project area or located in the State. Working with the project team, CGS developed presentation materials that were used to communicate information about carbon sequestration in northwest Colorado and the proposed Craig Geologic Characterization project. CGS made presentations to the Colorado State Land Board, the State of Colorado's Carbon Sequestration Task Force, the Tri-State Generation and Transmission Association Board of Directors (Tri-State), the Trapper Mine Board of Directors, to locally elected officials from the Town of Craig and to County Commissioners from Moffatt and Routt Counties. The State Land Board holds title to some of the surface rights and most of the mineral rights upon which the project was located. The geologic characterization well and the seismic surveys to be conducted for the project were all located on the Trapper Mine property. Tri-State operates the Craig generating station located adjacent to the Trapper Mine and uses all of the coal it produces. The Town of Craig is located just a few miles from the Trapper Mine, Craig Station and the RMCCS project. The Trapper Mine representatives were very helpful and accommodating in the completion of the seismic surveys and in the drilling of the characterization well. Presentations made to local elected officials also provided a forum for presenting information to members of the public about the project. Early contact with the public was an important aspect of the project that helped to develop a greater understanding of carbon storage in deep saline formations and build a foundation for good relationships. CGS also made presentations to the State Geologists of Utah, Arizona, and New Mexico to explain the DOE project and how the information to be collected would be useful. In many cases, the planning efforts were a useful preliminary step to satisfying requirements from landowners, mineral right owners and various state and local agencies, to conduct many of the activities required by the RMCCS project.

PERMITTING

It is required by state and local regulators to obtain permission from landowners, mineral right owners and various state and local agencies, to conduct many of the activities required by the RMCCS project. Specific requirements vary greatly from state to state and county to county, time of year and the nature of the work being done. It is strongly recommended that project leaders identify sub-contractors familiar with the permitting requirements in the specific area for any future projects. This pertains to gaining access to the drill site within the Trapper Mine, conducting of the surface seismic survey and the drilling of the RMCCS State No. 1 site characterization well. The objective of drilling the characterization well was to obtain valuable data from the subsurface and was classified as a "Stratigraphic Test". Since there would be no production or injection with the well, the permitting process was straight forward and relatively fast. In the project, no individual permit took longer than 60 days from the time of submission to approval. Obtaining approvals for permits to drill wells for the purpose of CO₂ injection take considerably longer. Even in projects where the ultimate purpose for a well is for injection it may be more expedient to initially permit the well as a stratigraphic test well, allowing drilling to proceed while the injection permits are being processed separately.

For the RMCCS project, permitting involved three different components. The first was obtaining permission from the Trapper Mine for access to the site that would be used for drilling the well. Selecting a well site within the boundaries of an operating surface mine added additional considerations in the permitting process. After significant work with the mine, the drill pad was located in a previously mined, inactive area, not yet reclaimed reducing reclamation expenses and mitigating much of the environmental risk associated with well drilling. The access permit obtained from the Trapper Mine specified the liability for any financial damages due to the drilling process

onto the RMCCS project, documented insurance requirements for Schlumberger as the owner of the well and all major sub-contractors to Schlumberger, and specified time limits for access to and from the well site under the agreement. The access agreement required approval by the Trapper Mine General Manager and also the mine insurance provider. For the RMCCS project there were two separate agreements, one for permission to conduct the seismic survey and the second agreement for well drilling. The process to obtain the permits took approximately six weeks from initial discussions to final approval for each agreement. A similar type of agreement will be typical when requiring access to any commercial industrial property.

The second permitting component involves obtaining permits from surface owners and mineral right owners to conduct a project surface seismic survey. A seismic survey was conducted to obtain detailed imaging of the subsurface using reflection of acoustic energy from rock layers deep below the surface. The permits included permission to access the property, a pre-negotiated damage fee and terms for compensation if additional damage occurs. For mineral right owners, the permits were to allow data to be acquired and specified who would be allowed to receive the data and what data, if any, would be given to the mineral rights owner. The permitting for the seismic survey was conducted by St. Croix Environmental, an organization specializing in seismic permitting.

The third, and most extensive, permitting component was for the drilling of the RMCCS State No. 1 characterization well. Although the permit requirements to drill a stratigraphic test well are the least complex to obtain, the number of permits and number of entities that need to be contacted is large. The primary agency regulating well drilling for the RMCCS project is the Colorado Oil and Gas Conservation Commission (COGCC). The land on which the well was drilled is owned by the State of Colorado and an exploration permit is required by the State Board of Land Commissioners. Additionally, Colorado's Department of Natural Resources - Division of Parks & Wildlife, Colorado's Department of Public Health & Environment and the federal Department of Labor's Mining Safety and Health Administration also has jurisdiction over various aspects of the operation. In order to assure all applicable requirements and jurisdictions were identified and fulfilled, Northwest Corporation, based in Grand Junction, Colorado, was employed as the project permitting agent. A forty-eight point compliance plan was developed summarizing all forms, notices and other requirements detailed. The primary permitting requirement for well drilling is the Application for Permit-to-Drill (APD). Prior to submitting the APD the drill pad site had to be surveyed and a layout of the site construction prepared. Detail information on the drilling rig, drilling fluid system, drilling plan and well completion plan was required to be developed and submitted with the application.

Once the engineering plan for the well drilling was complete, the drilling rig selected and the exact site located, a series of forms were required to be completed and submitted to the Colorado Oil and Gas Conservation Commission for approval. The forms included: Form 1 – Operator Application, Form 2 – Application for Permit-to-Drill, Form 2A – Oil and Gas Location Assessment, Form 3 – Performance Bond, Form 4 – Sundry Notice and Form 15 – Earthen Pit Permit. In addition to COGCC requirements, the project was required to obtain a waiver of wildlife stipulations from the Colorado Division of Parks & Wildlife which restricts drilling during winter months in certain areas in Moffat County. A mitigation plan was agreed upon to limit impact on elk common in the area by the well drilling. A Storm Water/Erosion Control Plan was submitted and approved by the Colorado Department of Public Health & Environment. The COGCC requested acknowledgement of drilling fluid containment, spill/release mitigation plans, and drill cuttings low moisture content requirements. Approval to drill was granted on October 27, 2011. A “letter of intent” to drill was sent to each land owner and to Moffat County after the COGCC approval was received. During the drilling operations a weekly storm water inspection was performed and sundry notices of key drilling operations were required to be provided to the COGCC. Typically the Occupational Health and Safety

Administration would have exercised jurisdiction over all field activities in regards to health and safety, however since the project site was located within the boundaries of the Trapper Mine, the Mining Safety and Health Administration (MSHA) exercised jurisdiction over the project. The special requirements for complying with MSHA regulations are extensive and are explained in the drilling section of this report.

Once the well was drilled and cored, and geophysical well logs were obtained, additional COGCC forms were required to be completed and submitted for plugging the well, restoring the drill pad and well abandonment. Form 6 – the Well Abandonment form was submitted and approved. In addition to the submission of COGCC Form 6, the RMCCS project was required to submit a letter from the Director of the Board of Land Commissioners, Craig Region, stating that the restoration of the site met the approval of the land board. Although the well has been abandoned in accordance with all state requirements, the well abandonment was engineered in such a way that it could be re-entered and put back into service with minimal cost.

PUBLIC OUTREACH

Upon receiving the RMCCS award from the DOE, the University of Utah began efforts to develop a web presence for the project. The first RMCCS project website for public use was developed by a University of Utah web development team and was housed on University of Utah servers. The rmccs.org website went “live” in late 2010. In May 2011 the rmccs.org web site (screenshot in Figure W1) was transferred to another University of Utah server (Apache), file system and RAID array purchased using RMCCS funds. The RMCCS website was built using standard HTML language with a flat (non-database) file system.

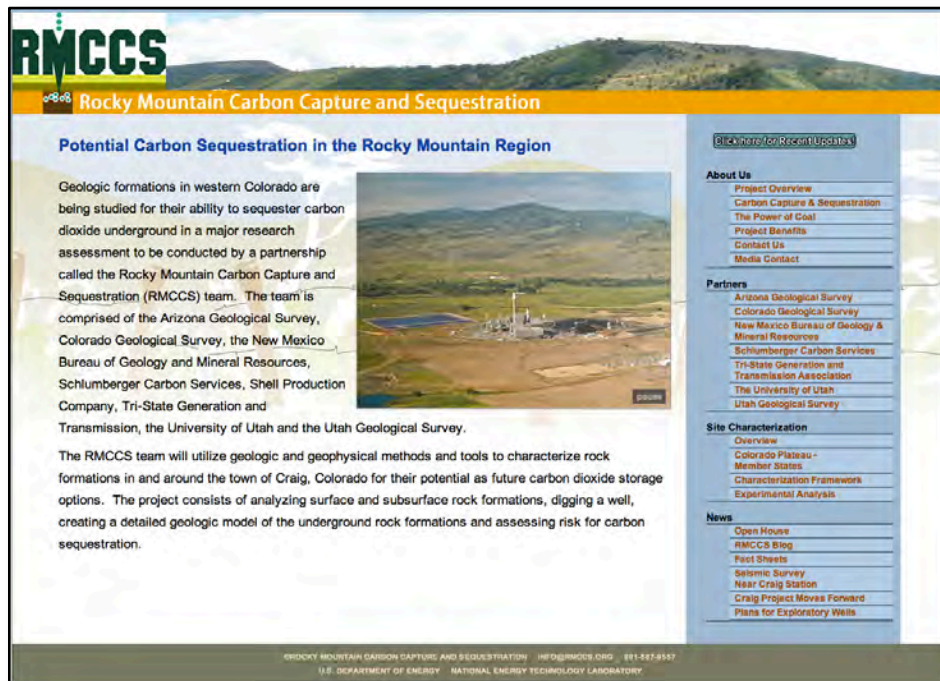


Figure 3.1. Screenshot of RMCCS.org website.

The initial RMCCS website introduced visitors to the concepts of CO₂ sequestration, the goals of the RMCCS project, and some economic background of northwest Colorado, including the benefits of coal mining and coal-fired electric power generation. As the project moved forward with surface field mapping, seismic surveys, well drilling, core analysis and modeling, the website was

updated by University of Utah staff, with input from RMCCS project partners. An “Update” link provided visitors with an up-to-the-minute status report of the well drilling progress and a “News” link provided information about open house events and press releases developed through the communications plan and other significant project developments. Significant website updates and changes were stored on secure, password protected subdomains (e.g. <http://testing.rmccs.org>) and passed along to the NETL/DOE for approval before being moved to the public site.

The RMCCS project also maintained an internal website, called “Unite”. Unite is a collaboration system used to assist multi-user groups and projects in their research efforts and goals. Unite for RMCCS (accessible from the main RMCCS website to authorized users) was intended to house all documents and data for the project, and to be a communication tool to discuss project tasks and deliverables. The RMCCS Unite site was prepared and presented to the RMCCS project team in September 2011, however, the project team never fully utilized the Unite system. Project team members eventually reverted to traditional means of communication and data-sharing, such as email and 3rd party file-sharing services.

Later in the project, the flat file/HTML system for the RMCCS website proved to be limiting for many of the project needs, especially for data-sharing and data-management (e.g. the dissemination of project core analysis results to the public). The RMCCS partners also wanted to better understand the organizations expressing the most interest in the data gathered by the RMCCS project to allow future site characterization and CCS/CCUS projects to more effectively reach stakeholders. To address these needs, the rmccs.org website was shifted to a dynamic, database-driven system (WordPress) in the summer of 2013. The updated site can be seen at <http://testing.rmccs.org/wordpress352/>. The new site maintains the overall look and feel of the original site, but benefits from an authentication system, where logged in users can create/edit pages, view pages and download analytical data, depending on predetermined permission levels. The public is able to register for access to all RMCCS data. The University of Utah, the RMCCS project, its partners and/or the NETL/DOE will not sell or otherwise provide the registration information (email address and organization) to any 3rd party.

The rmccs.org site served a total of 2,446 unique visitors, with over 15,000 page hits during the life of the project. Most site visitors were from Colorado and other locations in the United States.

The RMCCS project team also developed a comprehensive communications plan that worked in partnership with the website to define and prioritize the stakeholder groups impacted by the project, finalize necessary messages, materials and communication channels, prepare public relations efforts, and determine long-term campaign strategies, issues, milestones and initiatives. The outreach strategy included an on-site open house at the Trapper Mine and a viewing of core samples at Triple-O-Slabbing in Denver. Two press releases were submitted to media outlets to promote these events.

The written communications plan for RMCCS identified the project partners, state, county and city government stakeholders and external influencers such as the media and special interest groups. The plan defined the strategy and planning of communications for the project, outlined materials to be developed in the communication efforts, media relations protocol, community outreach including open houses at the project site and at the slabbing office, and programs, tools and tactics the RMCCS used for outreach efforts.

The first open house was held at the Trapper Mine in Craig, Colorado on January 24, 2012 from 4:00 pm to 7:00 pm. The open house was promoted to the Craig community through newspaper ads in the Craig Daily Press and postcards mailed to stakeholders identified in the communications plan. At the open house meeting, informational boards on the project were located throughout the conference room and team members were on hand to answer questions about the project. The

informational boards covered a general project overview, an overview of the project partners, information on carbon capture and sequestration, seismic testing, how a well for this type of project is drilled, safety of storing carbon underground and an update on the current drilling project at Trapper Mine. A tour of the drilling rig was offered at 3:00 pm just prior to the start of the open house meeting. Members of the public interested in the tour were taken by shuttle bus to the rig site where they were provided an overview of the drilling rig and progress on the overall project of drilling the well. A total of 21 people attended the open house, including two local county commissioners and a representative from US Senator Udall's office.

The second public event was an opportunity to view the core that was taken from the well drilled at the Trapper Mine and was held at Triple-O-Slabbing on August 16th, 2012 from 1:00pm to 2:00pm. Members of the press were invited to view core samples via a broadly distributed press release and through personal invitations. Several members of the project team were present for the core viewing and were available to discuss the potential for long-term carbon storage sites with the media. RMCCS received 33 media hits from this event, totaling 7,704,687 unique visitors. A total of four radio stories were aired as part of the media coverage. Barbara Walz of Tri-State gave an interview to Colorado Public Radio that subsequently air on the local radio station in Denver. KOA radio also attended the event and conducted interviews with Sarah Carlisle of Tri-State and Vince Matthews of the Colorado Geologic Survey that subsequently aired on the local radio station.

CONCLUSION

Effective communication and public outreach were critical to the success of the RMCCS project. Investing the time necessary to understand the requirements and establish good relationships with federal, state and local government agencies as well as members of the media and individual citizens made challenging issues more manageable. Access and permitting activities were required in all phases of the field activity from planning and execution through completion and abandonment. Project implementation required obtaining permits and complying with numerous terms and conditions that vary greatly from state to state depending on the specifics of the operation. For this reason it is highly recommended to engage sub-contractors that are experienced in permitting for the specific requirements of each project. Compliance with permit terms and access requirements was also an important component to successful project completion and for being a responsible community partner. Communication with the local and regional community provided education and acceptance for the viability of long term carbon storage in deep saline formations. Outreach efforts included providing internet access to general background information about CCS and the project specific data as well as locally hosted public events and television/radio/print media contacts. The outreach efforts successfully educated the public about the project, its perceived issues and promoted the use of long term carbon storage as a safe and effective strategy.

4. Geologic and geophysical studies at local characterization site

The Sand Wash Basin is a basin within the CSA in northwestern Colorado that was selected as the focus of this study. It contains the Craig Power Station and the location of the stratigraphic test well (RMCCS State #1) that was drilled as part of this study; it was the area of the most detailed mapping.

Two key objectives of the RMCCS partnership are to:

1. Characterize in detail the saline aquifers and their seals in the vicinity of a stratigraphic test well that was to be drilled as part of this project. The well was drilled in February and March, 2012, in the SW SE of Section 34, Township 6 North, Range 91 West, six miles south of Craig, Colorado and was named the RMCCS State #1.
2. Expand that characterization to the entire Colorado Plateau incorporating the data acquired from the drilling of the stratigraphic test.

To achieve these objectives, the CSA was examined at three scales (Figure 4.1):

1. At the local scale, a very detailed examination has been made of the geology within a single Laramide-age structure called the Yampa Block surrounding the site of the RMCCS State #1 stratigraphic test well.
2. At the basin level, the structural framework for a detailed three-dimensional geocellular model was created that covered the Sand Wash Basin and a portion of the adjacent Piceance Basin in northwestern Colorado.
3. At the regional level, the top and base of each of the saline aquifers were mapped within the Colorado portion of the Colorado Plateau.

To achieve the primary objective of characterizing the targeted saline aquifers and their seals, a three-dimensional geocellular model was created that covered the Sand Wash Basin study area (Figure 4.1). This will be used for simulating carbon dioxide injection into the RMCCS State #1 stratigraphic test well, which is to the south of the Craig Power Station. Characterization of the reservoir quality of the saline aquifers in the Sand Wash Basin was made by examining cores and cuttings; researching published porosity and permeability values for oil and gas fields within the basin; crossplotting porosity and permeability data from core analyses from existing wells; and mapping net sand, porosity and pore volumes from digital geophysical logs.

To achieve the secondary objective of expanding the characterization to the Colorado Plateau, maps were made depicting the structural tops and bases of the three saline aquifers and their equivalent formations, as well as the Mancos seal; these covered the CSA. Near the end of the project digital logs were obtained and were used to identify more accurately net sand, average porosity and pore volumes; maps of these parameters were constructed for the CSA.

Because the majority of this report was prepared prior to the simulation of CO₂ injection, analyses of geologic and structural controls on fluid flow are minimal.

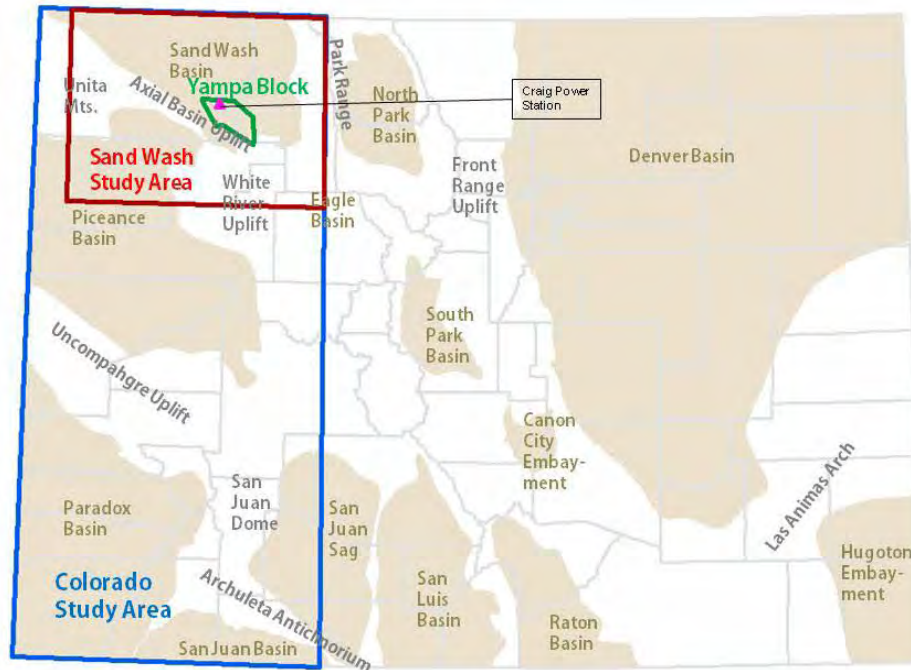


Figure 4.1. Extent of Colorado study areas including Yampa Block (green) and Sand Wash Basin (red).

Mapping of Structural Surfaces

Data

A goal of this project was to incorporate all existing publicly available data into maps depicting the structural configuration of the saline aquifers and their seals. The data utilized in this mapping included:

- Records from over 30,000 oil and gas wells. These were obtained primarily from the IHS commercial database for the Rocky Mountain region. This database was augmented by data from the Colorado Oil and Gas Conservation Commission's website. The locations of these wells are shown in Figure 4.2A.
- Raster images of geophysical logs from over 18,000 oil and gas wells in the CSA. These were purchased from MJ Systems, a company that scans and archives raster logs. Geophysical logs record the physical properties of the rocks and fluids that surrounding the wellbore and were used to determine the depths of the saline aquifers and other formations in the subsurface. They were also used to estimate porosity and net sand in the saline aquifer. Locations of wells with raster geophysical logs are shown in Figure 4.2B.
- One thousand surface measurements of bedding strikes and dips. Nearly 1500 measurements were collected by a team of geologists from the Colorado Geological Survey covering an area of approximately 800 square miles, predominantly in the region of the Yampa Block. 470 of these measurements were deemed less reliable and were not used. Approximately one thousand strike and dip measurements were used to modify hand contours depicting the structural configuration of the Dakota Formation in the subsurface. Figure 4.3 shows the locations of the strike and dip measurements used in this project.
- Approximately 70 miles of existing two-dimensional seismic data in 11 lines. These were purchased through Seismic Exchange, Inc. to help define the structures in the southern part

of the Yampa Block, which is updip from the stratigraphic test well, the direction that sequestered CO₂ is expected to migrate. The locations of these lines are shown in Figure 4.4.

- Approximately eight miles of two-dimensional seismic data in two lines were shot by Western Geco, a Schlumberger Company. These cross the stratigraphic test well location and were shot to define the subsurface structure in the immediate area of the test well. The locations of these lines are shown in Figure 4.4. For work on this portion of the project, these newly acquired lines were used qualitatively to manipulate the shape of the Dakota surface. The precise depth of the Dakota horizon was not picked from the seismic lines because existing maps of the structural configuration of the shallow Twenty-Mile Sand and the Trout Creek Sand, as well as surface strike and dip measurements, conflicted with the information in the deeper seismic horizons. More work can and should be done with these seismic lines assuming processing and calibration are robust.
- Published geologic maps that depict the rocks and structures at the surface. These include:
 - Outcrop patterns from surface geologic maps, including Tweto (1977).
 - Locations of fold axes from surface geologic maps, including Tweto (1977).
 - Elevations of surface contacts between the Dakota and the overlying Mowry Shale depicted on digital elevation models.
- Geologic publications that contain subsurface maps, cross sections, and/or rock characteristics and properties.
- Data collected from the drilling of the stratigraphic test well RMCCS State #1, including:
 - Geophysical well logs that help determine rock and fluid properties of the penetrated strata.
 - Full-diameter cores and sidewall cores from which direct measurements of rock properties of the saline aquifers and their seals can be obtained.

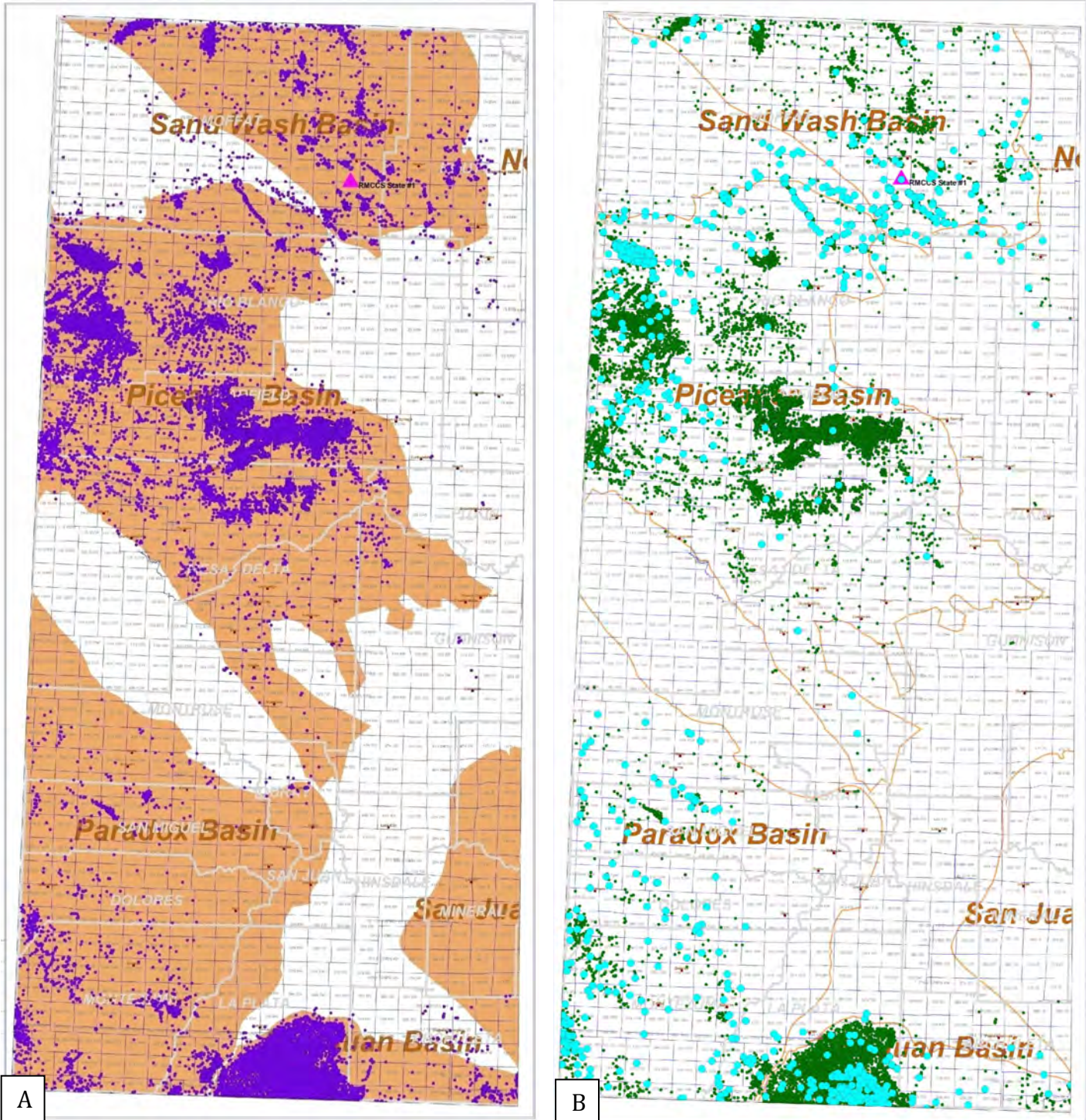


Figure 4.2: A.) Location of wells in the Colorado Study Area. B.) Location of wells in the Colorado Study Area with raster images(dark green, smaller dots) and digital logs (larger turquoise dots).

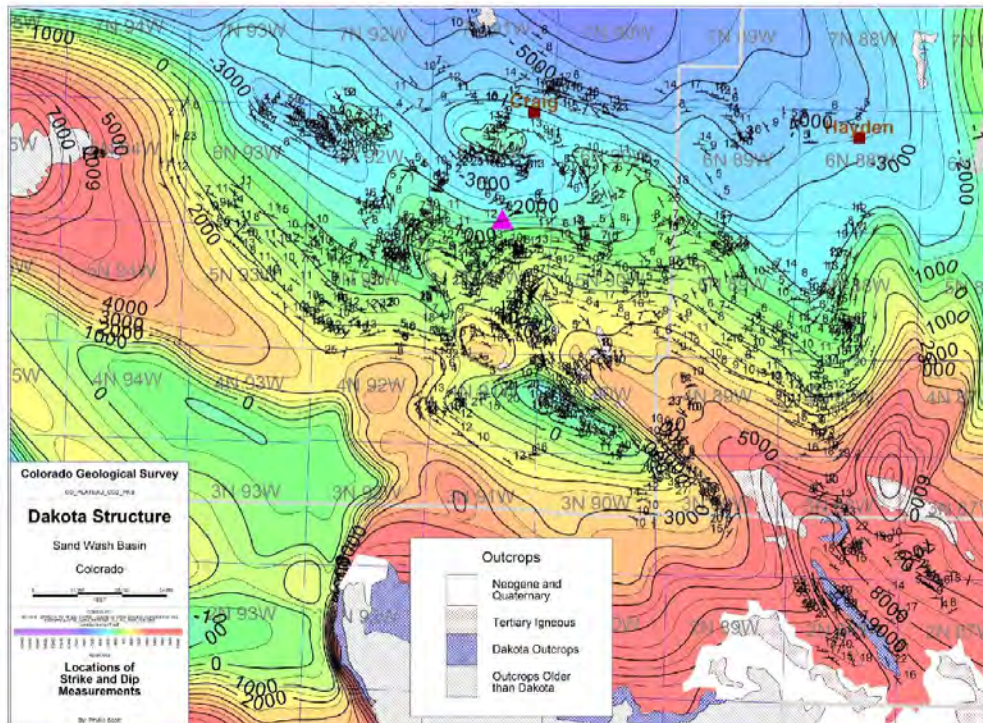


Figure 4.3: Location of surface strike and dip measurements made by the Colorado Geological Survey superposed on structure map on top of the Dakota sandstone.

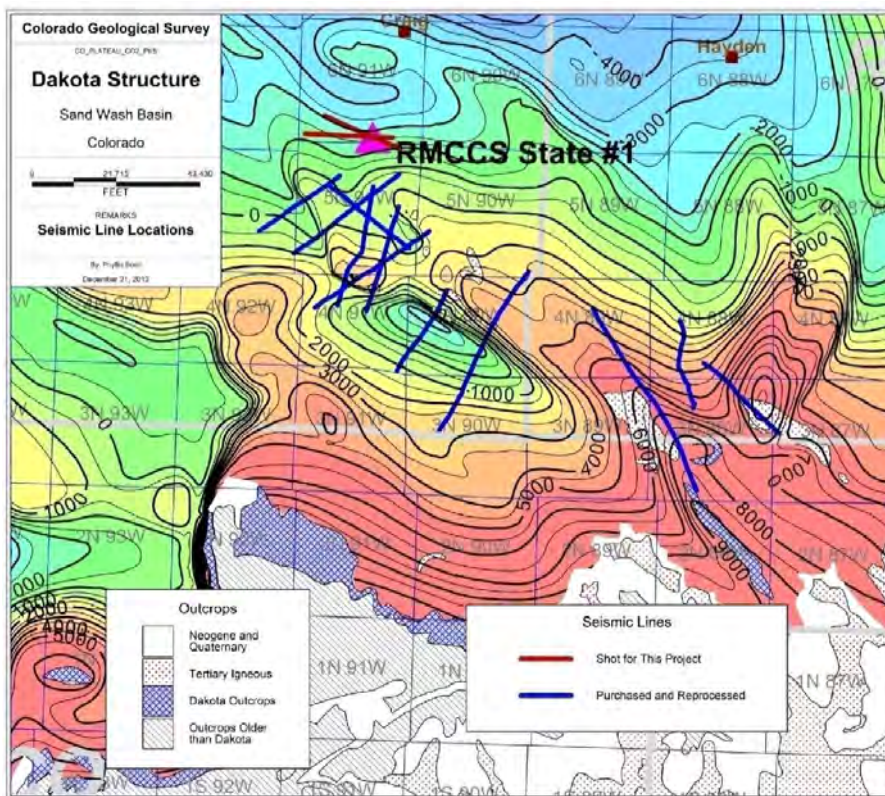


Figure 4.4: Location of seismic lines purchased or shot for the study superposed on top of Dakota structure map.

Extent of Maps of Structural Surfaces

The sequestration potential of the saline aquifers in Colorado has been examined at three scales as was shown in Figure 4.1:

1. Yampa Block: a very detailed analysis of the geology of the Laramide-age Yampa Block south of the town of Craig, Colorado. All of the data types listed above were used in this detailed study component. This block covers approximately 230 square miles and generally dips about 10 degrees to the north. It is bounded on all sides by forced folds.
2. Sand Wash Study Area: a detailed characterization of the three saline aquifers within a 40-mile radius of Craig. This study component augments the Yampa Block mapping with IHS data for oil and gas wells in the expanded area. Also utilized were additional geophysical logs, surface geologic maps and other published data. This characterization included most of the Sand Wash Basin and the adjacent Axial Basin Uplift that separates the Sand Wash and Piceance basins. The final products from this characterization were structure maps of fourteen formation top surfaces that were used for building a geocellular model.
3. Colorado Study Area: a regional scale mapping of the three saline aquifers and their equivalents. This report presents the maps created for Colorado portion of the Colorado Plateau, also referred to as the Colorado Study Area (CSA). Mapping from the Sand Wash Study Area was expanded to the CSA by incorporating more IHS well data, geophysical logs, surface geologic maps and other published data. The tops and bases of the three saline aquifers and their equivalents, as well as the top of the Mancos seal, were mapped at this scale.

Mapping Software

Three mapping software packages were used to create these maps:

1. Petra™: an IHS software package designed for geologic interpretation and mapping based on data from oil and gas wells. Petra was used to correlate formation tops and to create a detailed, hand-contoured map depicting the structural surface of the Dakota Sandstone.
2. Petrel™: a Schlumberger application for geocellular modeling and visualization. Petrel was used to generate multiple, sub-parallel formation surfaces using the Dakota structure map and other formation tops interpreted in Petra. A static geologic model was created from this framework that was ultimately used for fluid injection simulations.
3. ArcGIS™: a popular ESRI tool for GIS based mapping. ArcGIS™ has been chosen as the primary RMCCS spatial database format.

Methods

Overview

The general workflow consisted of correlating formation tops in Petra™ and creating a detailed, hand-contoured, Dakota structure map. The correlated tops and gridded Dakota structure map were transferred to Petrel™, which was used to create structure maps of other formations. Finally, the Petrel™ gridded surfaces were imported into ArcGIS™ where they were combined with surfaces created for other portions of the Colorado Plateau in the final report.

Sand Wash Basin

Petra™

Petra™ was the primary software tool used for analysis and interpretation. Well data from the IHS database and scanned geophysical log images from MJ Systems were central to this interpretation. Formation tops as reported by operators are notoriously unreliable, with inconsistencies common from company to company. Oftentimes tops do not correlate exactly, creating errors in mapped surfaces. To produce the most accurate maps, formation tops were identified and correlated anew throughout the study area. This detailed correlation process resulted in a high level of consistency throughout the area.

The tops correlated in this project were used to create a detailed structure contour map on the top of the Dakota Sandstone. The Dakota Sandstone was chosen as the key surface because it is regionally extensive and often easy to distinguish on geophysical logs. It is also the shallowest of the regionally targeted saline aquifers.

Initially only the Sand Wash Basin study area (including the Yampa Block and the Axial Basin Uplift) was examined and mapped. On the Axial Basin Uplift, the saline aquifer targets are near the surface, and in some cases have been removed by erosion. In contrast, deeper parts of the basin have thick sections of younger sediments overlying the saline aquifers, with few wells drilled deep enough to penetrate the aquifers. To overcome this problem, depths to the aquifers could be projected from the positions of shallower or deeper formations. Many more formation tops not associated with the targeted aquifers were correlated and mapped. From these the tops of the aquifers could be estimated in wells that did not actually penetrate the aquifers.

The Sand Wash study area contained 4924 wells, of which 2708 had at least one geophysical log. Of those wells with logs, 2000 had either an actual or projected Dakota formation top that was correlated for this project. Altogether, 37 formation tops ranging in age from the Cretaceous Fox Hills Sandstone to the Precambrian erosional surface were correlated for the Sand Wash study area totaling 15,000 individual tops.

The Dakota tops were hand contoured to incorporate the individual data points as well as all the other data sources. The structures were contoured as forced folds overlying the edges of fragmented and differentially uplifted basement blocks.

The Dakota structure map of the Sand Wash Basin study area, shown in Figure 4.5, was then imported into Petrel and subsequently used for generating other modeled surfaces .

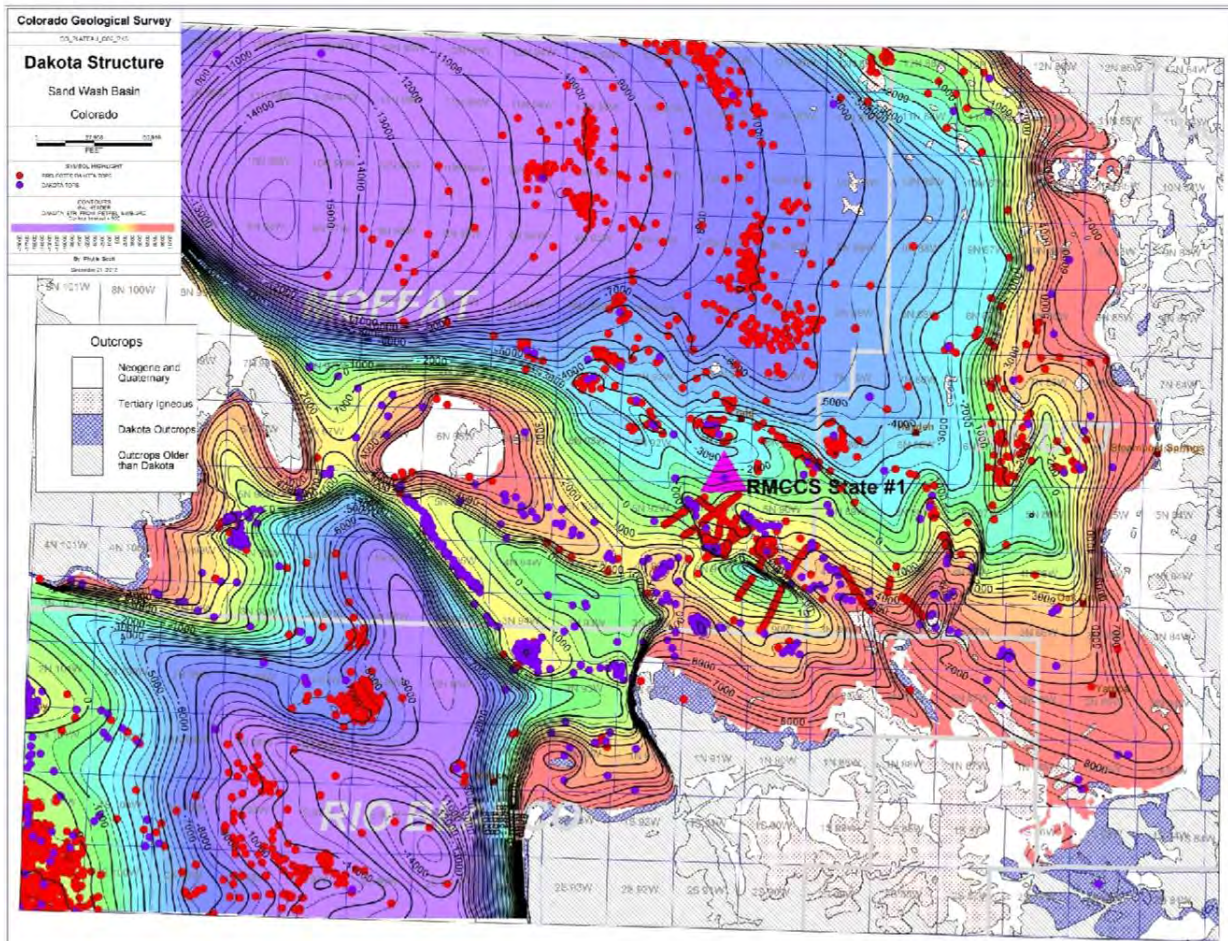


Figure 4.5. Petra™ structure map on top of the Dakota Sandstone saline aquifer, Sand Wash Basin Study Area. Locations of Dakota tops shown as purple dots; projected Dakota tops are shown as red dots.

Petrel™

Petrel™ is a software package designed by Schlumberger for generating and visualizing static geologic models from a myriad of oil and gas well data. Petrel™ was used to create a three-dimensional model within the Sand Wash Study area to be used as the structural framework for simulating the injection of CO₂ into the saline aquifers from the RMCCS State #1 well.

The Dakota surface that was generated in the Petra project was imported into Petrel along with the locations of wells within the study area and formation tops for those wells. Petrel used these data to map other surfaces by comparing formation tops for an unmapped surface with an adjacent mapped surface and creating a new, sub-parallel structure map. For example, the top of the Morrison was mapped by using the Dakota structural surface and Morrison formation tops to create a Morrison structural surface that is sub-parallel with the Dakota surface. The use of both a surface and the formation tops provides much more information for the creation of the secondary surface than tops alone. Relying only on formation tops to create surfaces in this structurally complex area usually resulted in impossible geometries with surfaces that intersected.

Fourteen surfaces were created in Petrel (Table 4.1 and Figure 4.6). From shallowest to deepest they are:

| Formations Mapped in the Sand Wash Basin Geostatic Model | | |
|---|-----------------------------------|---|
| Formation Top | Average Interval Thickness | Description |
| Mancos | 888 | The name of the group that comprises all of the formations deposited within the Cretaceous Seaway (including all formations down to the Dakota saline aquifer). The Mancos Group is the ultimate seal overlying the saline aquifers. |
| Morapos | 2311 | A prominent sand within the Mancos Group deposited in the Cretaceous Seaway |
| Niobrara | 1528 | A calcareous section within the Mancos Group deposited in the Cretaceous Seaway |
| Carlile | 199 | A shale within the Mancos Group deposited in the Cretaceous Seaway |
| Frontier | 295 | A coarsening-upward shale and sand unit deposited within the Cretaceous Seaway. |
| Mowry | 102 | A shale unit directly overlying the Dakota saline aquifer. It is the seal for the Dakota saline aquifer |
| Dakota | 166 | A saline aquifer comprised of fluvial and marine sands, silts and shales. |
| Morrison | 415 | Fluvial sands and shales. The Morrison top is the base of the Dakota saline aquifer. This unit is a seal for the Entrada saline aquifer, although there are some porous sandstones in the western part of the study area. |
| Curtis | 65 | A marine deposit of sand, shale and siltstone that forms the seal for the Entrada saline aquifer. |
| Entrada | 347 | A saline aquifer comprised of eolian sandstone. It includes the Navajo Sandstone in the western part of the study area. |
| Chinle | 779 | Sands and silts deposited by large river systems. The Chinle is the base of the Entrada/Navajo saline aquifer. This interval includes the Moenkopi, which underlies the Chinle. The entire interval is a seal for the Weber saline aquifer. |
| Phosphoria | 187 | Marine limestone, sandstone and shale that acts as a seal for the Weber saline aquifer. |
| Weber | 411 | A saline aquifer comprised of eolian sandstone. |
| Maroon | | Alluvial fan redbeds and the base of the Weber saline aquifer. |

Table 4.1. Summary of stratigraphic formations mapped for the Sand Wash Basin geostatic model.

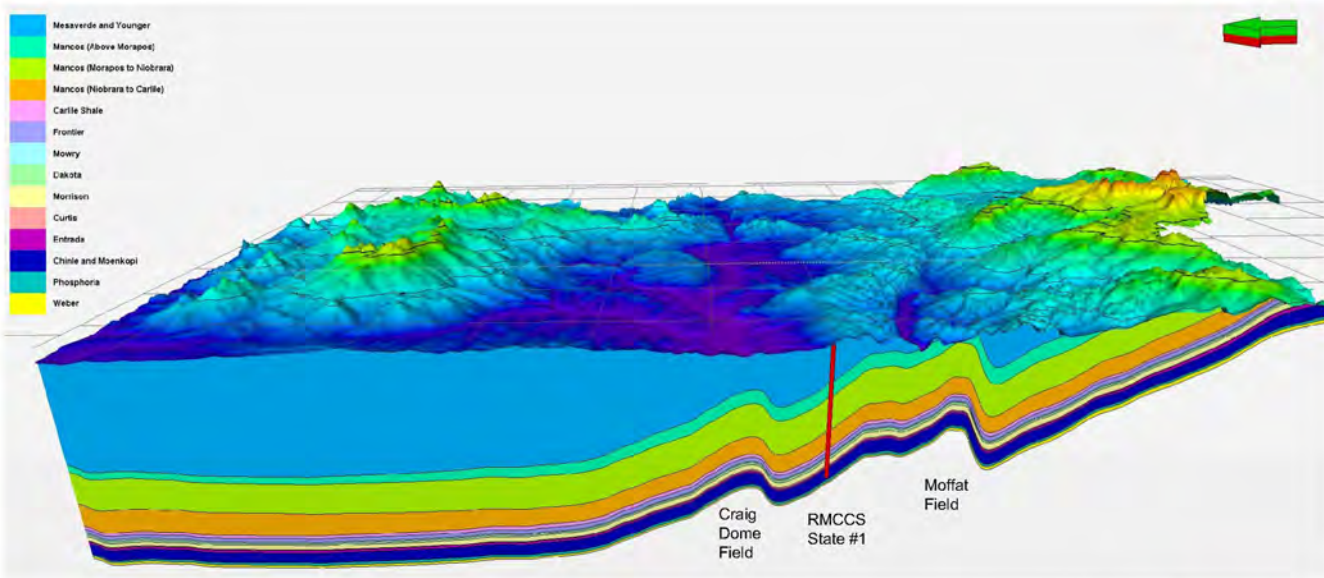


Figure 4.6. North-South cross section through Sand Wash Basin Petrel™ model. Wyoming border is at the left of the image and the White River Uplift (south) is on the right. The RMCCS State #1 stratigraphic test well is shown in red.

Geocellular Model

Surfaces for the geocellular model were generated using a minimum curvature algorithm and a grid size of 500 by 500 feet. A digital elevation model was imported into Petrel™ and used to trim each of the surfaces to prevent projections above the ground surface. Fourteen surfaces and their respective isopach maps were migrated from Petrel™ into Petra™ and ArcMap™ for visualization and database archiving. A cross section through the Petrel model is shown in Figure 4.6 which is a north-south cross section.

Discussion

Accuracy of Mapped Surfaces

Potential sources of error in the oil and gas well data and resultant maps include the following (listed in order of significance):

- In areas of sparse well control, the surfaces may be mapped incorrectly. Structural features, both faults and folds, may be completely missed if there are no well control or outcrop patterns that suggest that structures are present.
- The thickness of a formation (or the thickness between two formation tops) may appear to be highly variable. This can be due to:
 - The wellbore cutting a normal fault which has removed part of the section by extension, resulting in an anomalously thin isopach. Anomalous data points were ignored.
 - Incompetent formations such as the Mancos Shale appear to have been deformed and either thickened by compressional forces or thinned by extensional forces.

- o Steeply dipping beds make a section appear thicker than normal because a vertical wellbore does not penetrate the formation at a 90 degree angle. In areas of steep dip, anomalous sections should appear as elongate thicks or thins that parallel the strike of the section; however, computer gridding algorithms contour these anomalies as bullseyes when there are no other wells nearby for additional control. Because of this, other contoured surfaces that were made from the isopach maps would be in error. However, in areas of steep dip the contour lines are very close together, so a thicker section would result in a very small lateral shift in the contour lines.
- Tops may be miscorrelated because they are difficult to discern, especially on different types of geophysical logs that have been run over the years. Correlations were made on many formation tops above and below the saline aquifer tops in an attempt to insure accurate correlations.
- Formation tops oftentimes are gradational and difficult to pinpoint.
- The datum may have been measured incorrectly. Reported surface elevations were compared with digital elevation model data to gauge the correctness of the surveys.
- Locations may be misspotted. Data points that did not make sense were checked on the Colorado Oil and Gas Conservation Commission's website. If they could not be rectified, they were ignored.
- Wells may not be vertical. If this is the case, the measured depth of a formation top or an isopach interval may be too great. Anomalous points were ignored.
- Formation tops were picked with the geophysical logs compressed on the screen so that a longer section of the log could be viewed. Because of this, the top could be off by as much as 10 or 15 feet from where the actual pick would be if the log were enlarged.
- Because of the scale of the mapping project, the mapped surfaces are generalized and smoothed.

Potential Pathway for Injected CO₂

Detailed mapping suggests:

- There are barriers to the updip migration of sequestered CO₂ to the south, west and east of the RMCCS State #1 well.
- At this scale of mapping there are no clear barriers to the southeast that would prevent injected CO₂ from traveling from the wellbore updip to the Dakota outcrop.
- It is very possible that barriers exist either as faults that have not been identified or as permeability barriers. If an injection program is pursued, this potential pathway must be examined in greater detail.

Mapping of Reservoir Properties

Porosity and permeability, and therefore storage capacity, vary considerably over the lateral extents of the aquifers. They are affected by the environments that existed during deposition of the formations and also by subsequent factors that occurred during burial and lithification including cementation and diagenetic changes. Reservoir parameters can be measured from core analyses and from geophysical logs. These parameters were examined in this study in an attempt to depict their spatial distributions and to quantify storage capacity (Figure 4.7).

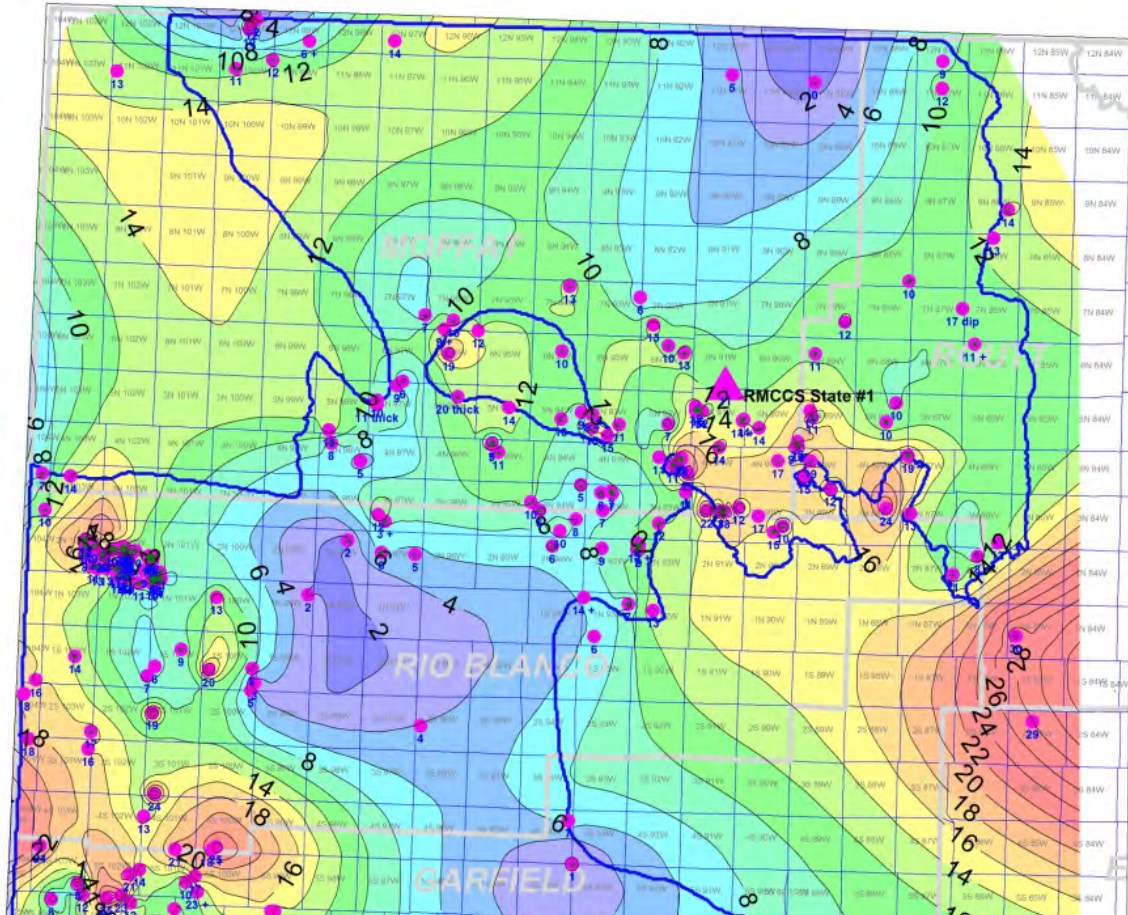


Figure 4.7: Pore thickness map (feet) for the Dakota saline aquifer in northwest Colorado. Purple dots show location of wells with data points.

Data

Data measuring reservoir properties were collected to understand the range and distribution of the properties that would affect storage capacity. These data include:

- Raster images of geophysical logs from over 18,000 oil and gas wells in the Colorado Study Area (CSA). These were purchased from MJ Systems, a company that scans and archives raster logs. Geophysical logs record the physical properties of the rocks and fluids that surround the wellbore. They were used to make an initial estimate of net sand within each saline aquifer. The locations of wells with raster geophysical logs are shown in Figure 4.2 B.

- In the final months of this study, digital logs were obtained for 818 wells in the (CSA) from IHS. These were used to map the reservoir parameters of net sand and porosity within the CSA. The locations of wells with digital geophysical logs are shown in Figure 4.2 B.
- Published average porosity and permeability values from field studies.
- Porosity and permeability measurements from older wells that had been cored and whose core analyses were available from the Colorado Oil & Gas Conservation Commission’s website.
- Data collected from the drilling of the stratigraphic test well RMCCS State #1, including:
 - Geophysical well logs that help determine rock and fluid properties of the penetrated strata.
 - Full-diameter cores and sidewall cores from which direct measurements of rock properties of the saline aquifers and their seals can be obtained.

Published Porosity and Permeability Values for Oil and Gas Fields

As a part of this study, a cursory examination of published porosity and permeability measurements was made in an attempt to better estimate the storage capacity of the saline aquifers.

Porosity and Permeability Crossplots

Additionally, core analysis data sheets were downloaded from the Colorado Oil & Gas Conservation Commission's website for wells in the Sand Wash Basin study area. Porosity and permeability measurements from six Dakota cores, three Entrada cores, and five Weber cores were manually entered into an Excel spreadsheet and crossplotted.

The data from the Dakota cores are shown in Table 4.2 and Figure 4.8; their average porosity is 13.7% and the median permeability is 19 md. One of the included cores had anomalously high permeability values. The porosity and permeability values are also dependent on the position of the core within the section; they vary greatly depending on whether the cores were cut through zones of the highest porosity or through more shaly intervals.

| Dakota Cores | | | | | Porosity % | | Permeability (md) | |
|--------------|--------------------|---------------|---------------------------|----------------|------------|--------|-------------------|--------|
| API Number | Location | Top of Dakota | Dist. from RMCCS State #1 | No. of Samples | Average | Median | Average | Median |
| 05-081-06683 | SE SW SW 20-5N-90W | 4893 | 6 mi SE | 8 | 11.7 | 12.8 | 84 | 43 |
| 05-081-06198 | NE SE SW 21-5N-90W | 4850 | 6mi SE | 35 | 16.4 | 16.4 | 16 | 1 |
| 05-107-06162 | NW SE 29-4N-89W | 3183 | 14 mi SE | 13 | 14.0 | 14.7 | 158 | 72 |
| 05-103-07055 | NE SE 1-2N-93W | 6996 | 20 mi SSW | 51 | 13.7 | 14.7 | 748 | 240 |
| 05-107-06133 | NW NE 36-4N-88W | 891 | 22 mi SE | 11 | 9.8 | 9.3 | 0.36 | 0.03 |
| 05-081-06666 | NE NW 30-5N-93W | 2752 | 16 mi | 7 | 8.3 | 7.5 | 9.1 | 0.16 |
| All 5 Cores | | | | 125 | 13.7 | 14.4 | 325 | 19 |

Table 4.2: Porosity and permeability data from COGCC public records.

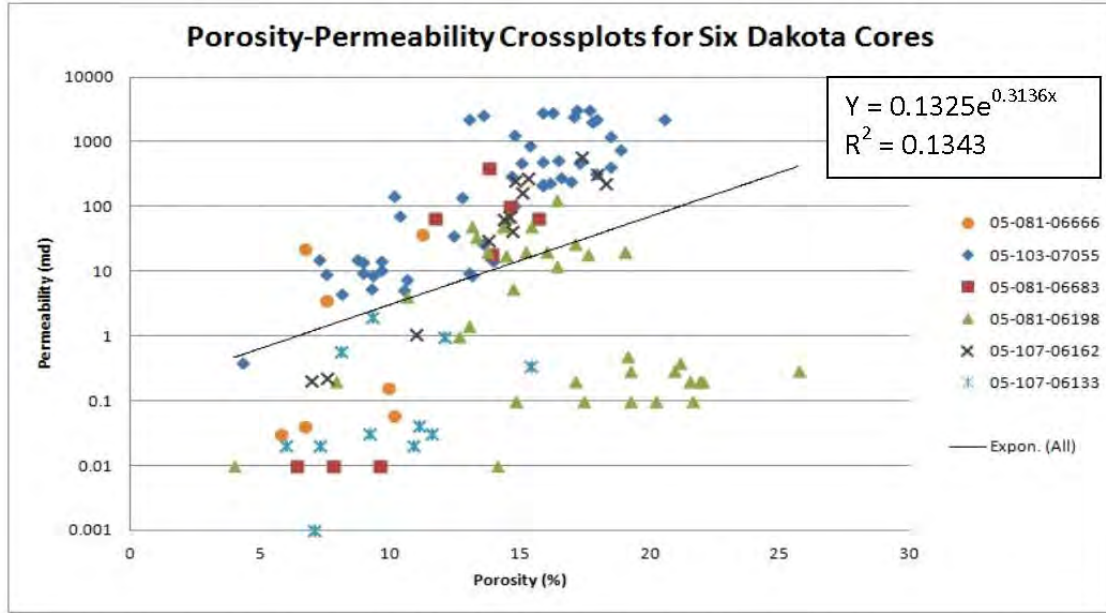


Figure 4.8: Cross-plot of permeability/porosity for 125 Dakota samples.

Table 4.3 and Figure 4.9 show the porosity and permeability data for the three Entrada cores. The table shows more detailed information for each individual core. The average porosity for the three cores is 15.0 percent and the median permeability is 23.5 md.

| Entrada Cores | | | | | Porosity % | | Permeability (md) | |
|---------------|------------------|---------------------|---------------------------|----------------|------------|--------|-------------------|--------|
| API Number | Location | Top of Entrada (MD) | Dist. from RMCCS State #1 | No. of Samples | Average | Median | Average | Median |
| 05-081-05278 | SW SE 20- 5N- | 5421 | 5.5 mi SE | 7 | 13.7 | 14.9 | 26 | 24 |
| 05-081-05284 | NW SW 13- 5N- | 5254 | 28 mi W | 10 | 18.8 | 21.2 | 187 | 161 |
| 05-107-06162 | NW SE 29- 4N-89W | 3814 | 13.7 mi SE | 45 | 14.4 | 14.7 | 21 | 18 |
| All 3 Cores | | | | 62 | 15.0 | 14.9 | 48 | 23.5 |

Table 4.3: Porosity and permeability data from COGCC public records.

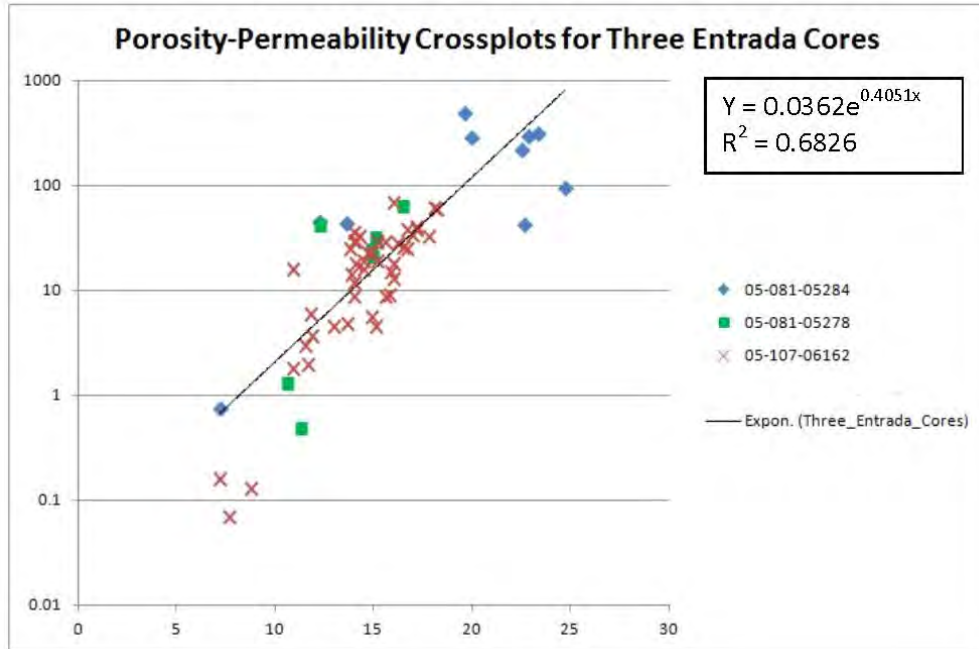


Figure 4.9: Cross-plot of permeability/porosity for 62 Entrada samples.

Table 4.4 and Figure 4.10 show the porosity and permeability data for five Weber cores. Four of these cores are from more than 60 miles to the west of the location of the RMCCS State #1 well. The one Weber core near the stratigraphic test well (05-081-06621) shows very low porosity and permeability. The Weber thins considerably from the west where the the other four cores were taken, to the east where this core was cut. However, the extremely low permeability in this core is somewhat misleading in that it was cut through a tight sandstone; a more porous zone containing about 40 feet of sand exists higher in the section.

| Weber Cores | | | | | Porosity % | | Permeability (md) | |
|-----------------|---------------------|-------------------|---------------------------|----------------|------------|--------|-------------------|--------|
| API Number | Location | Top of Weber (MD) | Dist. from RMCCS State #1 | No. of Samples | Average | Median | Average | Median |
| 05-081-06621*** | NW SW NW 20-5N-91W | 8300 | 4 mi SW | 17 | 2.9 | 2.2 | .04 | .01 |
| 05-081-06340 | NW NW 12-3N-104W | 9303 | 77 mi WSW | 31 | 9.4 | 8.8 | 2.6 | 0.24 |
| 05-103-09287 | NW NW SE 17-1N-100W | 9968 | 61 mi SW | 25 | 3.7 | 2.9 | 0.08 | 0.02 |
| 05-103-09262 | NE SE 1-2N-93W | 7661 | 69 mi SW | 26 | 8.0 | 7.5 | 0.75 | 0.23 |
| 05-103-08021 | NE SE 31-2N-101W | 6160 | 67 mi SW | 257 | 7.1 | 6.1 | 1.3 | 0.1 |
| All 5 Cores | | | | 356 | 6.9 | 6.15 | 1.3 | 0.1 |

Table 4.4: Porosity and permeability data from COGCC public records.

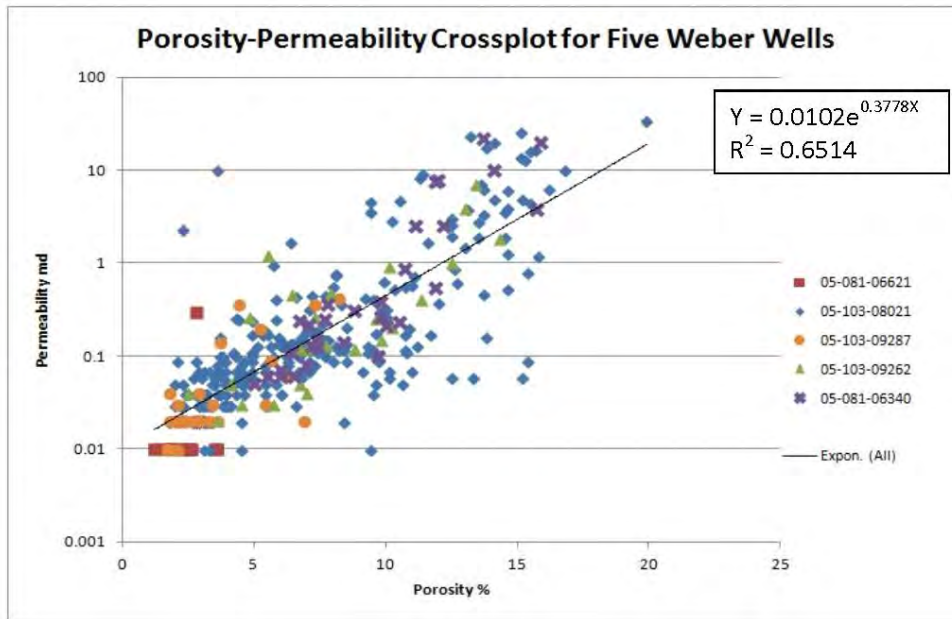


Figure 4.10: Cross-plot of permeability/porosity for 356 Weber samples.

5. Stratigraphic well drilling and coring

Pre-Drilling Activity Drilling Plan

The drilling of any well begins a minimum of six months prior to spudding, or initiating drilling operations. The approximate well location, projected depth of the target and the overall objectives of the well are required to begin planning. In the case of the RMCCS well there were two potential locations under consideration, both approximately 5 miles south of the town of Craig, Colorado in Moffat County. The deepest target formation was the Weber Sandstone with an estimated depth of 7,500 Ft, based on the best estimated available data at the time the project management plan was submitted in January 2010. The immediate area surrounding the potential locations were sparsely drilled and so this well would generally be referred to as a “Wildcat” well due to the lack of key data. The primary objectives were to: obtain full-bore core in three injection zones of interest and their respective sealing formations, obtain a full suite of geophysical well logs, and construct a well following current Department of Energy NETL best practices.

From this basic information a well budget, generally referred to in the oil and gas industry as an Authorization for Expenditure (AFE) was generated. Drilling bit records in the general area were analyzed to estimate drilling times, quotes obtained for all key costs elements, and drilling contractors meeting the selection criteria interviewed. For the RMCCS well the initial drilling contractor selected was Nabors Drilling in Q1 2011. In the RMCCS project there were two overriding external influences impacting the critical component surrounding securing a top tier drilling contractor. The first was a significant increase in drilling costs compared to estimates from 2010

when the project budget was developed and approved. This was primarily due to a historic boom in shale oil activity in North Dakota attracting a significant number of rigs from the Rocky Mountain region. This included Nabors Drilling which moved the rig selected to drill the RMCCS well from Colorado to ND. The second was the reluctance of the remaining drilling contractors in the area surrounding our location to mobilize a large distance to drill one well. After a prolonged search consuming all of Q3 2011, Patterson 166 was selected to drill the RMCCS well.

The final pre-drilling component was the selection of the actual drill site. Two viable sites were identified meeting all project criteria. The first was in Township 6N, Range 91W, a state section in Moffat County within the boundaries of Trapper Mine. Project partner, Tri-State Generation and Transmission, is a majority owner of Trapper Mining Company. The second location was in Township 5N, Range 90W, also a state section.

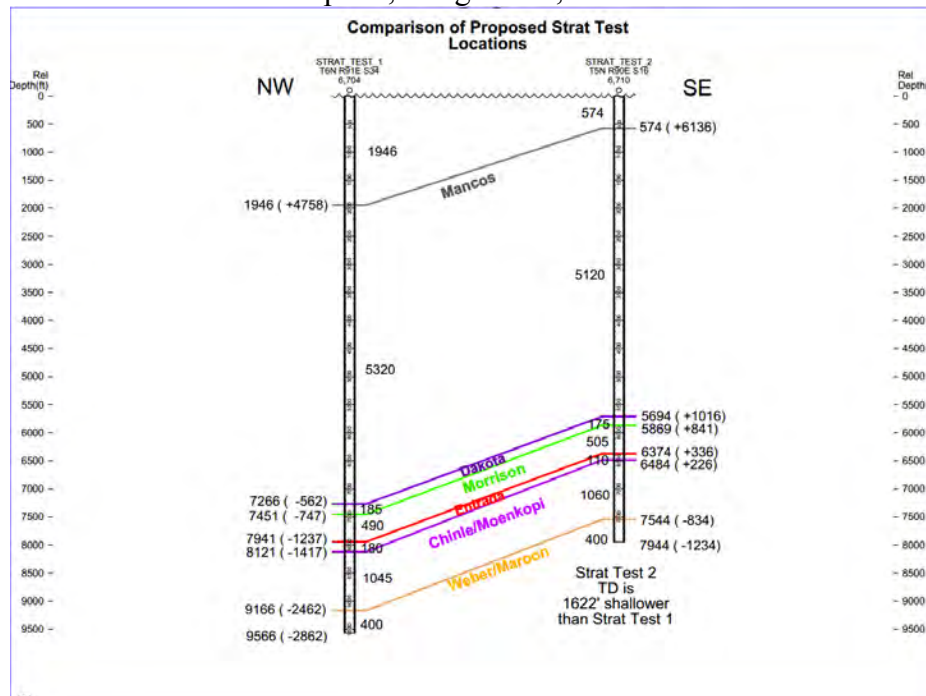


Figure 5.1: Cross-section with two potential drill sites

The second location had the advantage of a lower ground elevation that would reduce drilling cost, was not within the boundaries of an operating mine that added significant additional drilling safety regulations and rig access complexities. On the negative side, the location was long and narrow significantly increasing pad construction cost, was directly adjacent to a county road increasing public safety risk and was located on a drainage watershed that would make permitting more difficult and dramatically increase environmental risk and the cost of drilling insurance. The Trapper Mine site had the advantage of a large, flat surface area, low pad construction costs, proximity to the Craig Station power plant (for possible future sequestration demonstration) and very low environmental risk. After careful consideration by the RMCCS technical team, the Trapper site was selected. With all key pre-drilling decisions complete the well plan was developed. On November 10 and 11 representatives from all project partners and sub-contractors met to review the drilling plan in detail in what is referred to as a drill the well on paper (DWOP) workshop. The workshop was held in Ft Lupton, Colorado and each step of the drilling plan was reviewed and evaluated.



Figure 5.2: Drill Well On Paper workshop, Ft. Lupton, CO.

Pre-Drilling Risk Mitigation

Prior to initiating drilling operations a number of steps were taken to reduce risks associated with field activity. The first step was creating what is commonly referred to as a “Bridging Document”. This is a single document that combines the safety procedures for each of the primary organizations involved in the drilling operations. In the case of the RMCCS project this included Schlumberger, Patterson Drilling and Trapper Mining. A representative from each organization met and reviewed each organization’s respective safety programs and policies. A comprehensive unified document was prepared and in cases of conflicting requirements, the more stringent was always used. Once the final document was compiled, each organization signed off on the document signifying this was the safety document that all parties involved in field operations would adhere.

The second risk mitigation step was performing a drilling risk assessment. In the risk assessment, a team of drilling experts reviewed the operation, identified the potential risks and ranked them for likelihood and severity. Each identified risk outside of safe operating conditions was treated with a mitigation plan until it fell within safe operating levels. The highest identified risk was site access within the boundaries of the mine by the numerous subcontractors involved in drilling operations. To reduce this risk to a minimum a full time on-site Safety Supervisor was added to the project during field activity. The Safety Supervisor had extensive oilfield experience, was a trained Paramedic and a certified Mining Safety and Health Administration (MSHA) instructor. From the beginning of field activity to the end the safety supervisor was on duty twenty-four hours a day, seven days a week. The safety supervisor performed MSHA training for every subcontractor entering the mine for access to the drill site, escorted traffic on and off the site, conducted twice daily safety meeting with rig crew, safety meetings with each subcontractor prior to any operation, maintained safety statistics, acted on hazard identification efforts by field crews and generally managed all aspects of safety during the entire field operation. The results were zero safety incidents, including not even minor incidents, for the entire project. There were 293 individuals trained in MSHA site training and 19,426 man-hours worked without incident. This performance is outstanding and well outside the norm in even the best of circumstances.

The third risk mitigation step was to develop a plan to assure Mining Safety and Health Administration (MSHA) compliance throughout all field operations within the boundaries of the mine. Oilfield drilling operations are generally regulated by the Occupational Safety and Health

Administration (OSHA) and drilling contractors and all drilling service providers are organized to maintain compliance to OSHA regulations. However, all activities within the boundaries of an operating mine are regulated by MSHA. MSHA compliance standards are generally much more stringent and comprehensive than OSHA. Additionally, significant violations or repeated minor violations of MSHA regulations by RMCCS project subcontractors would potentially have devastating consequences for the project host, Trapper Mining. Therefore, every effort was made to fully comply with MSHA requirements. Numerous meetings were conducted with the MSHA field superintendent in Craig, Colorado and with Trapper Mining safety engineers to develop the compliance plan. Once the plan was completed a meeting was held in the MSHA Division office in Denver, including Schlumberger, Patterson and Trapper representatives, to review the plan in detail. The RMCCS MSHA Safety compliance plan was approved on December 1, 2011. An additional step was to have an MSHA certified inspector visit the selected rig, November 28, 2011, on location in Wyoming while it was drilling for another operator. The inspector identified modifications to be made to the rig to bring it within compliance to MSHA regulations.

An important lesson learned was to attempt to secure permission from the operator of the well the rig was drilling for, to complete as many the modifications while on this location. Four days at a daily rate of \$19,000 per day were used after rigging up on the RMCCS site making the necessary modifications. Overall, this MSHA compliance risk mitigation effort was also a motivating factor in having a dedicated safety engineer on site with MSHA certification. Overall, the MSHA compliance plan was extremely effective and there were zero MSHA citations for any project partner, service provider or subcontractor for the entire project.

Discussion and Key Learning's Drilling Under MSHA Oversight

Drilling a well for deep geologic storage draws heavily on people, equipment and expertise from the oil and gas industry. Safety for drilling rigs and operations in the oil and gas industry are generally regulated by the Occupational Safety and Health Administration (OSHA). Consequently, drilling rigs and procedures are constructed for compliance with OSHA rules and guidance. The RMCCS well was drilled within the boundaries of an operating coal mine and thus, under the oversight of the Mining Safety and Health Administration, or MSHA. Many coal-fired power plants are situated in close proximity to the mines supplying the coal reducing the cost of transporting the coal to the plant. Since CO₂ transportation is a major cost component for geologic storage as well, having injection wells placed within the boundaries of a mine will not be uncommon. For this reason, the lessons learned by drilling the RMCCS State No. 1 within the boundaries of the Trapper Mine will be valuable for future operations. Many of the issues surrounding site access, rig worker certification and transportation to and from the site have been discussed. However, conducting drilling operations with a drilling rig and rig crews under MSHA oversight, rather than OSHA, had considerable impact on the cost of drilling the RMCCS well. This impact was due almost exclusively to modifications necessary to the rig and drill pad living quarters to make them compliant with MSHA regulations.

To proactively assess the condition of the rig we were to use for drilling the RMCCS well, we contacted the drilling company and the operator of the well they were drilling for and obtained permission to have an MSHA inspector visit the rig. On November 28, 2011 the unofficial inspection was conducted by an MSHA certified electrician. None of the observations were considered serious and it was estimated that it would take minimal time to bring the rig into compliance. A local MSHA certified electrician in the Craig, Colorado area was identified and secured to begin preparing the rig for MSHA certification once it arrived at the RMCCS

site.

On January 3rd, the rig was released by the operator of the preceding well and by January 7 the entire rig was at the location. Rig up activity took an additional three days and under normal conditions, the rig would have been ready to begin drilling on January 10. However, it would take another five days to get the rig operational and fully compliant with Mining Safety and Health Administration (MSHA) regulations. The difficulty was in complying with Federal Metal and Nonmetallic Mine Training, Safety & Health Standards CFR 30 Section II, subpart K.12001 – K.12038 related to electrical overload protection, conductors, distribution boxes and grounding. The time and effort to bring the rig and living quarters to compliance was much greater than anticipated. It is important to note that it is not the electrician hourly wages and material cost that impacted the project budget. It is the fact the once the rig is functionally ready to commence drilling operations the rig goes on “Day Rate” or begins charging a daily sum as specified by the drilling contract. In the case of the RMCCS well, the negotiated day rate was \$19,000 per day. Additionally, all daily rental fees associated with living quarters, rental tools and expendables increased the daily cost to \$27,950 per day. Consequently, the 5 day cost of bringing the rig into MSHA compliance was \$139,750.

✚ *When drilling a well for geologic storage under MSHA regulations, make every attempt to have the rig pass an inspection by MSHA prior to taking possession of the rig.*

For future drilling operations within the jurisdiction of MSHA guidelines, there are three potential actions to mitigate the cost of bringing compliance of a drilling rig generally operating under OSHA regulations up to the much more stringent MSHA standards. The first is to attempt to secure a rig that has already been made MSHA compliant. The second is to attempt to gain a waiver from the MSHA District Superintendent from MSHA oversight. In the case of the RMCCS well a partial waiver was obtained in regard to training of the rig workers, but not to drilling operations oversight. There is a potential pathway to obtaining a waiver that should be rigorously pursued. There is a “Memorandum of Understanding” between OSHA and MSHA that allows oversight by OSHA within specific areas within the boundaries of the mining operation under certain circumstances. This avenue was pursued in the RMCCS project but a waiver not granted. The third option is to attempt to gain access to the rig while it is either idle or “stacked”, or obtain permission to work on the rig while drilling for another operator, bringing the rig into compliance without being subject to the rig and associated day rate.

Coring Operations

In most drilling applications there are nearby wells penetrating the same formations providing an accurate geologic cross-section allowing the well-site geologist to make an accurate estimation of the depth that equivalent formation to be encountered in the well being drilled. In these cases, if a particular formation is to be cored, the well-site geologist can determine the point at which the drilling of the desired formation is imminent and at what point to pull the drill bit out of the well-bore and re-enter with the coring assembly. The general objective for coring in the RMCCS project was to attempt to obtain full diameter core (4”) from the bottom of the sealing formation and into the top of each of the three potential storage targets. Three target seal combinations are: Mowry Shale / Dakota Sandstone, Curtis Shale / Entrada Sandstone, Phosphoria / Weber Sandstone. The plan was to attempt to core through the contact interface between each seal/injection formation pair. In the case of typical coring operations there is a single formation that core is to be obtained in each coring run. In this instance, the geologist observes drill cuttings to watch for evidence that the bit is penetrating the desired formation. To core through the interface between two formations, the geologist must have an accurate prediction of the thickness of the first formation to be able to predict at what point the core bit will approach the top of the interface.

If the first interval is thinner than predicted the drill bit could unexpectedly pass all the way through the interface. If the first formation is thicker than predicted and the coring begins too soon, it is possible to fill the 90' core barrel with the first (sealing) formation, thus requiring adding a second core run to continue into the target injection formation. At depths typical to geologic storage, it takes from eight to sixteen hours to pull out of the well with a core barrel, retrieve the core, and go back into the well to either resume drilling or resume coring. Therefore, picking the core point too early or too late can have significant impact on the scientific objectives of the well, or significantly increase drilling cost.



Figure 5.7 – Core obtained from the RMCCS Well.

In areas where there are few nearby well penetrations, such as the case for the RMCCS well, it is difficult to predict the relative thickness and depth at which the bit will penetrate the intervals to be cored. Matching drill cuttings to well correlations to distant wells resulted in too much uncertainty for predicting proper core points. It was decided to add a gamma ray measurement to the bottom hole drilling assembly. Having a more precise depth correlation and a measurement that could be compared to similar measurements in the correlation wells dramatically improved the confidence in the depth of the drill bit in relation to the geologic structure and the desired intervals to core. Therefore, it is highly recommended to add a gamma ray measurement, at a minimum, to the drilling assembly, if full core is to be obtained in a well without nearby wells (within one to three miles). Additional measurements, such as resistivity and porosity, can be added to further reduce uncertainty, if the budget allows.

Managing Drilling Cost

The single largest budget component for the entire RMCCS project was the cost to drill the characterization well. The primary objective in drilling the well was obtaining the site specific data necessary to complete the scientific objectives of the project. This data includes geophysical well logs and full core to permit detailed characterization of the injectivity and capacity of the Dakota, Entrada and Weber formations, and their respective sealing formations. However, the lessons learned in performing the drilling and coring operations provide additional significant benefits to further the development of best practice documentation by the NETL and providing a significant economic impact to the local economies.

The initial drilling budget was developed in the spring of 2009 for the original grant proposal. At the time, rig availability, drilling supplies, third-party contractors, trucking, tubulars and all of the costs associated with drilling, were generally plentiful. The estimated well total depth was estimated at 7,500' and not for a specific site, but was thought to be a representative depth for the general area. Furthermore, the cost estimate was based on typical drilling practices and bit records gleaned from oil and gas development wells were from the Piceance Basin to the south, where the vast majority of drilling activity in NW Colorado was underway. The

development of the drilling budget started by defining a percentage of the available funding, the available cost share and was distributed proportionally by the cost expectations of completing all of the proposal tasks. Consequently, the drilling budget started at roughly one-third of the total project budget. The original drilling budget dated July 31, 2009 was \$1,005,302. The final AFE amount, prior to drilling, with an expanded Niobrara coring program and projected total depth of 10,380' was \$4,119,721. The final actual drilling cost was \$4,666,757 with an actual total depth of 9,745'.

There were several categories of drilling expenditures significantly higher than the initial drilling budget (AFE). The "Preparation and Termination" category exceeded the budget by \$106,312. The majority of the overages within this category are directly attributable to the additional expense of bringing the rig and location within MSHA regulation requirements. Alterations of the well pad, camp facilities, and electrical work and rig costs associated with approximately four days of extended rig up were all required to pass inspections and meet the MSHA standards.

A second area of significant overage are related to the loss circulation encountered in drilling the surface section prior to setting the intermediate protection casing at 5,340'. Lost circulation occurs when the pressure exerted by the column of drilling fluid encounters open fractures, extremely permeable formations or rock layers with pore pressures much less than hydrostatic. The weight of the drilling fluid must be maintained to prevent the potential for blowout. Drilling through multiple coal layers within the surface strata made the potential of a blowout caused by drilling into trapped accumulations of methane a significant project risk. However, the rock formations in this interval were not able to support the slight overbalance in the mud weight and consequently, thousands of gallons of excess water and drilling fluid materials had to be trucked in on a continual basis until casing was cemented in place to prevent the lost circulation. The impact on the drilling costs were \$93,190 in additional "Mud Chemical and Engineering Services" and \$62,363 in Water.

A third category of drilling cost exceeding the budget is directly related to the drilling environment. The toughness of the rock layers is higher than expected, lowering bit efficiency and resulting in the utilization of additional bits, both for drilling and coring. The expense for "Bits, Reamers and Coreheads" exceeded the budget by \$85,649. The well also exhibited a tendency to drift to the south due to formation dip. The drilling manager felt it was critical to maintain a deviation from vertical less than 10 degrees, and ideally less than 3 degrees. This was to assure the successful retrieval of core barrels and reduce the risk of sticking the logging tools. To combat the well deviation and the development of doglegs in the well trajectory, directional drilling capabilities were added to the bottom-hole assembly (BHA). Later, a gamma ray tool was also added to the BHA to help the wellsite geologist correlate the well to distant offset well control to aid in picking core points. Both of these additions to the BHA resulted in \$260,616 to the drilling costs above the budget.

In addition to the drilling related cost overages described, there was \$209,771 in additional "General" expenses directly attributable to cost inflation experience in the period between preparing the drilling budget (2010-2011) and the beginning of 2012. The cost inflation was a result of a rapid drain of available service capacity driven by an historic boom in activity in North Dakota with the success of drilling efforts in the Bakken Oil Shale. The final drilling expenditures exceeded the budget by \$545,771 (13%) necessitating the curtailing of the core plan and abandoning the attempt to drill to the deepest formation of interest, the Weber Sandstone. To cover the additional drilling costs \$90,000 were moved from the regional characterization budget of the state geological surveys and Shell provided an additional \$507,000 in cost share to allow

drilling to continue and to preserve logging a full and comprehensive wireline logging suite to augment the full core in developing the site specific characterization project task.

✚ *Exercise caution in basing drilling cost estimates on nearby oilfield experience.*

There are several cost efficiencies built into drilling expenditures in the oil and gas industries providing an important analog for drilling wells for geologic storage. However, it is important to consider unique differences that may impact drilling costs. The majority of wells drilled for oil and gas development are in areas where a great number of wells have been drilled previously and a particular drilling technique is more fully optimized. Additionally, it is common practice to add 10% - 15% to the estimated drilling expense (AFE) to cover overages that are common, but difficult to anticipate in what category the overages may occur. Very seldom does every cost group fall within the AFE amount in normal oil and gas drilling activities, even in mature areas. Periodically there will be an extreme overage, as much as 100% or more of the AFE cost, and is absorbed within the long term asset budget not tied to an individual well budget. A relevant example is the well drilled by the Patterson 166 just prior to moving to the RMCCS well. The operator encountered unanticipated drilling hazards that increased total drilling time from the original 30 day estimate to 65 days, increasing the drilling cost by an estimated 80% and delaying the start of the RMCCS well.

✚ *Well construction for Geologic Storage has lower risk acceptance than drilling for oil and gas and extra drilling methods need to be used to mitigate risk to as low as reasonably possible.*

Oil and gas exploration and production is a high risk – high reward activity. Typical rate of return on expenditures is generally over 25%, even with below average commodity prices. Consequently, operators have the ability to absorb significant, unexpected costs. Commercial operations engaging in industries producing anthropogenic CO₂ often operate at lower margins or have margins regulated and have a much lower risk tolerance. Additionally, for geologic storage in a saline reservoir, there are few surrounding wells to provide nearby drilling experience inherently increasing the risk. In the case of the RMCCS well, risk tolerance is also low, due to a fixed budget and high visibility associated with a publically funded demonstration project. In such cases it is prudent to perform a thorough and complete risk assessment for the drilling operation and apply mitigation strategies to bring all identified risks within an acceptable range. It is often above and beyond what may be acceptable risk in oil and gas operations. For the RMCCS well, a risk assessment was initiated on June 24, 2011 and completed, presented and approved on July 7, 2011. Some of the significant mitigation strategies employed in the RMCCS project included: securing a high performing rig and crew with local drilling experience, utilizing a rig with greater than 200 ton hook capacity to minimize the risk of sticking the bottom hole drilling assembly, a sub-structure to accommodate the required Blow-Out-Preventer, maintaining well deviation below 3 degrees, twenty-four hour on-site safety supervision, setting an intermediate casing string above intervals to be cored, close engagement with district and local MSHA managers and Trapper Mine managers.

✚ *Well construction costs can be quite volatile for intervals as short as six months. The volatility is tied to oil price, and to a lesser extent, the price for natural gas. The impact on well construction is compounded if the site is greater than 50 miles from centers of oilfield activity, which is often the case for geologic storage into saline aquifers.*

The cost of drilling rigs and services is closely tied to rig utilization, which is in turn closely tied to the price of oil and gas. The fleet of available drilling rigs and skilled personnel is relatively stable for periods of two to three years. This is due to the cost to build new rigs and infrastructure cost required to increase service availability limits the ability to match supply with

demand. Conversely, a drop in oil prices results in a reduction in drilling activity and an accompanying drop in rig costs. The variability goes beyond daily drilling rates, but extend to contract terms as well. When rig availability is high, rig owners are willing to negotiate contract terms potentially extending to offering turnkey contracts where the driller agrees to reach a specified depth for a fixed price and often absorb some or all of the cost to mobilize and demobilize to the drill site. A turnkey contract significantly reduces drilling risk for the well operator. When rig availability is tight, drillers generally adhere to general contract terms outlined by the International Association of Drilling Contractors, or IADC. The general terms of a standard IADC specify a day rate for the rig, pass all mobilization costs, possibly de-mobilization costs and place virtually all risk associated with the drilling operations on the well operator. In the case of tight rig availability, the effect on geologic storage into saline aquifers can be compounded. Many potential sites for saline aquifer storage are in areas remote from concentrated oil and gas activity. Any distance greater than 50 miles from centers of oilfield activity place additional burdens on well construction costs. The cost of rig mobilization, fuel, casing, wellheads, etc., are directly related to distance from the service center. At the time of the drilling of the RMCCS well (2012) the typical cost to move a rig was roughly \$1,000/mile. Additionally, the greater the distance a rig must move, the more reluctant a drilling contractor is to leave a particular area because the day rate only applies when the rig is on site and operational; the drillers favoring multiwell contracts and short moves.

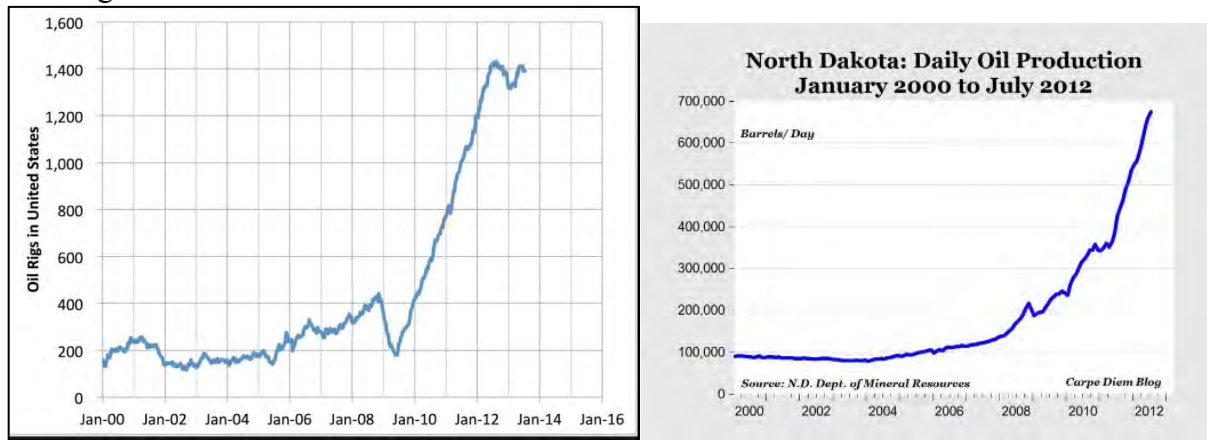


Figure 5.8 – Rig Utilization during RMCCS project primarily as a result of oil boom in North Dakota.

All of these factors related to rig utilization impacted the RMCCS project. At the time the original proposal and budget were being prepared in mid-2009, rig utilization was low as seen in figure 5.8. At this time, rig day rates were moderate, service costs low and drilling contractors willing to consider favorable contract terms. At that time, Nabors drilling was identified as the best option and the drilling budget was based on prevailing costs at that time. By the time the project schedule was ready for the well in mid-2011 the landscape had experienced dramatic change. An increase in oil prices, coupled with technical success in applying new hydraulic fracturing technology in the Williston Basin of North Dakota had initiated a boom in activity there of historic proportions. This initiated a drain in rig capacity, skilled personnel and services in NW Colorado to North Dakota. This included Nabors moving our designated rig there. Additionally, the remaining rigs in NW Colorado were generally engaged in long-term, multi-well projects in the Piceance Basin 50 miles to the south of Craig. It took many months to find a drilling rig willing to mobilize to Craig, Colorado to drill the RMCCS well. Fortunately, by September of 2011, we were able to come to contract terms with Patterson Drilling rig 166. The impact of the

volatility of drilling costs within the oil and gas industry was evident with the RMCCS project. When drilling actually began in January 2013, the drilling spread rate, or total daily costs for well drilling, had nearly doubled from \$37,500 in 2009 to \$71,000 in 2012.

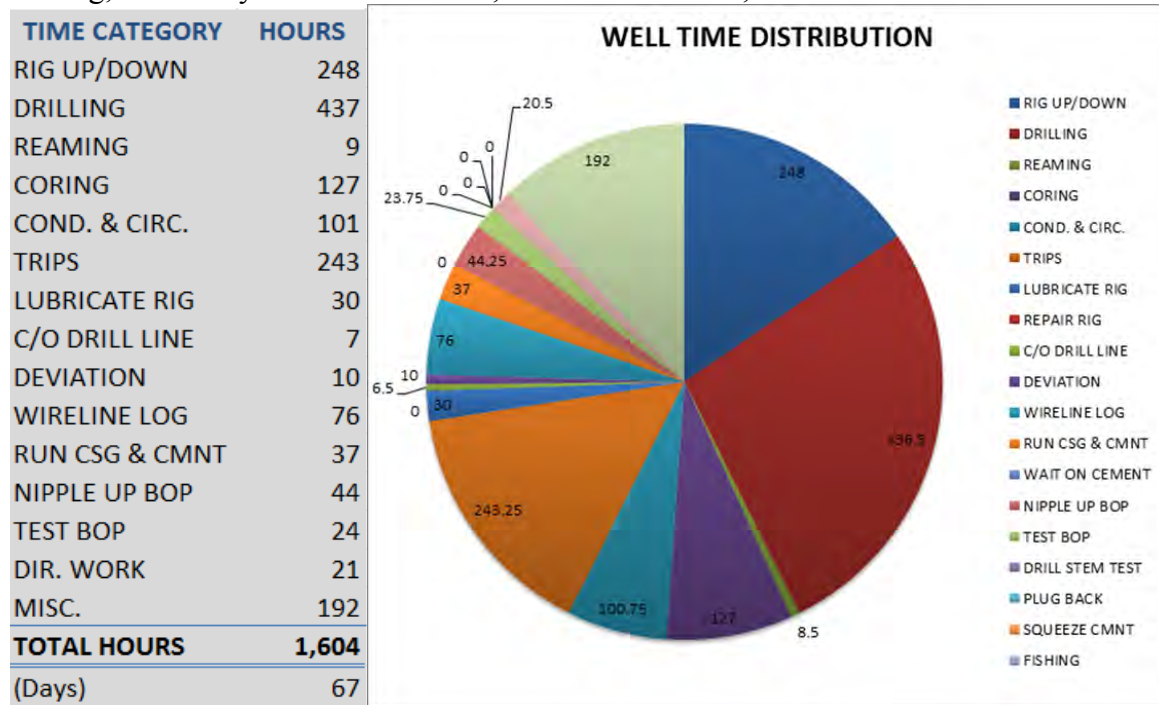


Figure 5.9 – Cost element distribution by hours.

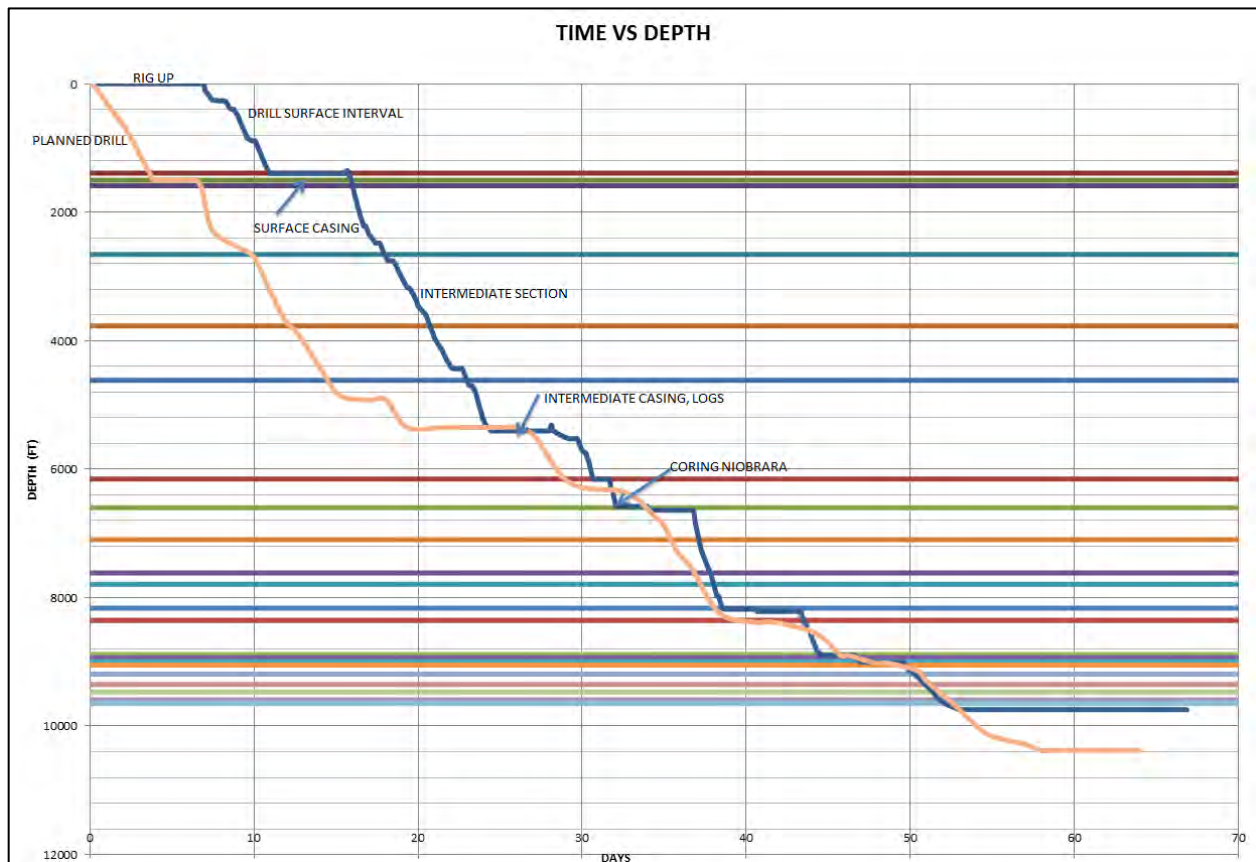


Figure 5.10 – Drilling time, projected VS actual.

- ✚ *Well construction with a fixed budget requires additional cost tracking methods beyond what is normally employed in oil and gas operations where reserve funding is readily available with approval by asset management.*

In normal oil and gas drilling operations a drilling budget, or AFE, is developed prior to initiating drilling. A contingency item of 10%-15% is included as a line item in virtually all cases. Cumulative daily costs are distributed each morning. If drilling costs are exceeding the AFE amount, the partners are contacted and if approved, additional funds are made available. In rare instances, the decision is made to stop at an intermediate point and abandon the original objective. Although projecting the final cost as drilling in progress, it is seldom rigorously done.

In the case of many scientific projects, the overall budget is fixed and cannot be exceeded. This was the case with the RMCCS well. Although there is the ability to change scope and move budget dollars between tasks, drilling expenses can escalate quickly and overwhelm a project's ability to absorb overages. Therefore, continually projecting the total costs forward to completion in drilling a well with a fixed budget is critical. Costs associated with drilling operations are in three categories: time driven, episodic and depth driven.

Time driven costs include the rig day rate, rental tools and equipment, fuel, trailers, and supervision. All combined these costs are referred to as the spread rate. The spread rate for the RMCCS well was approximately \$71,000 per day. During drilling the time driven costs remaining are computed by the penetration rate times the thickness of the remaining formations, plus number of bit trips times average trip time, plus logging time, plus completion time and rig down time. Time driven costs are the dominant costs determining the

Episodic costs include running casing, running geophysical well logs, well completion or plug and abandonment, rig demobilization, site restoration and reclamation.

Depth driven costs generally become components of the time driven costs and episodic costs. For example, the time it takes to come out of the hole to change drill bits and go back to bottom to resume drilling (referred to as trip time) is a function of depth. The cost to run casing is a function of depth based on the number of joints of casing required. The cost of geophysical well logs has a depth component.

For the RMCCS well the estimated cost going forward using this methodology was computed daily and provided to project partners. This allowed "what-if" scenarios to be calculated to continually adjust scope to assure there would be remaining budget to finalize all necessary work all the way through to rig demobilization and site restoration. It was using this methodology that the determination was made that there would be insufficient remaining funds to drill to the ultimate objective of 200' below the top of the Weber formation. This resulted in achieving most of the scientific objectives of the well while finishing all well related work without exceeding the available budget.

Conclusion

The drilling of the RMCCS State No. 1 well provided an abundance of critical site-specific scientific data. This data is the foundation for developing a detailed geologic description of the Dakota and Entrada formations, two of the primary targets for potential future geologic storage, and their respective sealing formations. Equally important is the operational experience, lessons learned and recommended best practices gathered through the drilling operations.

6. Core analysis and interpretation with other geological and geophysical data

Core Sampling and Inventory

Due to technical and budgetary issues related to drilling, coring and core recovery, as described in previous sections, only 131 feet of RMCCS core was obtained for the project. Initial plans for the project called for 780 feet of core, from the Dakota, Entrada and Weber sandstones, and their associated seals: the Mowry, Curtis and Moenkopi shales, respectively. Sub-cores (plugs) of these three formations and their seals were to provide a comprehensive evaluation of the capacity, injectivity and seal integrity of the most promising CO₂ sequestration targets on the Colorado Plateau. The 131 feet of core obtained only included the Mowry, Curtis and Entrada Formations. However, several downhole trips with a rotary sidewall coring tool were able to obtain small plugs of the Carlile, Frontier, Dakota, Morrison, Curtis (Sand), Entrada, Chinle, Shinarump and Moenkopi Formations.

Plug Acquisition

The full diameter core was transferred from the RMCCS drill site to CoreLab of Denver for acquisition of sub-core/plugs. Based on in-person consultations from Rich Esser, Tony Rice, Chris Eisinger and Dave Noe after viewing the core, sample points (n=537, including “duplicates”) along the 131 feet of core were chosen. The RMCCS team elected to plug the core prior to slabbing to maximize sample size and recovery. It was also decided to plug the shale core (Mowry and Curtis) at 1.0 inches in diameter and the Entrada core and 1.5 inches in diameter in an effort to maximize recovery of coherent plugs. The three principle orientations (horizontal, vertical and 45°, relative to the axis of the core) were selected throughout the cored section to assess anisotropy of the analytical data. Where the full diameter core was deemed sufficiently coherent, multiples from a single location (i.e. immediately adjacent location) were attempted to accommodate duplicate analyses for QA/QC purposes. Table 6.1 shows the plug locations, orientations and multiples requested by the RMCCS team.

In the interest of posterity and/or any petrophysical tests requiring larger diameter core, a 21-inch section of the RMCCS core from the Entrada Formation was spared from plugging and slabbing activities. The unadulterated, full diameter (4.0 inch) core spans from 9038 ft to 9039.75 ft. It is currently housed at the University of Utah.

Table 6.1. Requested plug attempts from RMCCS team to CoreLab. In some cases, multiples of a specific location were requested (x2, x3, x4) to accommodate duplicate analyses.

RMCCS Core plugging plan (based on observations from CoreLab visit of March 28, 2012)

| | | |
|---|-------|----------------------------|
| 1 inch diameter plugs (by at least two inches long) | Hor | - parallel to bedding |
| 1.5 inch diameter plugs (by at least three inches long) | Vert | - perpendicular to bedding |
| | 45Deg | - 45° to bedding |

| Formation | Core | Box | Depth (in feet) | | | | | | | | | | | |
|----------------------------|------|-----|-----------------|-------------|-------------------|-------------|-------------|-------------|-------------|-------------|-------------|------------|------|--|
| | | | Hor1 | Vert1 | 45Deg1 | Hor2 | Vert2 | 45Deg2 | Hor3 | Vert3 | 45Deg3 | | | |
| Mowry (~8180-8206 ft) | 1 | 1 | | 8180 | | | | | | | | | | |
| | 1 | 2 | | | | | | | | | | | | |
| | 1 | 3 | 8187 | 8187 | 8187 ¹ | 8187.6 | 8187.6 | | | | | | | |
| | 1 | 4 | | 8189.4 | | 8191.7 | 8191.7 | 8191.7 | | | | | | |
| | 1 | 5 | 8192 | 8192 | 8192 | 8194.4 | 8194.4 | 8194.4 | | | | | | |
| | 1 | 6 | 8195 | 8195 | ary 1 | 8197 | 8197 | | | | | | | |
| | 1 | 7 | 8198 | 8198 | 8198 | 8199 | 8199 | | | | | | | |
| | 1 | 8 | 8201 (x2) | 8201 (x2) | 8201 (x2) | 8203 | 8203 | | | | | | | |
| | 1 | 9 | 8204 (x2) | 8204 (x2) | 8205 | 8206 | 8206 | | | | | | | |
| | 1 | 10 | 8206 | 8206 | 8206 | | | | | | | | | |
| Mowry (~8216-8261 ft) | 2 | 1 | 8216 (x2) | 8216 (x2) | 8216 (x2) | 8217 (x2) | 8217 (x2) | 8217 (x2) | 8218 | 8218 | | | | |
| | 2 | 2 | 8219 | 8219 | 8219 | 8221 (x2) | 8221 (x2) | 8221 (x2) | | | | | | |
| | 2 | 3 | 8223 (x2) | 8223 (x2) | 8223 (x2) | | | | | | | | | |
| | 2 | 4 | 8226.8 | 8226.8 | 8226.8 | 8227.6 | 8227.6 | | | | | | | |
| | 2 | 5 | 8228.9 | 8228.9 | 8228.9 | 8230.9 | 8230.4 | | | | | | | |
| | 2 | 6 | 8233 (x2) | 8233 (x2) | 8233 (x2) | | | | | | | | | |
| | 2 | 7 | 8235 | 8235 | 8235 | 8236 | 8236 | | | | | | | |
| | 2 | 8 | 8238 | 8238 | | 8240 | 8240 | 8240 | | | | | | |
| | 2 | 9 | 8241.9 | 8241.9 | 8241.9 | 8243 (x2) | 8243 (x2) | 8243 | | | | | | |
| | 2 | 10 | 8244 | 8244 | 8244 | 8245 | 8245 | | 8246 | 8246 | 8246 | | | |
| | 2 | 11 | 8246.8 | 8246.8 | 8246.8 | 8249.6 | 8249.6 | | | | | | | |
| | 2 | 12 | 8250 | 8250 | 8250 | 8251 | 8251 | | | | | | | |
| | 2 | 13 | 8253.4 | 8253.4 | 8253.4 | 8254.5 | 8254.5 | 8254.5 | | | | | | |
| | 2 | 14 | 8255.5 | 8255.5 | 8255.5 | 8258 | 8258 | 8258 | | | | | | |
| | 2 | 15 | 8259.5 | 8259.5 | 8259.5 | 8260.6 | 8260.6 | 8260.6 | | | | | | |
| Curtis (~8896-8924 ft) | 3 | 1 | 8896 | 8896 | | 8897.2 | 8897.2 | 8897.2 | | | | | | |
| | 3 | 2 | 8898.5 | 8898.5 | | 8900.5 | 8900.5 | | | | | | | |
| | 3 | 3 | 8902.5 | 8902.5 | | 8903.5 | 8903.5 | | | | | | | |
| | 3 | 4 | 8904 | 8904 | 8904 | 8905 | 8905 | | 8906 | 8906 | 8906 | | | |
| | 3 | 5 | 8907 | 8907 | | 8908 | 8908 | | | | | | | |
| | 3 | 6 | 8909 | | | 8910 | | | | | | | 8911 | |
| | 3 | 7 | 8911.8 | 8911.8 | | 8913 | 8913.4 | | 8914 | 8914 | 8914 | | 8914 | |
| | 3 | 8 | 8915 | 8915 | | 8916 | 8916 | 8916 | | | | | | |
| | 3 | 9 | 8918 | 8918 | | 8919.8 | 8919.8 | 8919.8 | | | | | | |
| | 3 | 10 | | | | | | | | | | | | |
| | 3 | 11 | 8924 | 8924 | | | | | | | | | | |
| Entrada (~9011-9046 ft) | 4 | 1 | 9011 (x4) | 9011 (x4) | 9011 (x3) | 9012 (x4) | 9012 (x4) | 9012 (x3) | 9013.5 (x4) | 9013.5 (x4) | 9013.5 (x3) | | | |
| | 4 | 2 | 9015 (x4) | 9015 (x4) | 9015 (x3) | 9016 (x4) | 9016 (x4) | 9016 (x3) | 9017 (x4) | 9017 (x4) | 9017 (x3) | | | |
| | 4 | 3 | 9017.5 (x3) | 9017.5 (x3) | 9017.5 (x3) | 9019.5 (x3) | 9019.5 (x3) | 9019.5 (x3) | | | | | | |
| | 4 | 4 | 9020.1 (x4) | 9020.1 (x4) | 9020.1 (x3) | 9021.2 (x4) | 9021.2 (x4) | 9021.2 (x3) | 9022.2 (x4) | 9022.2 (x4) | 9022.2 (x3) | | | |
| | 4 | 5 | 9023.2 (x4) | 9023.2 (x4) | 9023.2 (x3) | 9024 (x4) | 9024 (x4) | 9024 (x3) | 9025.2 (x4) | 9025.2 (x4) | 9025.2 (x3) | | | |
| | 4 | 6 | 9026 (x4) | 9026 (x4) | 9026 (x3) | 9027 (x4) | 9027 (x4) | 9027 (x3) | 9028 (x4) | 9028 (x4) | 9028 (x3) | | | |
| | 4 | 7 | 9029 (x4) | 9029 (x4) | 9029 (x3) | 9030 (x4) | 9030 (x4) | 9030 (x3) | 9031 (x4) | 9031 (x4) | 9031 (x3) | | | |
| | 4 | 8 | 9032 (x4) | 9032 (x4) | 9032 (x3) | 9033 (x4) | 9033 (x4) | 9033 (x3) | 9034 (x4) | 9034 (x4) | 9034 (x3) | | | |
| | 4 | 9 | 9035 (x4) | 9035 (x4) | 9035 (x3) | 9036 (x4) | 9036 (x4) | 9036 (x3) | 9037 (x4) | 9037 (x4) | 9037 (x3) | | | |
| | 4 | 10 | 9037.5 (x4) | 9037.5 (x4) | 9037.5 (x3) | | | | | | | | | |
| | 4 | 11 | 9040 (x4) | 9040 (x4) | 9040 (x3) | 9041 (x4) | 9041 (x4) | 9041 (x3) | 9042 (x4) | 9042 (x4) | 9042 (x3) | | | |
| | 4 | 12 | 9042.8 (x4) | 9042.8 (x4) | 9042.8 (x3) | 9043.7 (x4) | 9043.7 (x4) | 9043.7 (x3) | | | | | | |
| Total Count | | | 84 | 84 | 62 | 74 | 75 | 47 | 40 | 40 | 31 | 537 | | |

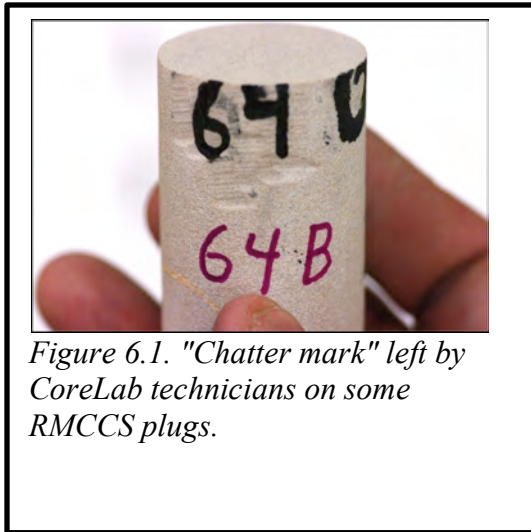


Figure 6.1. "Chatter mark" left by CoreLab technicians on some RMCCS plugs.

CoreLab technicians utilized a drill press with diamond coring tools and liquid nitrogen as a drilling lubricant to attempt to cut as many of the plugs at the orientations requested (some plugs in the Entrada were drilled with a salt water solution). Due to the fractured nature of the core, in particular the shale sections, only about 60% (313 out of 537 plugs) were considered a “good” recovery by CoreLab. The remaining plug points were either not attempted by CoreLab because of the poor quality of the core section, or the plug recovery was too poor to be useable/saved. However, of the 313 recovered plugs that were labeled “good” by CoreLab, only 183 were longer than 1 inch, a length sufficient for many of the petrophysical analyses that were going to be attempted by the project. CoreLab labeled most of the plugs as an “A” on their Core Quality Index (CQI – a visual description of core grain recovery based on core quality (e.g. shattering, fracture, mud invasion, etc) and core recovery size (i.e. length)) though some of the plugs exhibited “chatter marks” (Figure 6.1), where the core barrel left grooves around the plug leaving it generally unusable for petrophysical testing.

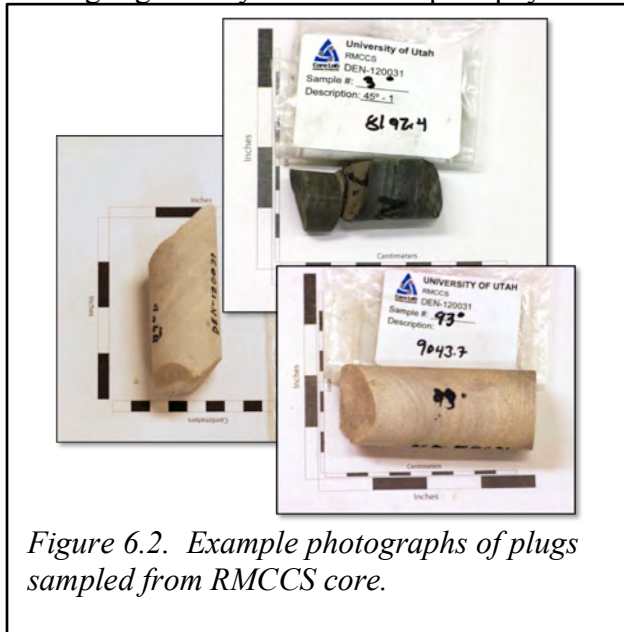


Figure 6.2. Example photographs of plugs sampled from RMCCS core.

The RMCCS plugs were wrapped in plastic and aluminum foil, to minimize significant dehydration, and shipped to the Energy & Geoscience Institute at the University of Utah. Each plug was unwrapped, inspected, measured and photographed (Figure 6.2). From this assessment, a matrix was constructed listing all available plugs, their core depth, formation of origin, size, orientation, length, CQI, extra notations and potential for various petrophysical tests. In general, it is preferable if plugs have a 2:1 length to diameter ratio, especially for geomechanics tests. The matrix visually identifies those samples adhering to this 2:1 ratio (green icons). Likewise, certain hydraulic tests ideally should have samples of a certain length (relative permeability tests should be at least 1.5” inches in length, but more accurate results are yielded when samples are at least 2 inches in length).

Table 6.2 shows an excerpt from the sample matrix.

Table 6.2. RMCCS sample matrix showing physical measurements and description of each plug sampled from the full core. Based on diameter, length and CQI, each plug received a grade potential for petrophysical tests. A green icon indicates sufficient material, a red icon indicates insufficient material, and a yellow icon indicates marginally sufficient material.

| Depth | Plug orientation | Plug No. | Formation | Size (inch diameter) | Max Size (inches) | Recovery Size | CQI | Petrophysical Test Potential | | | | | | | | |
|---------|------------------|----------|-----------|----------------------|-------------------|---------------|-----|------------------------------|-----|-------------|----------|--------------|---------------|----------------|----|--|
| | | | | | | | | MWD | SEM | Petrography | Porosity | Permeability | Relative Perm | Capillary Pres | | |
| 8188.17 | | | Mowry | | | | | | | | NMT | | | | | |
| 8188.92 | | | Mowry | | | | | | | | NMT | | | | | |
| 8191.6 | Hor | | Mowry | 1.0 | | | | | | | | | | | | |
| 8191.65 | Vert | 2V | Mowry | 1.0 | 0.2 | 1 | D | | | | | | | | | |
| 8191.65 | Vert | 2VB | Mowry | 1.0 | 1.1 | 4 | B | | | | TT | TT | | | | |
| 8191.85 | 45° | 2'B | Mowry | 1.0 | 1.3 | 4 | B | | | | | | | | | |
| 8192 | Hor | 3H | Mowry | 1.0 | 1.0 | 3 | B | | | | TT | TT | | | | |
| 8192.1 | Vert | 3V | Mowry | 1.0 | 0.9 | 3 | A | | | | | | | | | |
| 8192.4 | 45° | 3* | Mowry | 1.0 | 0.8 | 3 | C | NMT | | | | | | | | |
| 8193.5 | | | Mowry | | | | | | | | NMT | | | | | |
| 8194.4 | Hor | 3HB | Mowry | 1.0 | 1.1 | 4 | B | | | | | | | | | |
| 8195.1 | Hor | 4H | Mowry | 1.0 | NR | | D | | | | | | | | | |
| 8195.1 | Vert | 4V | Mowry | 1.0 | 0.3 | 1 | D | | | | | | | | | |
| 8195.65 | 45° | 4* | Mowry | 1.0 | NR | | D | | | | | | | | | |
| 8197.3 | Hor | 4HB | Mowry | 1.0 | 0.2 | 1 | C | | | | | | | | | |
| 8197.67 | | | Mowry | | | | | | | | NMT | | | | | |
| 8198.1 | Hor | 5H | Mowry | 1.0 | NR | | D | NMT | | | | | | | | |
| 8198.15 | Vert | 5V | Mowry | 1.0 | 0.7 | 3 | C | | | | | | | | | |
| 8199.45 | Hor | 5HB | Mowry | 1.0 | 1.6 | 4 | B | | | | | | | | | |
| 8199.45 | Vert | 5VB | Mowry | 1.0 | NR | | D | | | | | | | | | |
| 8200.5 | Hor | 7HA | Mowry | 1.0 | NR | | C | | | | | | | | | |
| 8200.6 | Hor | 7HB | Mowry | 1.0 | 1.3 | 4 | B | | | | | | | | | |
| 8200.5 | Vert | 7VA | Mowry | 1.0 | 0.4 | 2 | D | | | | | | | | | |
| 8201.1 | Vert | 7VB | Mowry | 1.0 | 0.7 | 3 | D | | | | | | | | | |
| 8201.5 | 45° | 7* | Mowry | 1.0 | 0.8 | 3 | B | | | | | | | | | |
| 8201.5 | 45° | 7'B | Mowry | 1.0 | 0.4 | 2 | D | | | | | | | | | |
| 8203 | Hor | | Mowry | 1.0 | 1.5 | 4 | A | | | | | | | | | |
| 8203.75 | Hor | | Mowry | 1.0 | 1.5 | 4 | A | NMT | | | TT | TT | | | | |
| 8203.83 | | | Mowry | | | | | | | | NMT | | | | | |
| 8204 | Hor | 9H | Mowry | 1.0 | 2.7 | 4 | A | | | | NMT | | | | | |
| 8204 | Hor | 9HB | Mowry | 1.0 | 1.6 | 4 | A | | | | | | | | | |
| 8204.3 | Vert | 9V | Mowry | 1.0 | 0.9 | 3 | B | | | | | | | | | |
| 8204.3 | Vert | 9VB | Mowry | 1.0 | 0.9 | 3 | B | | | | | | | | | |
| 8205 | 45° | 9* | Mowry | 1.0 | NR | | D | | | | | | | | | |
| 8205 | 45° | 10* | Mowry | 1.0 | 1.3 | 4 | A | | | | | | | | | |
| 8206 | Hor | 10H | Mowry | 1.0 | 1.6 | 4 | A | | | | TT | TT | | | | |
| 8206 | Hor | 10HB | Mowry | 1.0 | 1.3 | 4 | A | | | | CL | CL | | | CL | |
| 8206 | Vert | 10V | Mowry | 1.0 | 1.0 | 3 | A | | | | | | | | | |
| 8206 | Vert | 10VB | Mowry | 1.0 | 1.6 | 4 | A | | | | | | | | | |
| 8216 | Hor | | Mowry | 1.0 | | | | | | | | | | | | |
| 8216 | Hor | 11HB | Mowry | 1.0 | NR | | D | | | | | | | | | |
| 8216 | Vert | 11V | Mowry | 1.0 | NR | | D | | | | | | | | | |

Core Slabbing

Following core plugging at CoreLab (Denver), the whole core was transferred to Triple-O Slabbing where it was slabbed to 1/3 to allow for more precise observations of petrology and sedimentary features by the team geologists. Figure 6.3 shows one box of

the seven slabbed core. Soon after the core was slabbed, Triple-O hosted a viewing event for the RMCCS team, its partners and local media.



Figure 6.3. Sample photograph of the slabbed RMCCS core.

The slabbed core was housed at Triple-O’s Denver facility for the active period of the RMCCS project. In October of 2013, the core and ownership was to be transferred to the USGS Core Research Center at the Denver Federal Center in Colorado.

In December of 2012, Dr. Daniel Soeder of the National Energy Technology Laboratory in Morgantown, West Virginia contacted the RMCCS team and inquired about the possibility of obtaining a selection of plug samples from the RMCCS well (Table 6.3). Dr. Soeder was interested in conducting “lithologic and petrophysical analyses of porosity, permeability, two-phase flow, and response to net stress on gas shales to determine how they may behave as carbon dioxide storage reservoirs after depletion”. As the samples were not earmarked for analysis by the RMCCS team, they were shipped to Dr. Soeder in early 2013. All analyses performed by Dr. Soeder are presumed to be “destructive” and no expectation of sample return is expected by the RMCCS project.

Table 6.3. RMCCS plug samples sent to Dr. Soeder (NETL) for testing.

| Depth (ft) | Plug orientation | Plug No. | Formation |
|------------|------------------|----------|-----------|
| 8221 | Hor | 15H | Mowry |
| 8221 | Hor | 15HB | Mowry |
| 8221 | Vert | 15V | Mowry |
| 8223.15 | Hor | 16H | Mowry |
| 8223.15 | Hor | 16HB | Mowry |
| 8223.45 | Vert | 16V | Mowry |
| 8226.5 | Hor | 17H | Mowry |
| 8226.6 | Hor | 17HB | Mowry |

| | | | |
|---------|----------|------|----------|
| 8241 | Vert | 24V | Mowry |
| 8241 | 45° | 24° | Mowry |
| 8254.3 | Hor | 34H | Mowry |
| 8254.3 | Vert | 34V | Mowry |
| 8254.55 | 45° | 34° | Mowry |
| 8898.5 | Hor | 43HA | Curtis |
| 8900.5 | Hor | 44HA | Curtis |
| 8900.5 | Vert | 44V | Curtis |
| 8903.5 | Vert | 46V | Curtis |
| 8911 | 45° | 54° | Curtis |
| 8911.6 | Hor | 54H | Curtis |
| 8911.6 | Vert | 54V | Curtis |
| 8916.3 | Vert | 58V | Curtis |
| 9012.1 | Hor | 63H | Entrada |
| 9022.1 | Hor | 72H | Entrada |
| 9022.3 | Hor | 72HB | Entrada |
| 9022.5 | 45° | 72° | Entrada |
| 9042.55 | Hor | 92H | Entrada |
| 9042.6 | Hor | 92HB | Entrada |
| 9042.9 | Vert | 92V | Entrada |
| 7863.00 | Sidewall | 99 | Frontier |
| 8515.00 | Sidewall | 16 | Morrison |

Core Analysis

The objective of the core analysis program was to obtain essential lithologic descriptions and hydraulic/geochemical/geomechanical properties of the cored rock formations. These parameters were going to be used to populate models and simulations that evaluate the potential for CO₂ storage at the RMCCS site, the region and the Colorado Plateau. The RMCCS team originally elected to perform a comprehensive suite of petrophysical tests to gather conventional petrophysical (porosity, permeability), mineralogy (XRD), chemistry (Total Organic Carbon, noble gases), physical (CT Scans, petrography, SEM), SCAL (capillary pressure, relative permeability) and geomechanics (scratch test, compressive strength, triaxial) data. The testing was going to be split between New Mexico Tech, the University of Utah and at least two commercial laboratories. However, because of budgetary constraints and analytical “overreach” (i.e. analyses that were not going to be incorporated into final RMCCS models or simulations), the planned testing was scaled back. Table 6.4 lists the petrophysical tests and number conducted by the RMCCS team on plugs sampled from the RMCCS whole core.

Table 6.4. Petrophysical tests conducted by the RMCCS project on plugs sampled from the whole core.

| Analysis | New Mexico Tech | University of Utah | Service Company (TerraTek, CoreLab) |
|-----------------------|-----------------|--------------------|-------------------------------------|
| XRD | 80 | 0 | 0 |
| Petrography | 41 | 0 | 0 |
| Porosity | 0 | 22 | 31 |
| Permeability | 0 | 22 | 31 |
| Relative Permeability | 0 | 2 | 4 |
| Capillary Pressure | 0 | 0 | 13 |
| TOC | 0 | 2 | 0 |

Total Organic Carbon (TOC)

Total Organic Carbon (TOC) analyses were performed on two samples from the Curtis Formation for the purposes of assessing CO₂ adsorption potential (CO₂ capacity) of the seal unit immediately overlying the Entrada. Table shows the TOC results from analyses performed at the University of Utah. By comparison, the TOC contents of the Curtis Shale are significantly less than those yielded by the Niobrara Formation (TOC range from 2.35% to 4.10%), courtesy of Shell.

Table 6.5. TOC results on 2 samples from the Curtis Formation, obtained at the University of Utah.

| Sample ID | Formation | Sample Mass (mg) | Organic Carbon (mg) | TOC (%) |
|-----------|-----------|------------------|---------------------|--------------|
| 47V0 a | Curtis | 88 | 0.128 | 0.15% |
| 47V0 b | Curtis | 171 | 0.954 | 0.56% |
| 47V0 c | Curtis | 128 | 0.583 | 0.46% |
| | | | Mean | 0.39% |
| 59H0 a | Curtis | 135 | 0.267 | 0.20% |
| 59H0 b | Curtis | 128 | 1.106 | 0.86% |
| 59H0 c | Curtis | 108 | 0.222 | 0.21% |
| | | | Mean | 0.42% |

X-Ray Diffraction (XRD)

Dr. Dana Ulmer-Scholle of New Mexico Tech performed XRD analyses on 80 samples obtained directory from the core and from plugs sampled for petrophysical testing. Figure 6.4 shows XRD data for some key CO₂ sequestration-significant minerals within the Entrada Sandstone and its immediately overlying seal, the Curtis Shale. Although specific reactive transport simulations are beyond the scope of this section, the mineralogy data will be useful for determining long-term trapping mechanisms within the Entrada reservoir as well as seal efficiency of the Curtis and Mowry Shales.

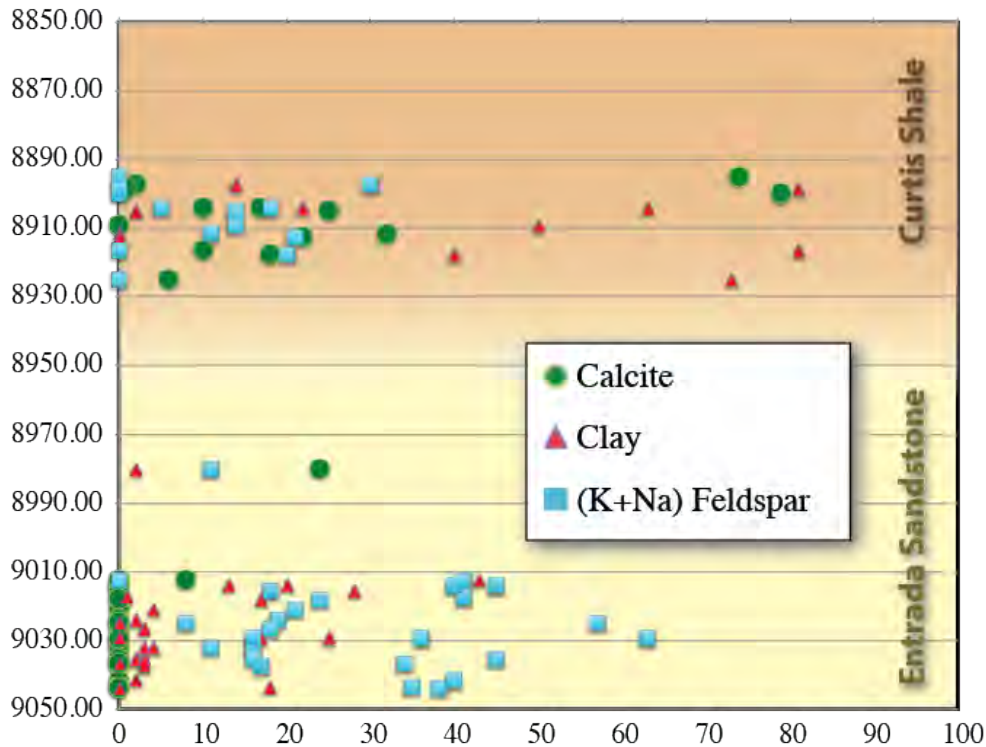


Figure 6.4. Plot of Calcite, Clay and Feldspar totals from the XRD analyses for the Entrada Sandstone and the overlying Curtis Shale. Of importance are the differences in reactive constituents between the two formations.

Spectral Core Gamma (SCG)

CoreLab performed Spectral Core Gamma (SCG) scans on the whole core when it was received from the RMCCS wellsite. The SCG System measures the natural radioactivity and is primarily used to calibrate core depths to downhole logging tools.

Fracture Analysis

Prior to plugging operations, the whole core was examined by CoreLab geologist Ron Cormier for lithologic/fracture descriptions. Additionally, seven core sections were scanned by X-Ray CT to determine interior structures.

Porosity and Permeability

RMCCS plugs and rotary sidewall cores were tested for (Helium) porosity and permeability using standard methods. Table 6.6 lists all of the values obtained by the University of Utah, CoreLab and TerraTek. All values reported in this section and in Table 6.6 were obtained using a Net Confining Stress (overburden) calculated from the depth the individual plugs were sampled. Nine unique formations were tested for porosity and permeability, but the majority of samples were from the Mowry Shale and Entrada Sandstone. The Mowry plugs yielded an average porosity of 2.25% (min=0.63%; max=5.95%) while the average permeability was 0.25 mD (min=0.07 mD; max=0.58 mD). The Entrada plugs yielded an average porosity of 8.57% (min=1.22%; max=18.60%) while the average permeability was 15.48 mD (min=0.05 mD; max=307 mD). While anisotropy of the individual formations is difficult to assess with the limited

number of oriented samples, it is worth noting that the average vertical permeability of the Entrada Sandstone is 3.83 mD, while the average horizontal permeability is 8.03 mD.

Correlating the Helium porosity values from the plugs to downhole log data is tenuous given the sparseness of the plug data. However, for the section of the Entrada core that has sufficient Helium porosity data, the values correlate well to the neutron porosity values obtained from the wireline logs (

Figure 6.5).

At the net confining stress values for each sample (>3500 psi), many of the values of porosity and permeability were too low (labeled as “N.A.” in Table) to be determined by the individual method or instrument. This minimum limits are generally approximately <<0.1% for porosity and <<0.001 mD for permeability.

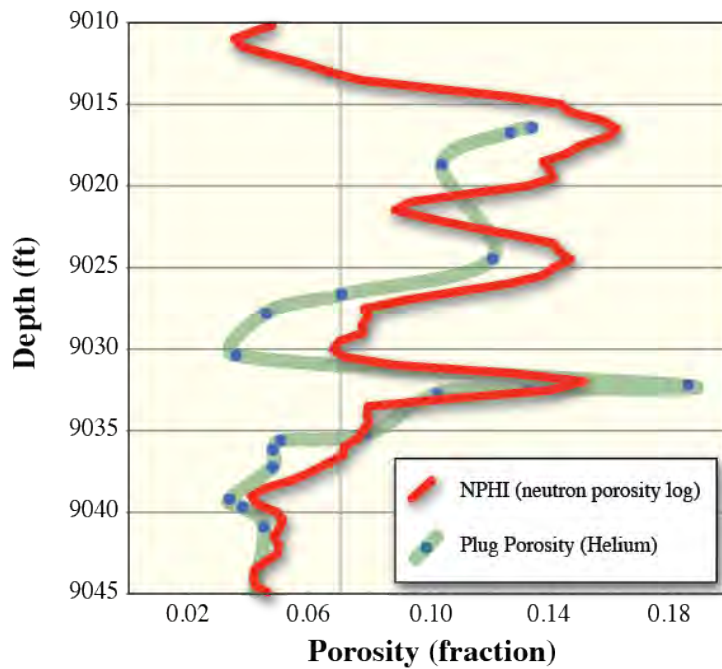


Figure 6.5. Correlation between Helium porosity values from the RMCCS plugs and the NPHI wireline log data. It must noted that there is an apparent ~3 ft offset between the two curves to maximize correlations.

Table 6.6. Porosity and Permeability results for plugs and rotary sidewall core from the RMCCS well. "N.A." indicates porosity and/or permeability values below detectable limits, at Net Confining Stress (i.e. overburden – greater than 3000 psi).

| Depth | Plug (orientation) or Sidewall | Sample ID | Formation | Helium Porosity (% , confined) | Permeability (md, water/Klinkenberg) |
|---------|--------------------------------|-----------|-------------|--------------------------------|--------------------------------------|
| 8191.65 | Vertical | 2VB | Mowry | 1.98 | N.A. |
| 8192 | Horizontal | 3H | Mowry | 0.98 | N.A. |
| 8206 | Horizontal | 10HB | Mowry | 5.40 | 0.09 |
| 8206 | Horizontal | 10H | Mowry | 5.95 | N.A. |
| 8218.3 | Horizontal | 13H | Mowry | 1.39 | 0.07 |
| 8228.9 | Horizontal | 18H | Mowry | 1.55 | 0.00 |
| 8235 | Horizontal | 21HB | Mowry | 1.60 | 0.58 |
| 8235 | Horizontal | 21H | Mowry | 1.98 | N.A. |
| 8243.15 | Horizontal | 25HA | Mowry | 1.29 | N.A. |
| 8258 | Horizontal | 36H | Mowry | 0.63 | N.A. |
| 8259.5 | Horizontal | 37H | Mowry | 1.95 | N.A. |
| 8288.00 | Sidewall | 42 | Dakota | 4.95 | N.A. |
| 8358.00 | Sidewall | 40 | Dakota | 5.66 | 0.01 |
| 8490.00 | Sidewall | 17 | Morrison | N.A. | N.A. |
| 8780.00 | Sidewall | 14 | Morrison | N.A. | N.A. |
| 8807.00 | Sidewall | 36 | Morrison | 5.22 | N.A. |
| 8882.00 | Sidewall | 35 | Morrison | 7.83 | 0.02 |
| 8896.1 | Horizontal | 41HA | Curtis | 0.51 | N.A. |
| 8904 | Horizontal | 47H | Curtis | 0.32 | N.A. |
| 8916.35 | Horizontal | 58H | Curtis | 2.58 | 0.03 |
| 8992.00 | Sidewall | 34 | Curtis Sand | N.A. | N.A. |
| 9012.3 | 45° | 63° | Entrada | 11.40 | 1.40 |
| 9012.8 | Vertical | 63VB | Entrada | 11.90 | 5.24 |
| 9012.8 | Vertical | 63V | Entrada | 12.40 | 2.84 |
| 9013.3 | Horizontal | 64H | Entrada | 13.40 | 2.11 |
| 9013.4 | 45° | 64° | Entrada | 12.25 | 5.22 |
| 9013.6 | Horizontal | 64HB | Entrada | 12.70 | 4.59 |
| 9015.6 | Horizontal | 65HB | Entrada | 10.40 | 0.64 |
| 9015.85 | 45° | 65° | Entrada | 12.10 | 3.04 |
| 9021.35 | Horizontal | 71HB | Entrada | 12.10 | 13.90 |
| 9021.55 | 45° | 71° | Entrada | 11.80 | 3.64 |
| 9023.35 | Vertical | 73V | Entrada | 13.10 | 3.41 |
| 9023.55 | Horizontal | 73H | Entrada | 7.10 | 19.80 |
| 9024.65 | Horizontal | 74HB | Entrada | 4.60 | 0.64 |
| 9026.7 | 45° | 76° | Entrada | 5.80 | N.A. |
| 9027.3 | Horizontal | 77H | Entrada | 3.60 | 0.17 |
| 9027.45 | Horizontal | 77HB | Entrada | N.A. | 0.18 |
| 9027.8 | 45° | 77° | Entrada | 1.22 | N.A. |
| 9029.15 | Horizontal | 79H | Entrada | 18.60 | 307.00 |
| 9029.35 | Horizontal | 79HB | Entrada | 13.30 | 10.66 |
| 9029.6 | Horizontal | 79HC | Entrada | 10.30 | N.A. |
| 9032.15 | Horizontal | 82H | Entrada | 7.87 | 1.41 |
| 9032.5 | Horizontal | 82HB | Entrada | 5.05 | 0.16 |
| 9033.1 | Horizontal | 83H | Entrada | 4.80 | 0.10 |
| 9034.1 | Horizontal | 84H | Entrada | 4.80 | 0.46 |
| 9036.1 | Horizontal | 86H | Entrada | 3.35 | 0.26 |
| 9036.6 | Horizontal | 86HB | Entrada | 3.80 | 0.10 |
| 9037.8 | Horizontal | 88HB | Entrada | 4.50 | 0.07 |
| 9042.1 | Horizontal | 91H | Entrada | 4.20 | 0.05 |
| 9043.7 | 45° | 93° | Entrada | 3.48 | N.A. |
| 9380.00 | Sidewall | 6 | Chinle | 2.83 | N.A. |
| 9603.00 | Sidewall | 2 | Shinarump | N.A. | N.A. |
| 9675.00 | Sidewall | 26 | Moenkopi | N.A. | N.A. |

Noble Gas Tracers

The RMCCS team, with the assistance of Dr. Kip Solomon of the Geology and Geophysics Department at the University of Utah, collected eight sub-samples of core to perform noble gas tracer analyses (Table 6.7). Noble gas (i.e. ³He and ⁴He) profiles have been used successfully as analogs to evaluate gas/fluid diffusion in seal units. Though the 8 samples (from the Curtis and Entrada Formations) were sampled (directly from the core at the well site) in February of 2012, the samples are required to sit and outgas in a vacuum-tight canister for at least several months. The “head space” gas in the canister is then analyzed for the isotopic signature of the noble gases. Unfortunately, a series of breakdowns and ultimately a significant laboratory upgrade by Dr. Solomon pushed the noble gas analyses back into late 2013. As of the end of the RMCCS project, the noble gas samples have not been analyzed. However, the integrity of the vacuum vessels remains intact and Dr. Solomon is committed to the analyses of the RMCCS noble gas samples and a publication of their results at a near future date.

Table 6.7. Samples collected by Dr. Kip Solomon for Noble Gas profiles.

| Sample ID (Depth(ft)) | Formation | Exposure Time (s) | Total Mass (g) | Mass in Flask (g) |
|--------------------------|-----------|----------------------|----------------------|----------------------------|
| 8901 | Curtis | 1020 | 1417.13 | 287.53 |
| 8907 | Curtis | 5880 | 1403.44 | 215.04 |
| 8913 | Curtis | 6720 | 1026.26 | 215.16 |
| 8919 | Curtis | 6720 | 1268.26 | 234.36 |
| 9020 | Entrada | 4560 | 1096.6 | 208.63 |
| 9026 | Entrada | 4980 | N.A. | 197.67 |
| 9032 | Entrada | 5340 | 892.6 | 241.19 |
| 9038 | Entrada | 5820 | 631.3 | 217.42 |

Capillary Pressure

Thirteen samples (plugs) from the RMCCS core were selected for capillary pressure measurements, two of which were duplicates to evaluate quality control between the two service companies performing the analyses (TerraTek and CoreLab). Additionally, the three plug samples sent to CoreLab were analyzed using both high-pressure mercury injection method and the centrifugal method. Table 6.8 lists the samples for which capillary pressure measurements were performed.

Table 6.8. RMCCS Plug samples where capillary pressure values were determined.

| Sample ID | Service Company | Method |
|-----------|-----------------|------------|
| 21HO | TerraTek | HPMI |
| 36HO | TerraTek | HPMI |
| 37HO | TerraTek | HPMI |
| 41HA | TerraTek | HPMI |
| 48HO | TerraTek | HPMI |
| 63DO | TerraTek | HPMI |
| 63VO | TerraTek | HPMI |
| 64HB | TerraTek | HPMI |
| 79HO | TerraTek | HPMI |
| 93DO | TerraTek | HPMI |
| 64HO | CoreLab | HPMI & Cfg |
| 21HB | CoreLab | HPMI & Cfg |
| 10HB | CoreLab | HPMI & Cfg |

HPMI: High Pressure Mercury Injection
 Cfg: Centrifugal

Figure 6.6 and Figure 6.7 show the capillary pressure (drainage) curves for the Entrada and Mowry plugs, respectively (TerraTek analyses only). Overall, the Corelab and TerraTek data yield entry pressures for the shales (Mowry and Curtis) between 3,357 and 10,031 psi, with a mean of 7085 psi. In general, the capillary pressures curves suggest that the Mowry and Curtis Shales will act as good CO₂ seals provided the entry pressures are not exceeded. Note: Capillary pressure curves from TerraTek and CoreLab on duplicate samples (Figure 6.8 and Figure 6.9) show good agreement between the two laboratories.

The mercury injection method yields pore throat size distributions that are expected for shales and sandstones.

Figure 6.10 shows typical pore throat size histograms for the two rock types. In general, the shales yield pore throat sizes ranging from 0.002 to 0.05 µm in diameter. The sandstones yield pore throat sizes greater than 0.05 µm in diameter.

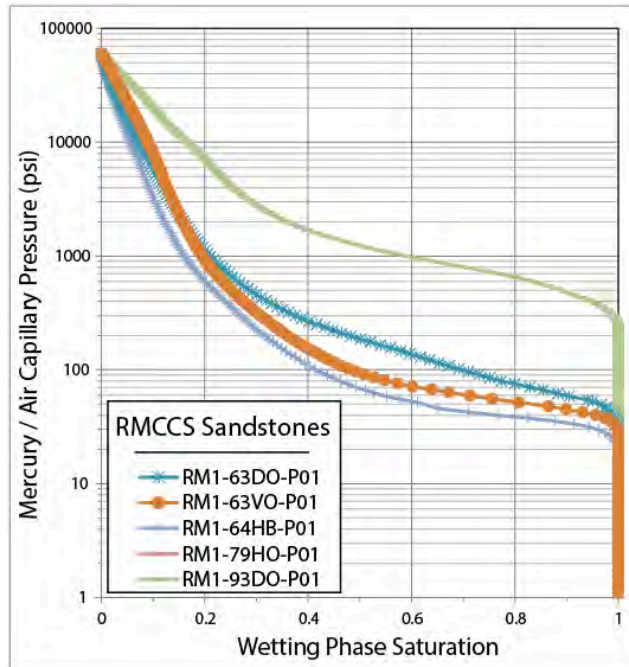


Figure 6.6. Capillary pressure curves for the Entrada Sandstone plugs sampled from the RMCCS core (TerraTek analyses).

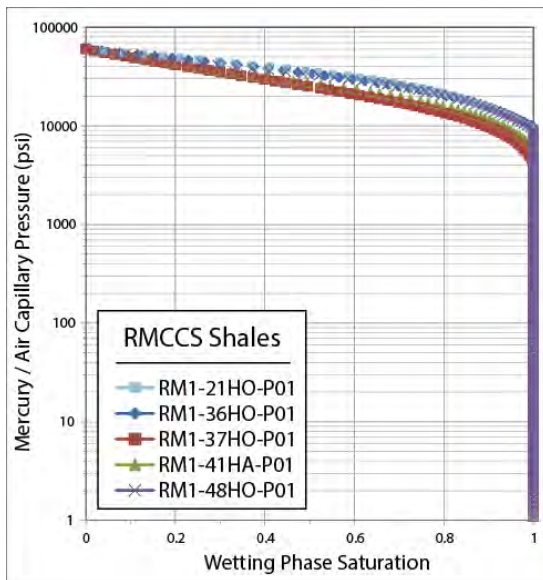


Figure 6.7. Capillary pressure curves for the Mowry Shale plugs sampled from the RMCCS core (TerraTek analyses).

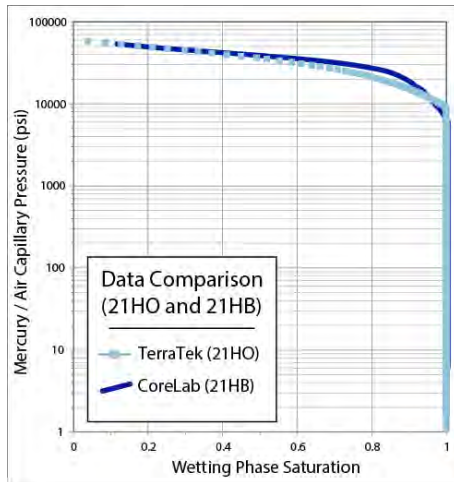


Figure 6.8. Data comparison of Capillary Pressure curves between TerraTek and CoreLab for plug 21H.

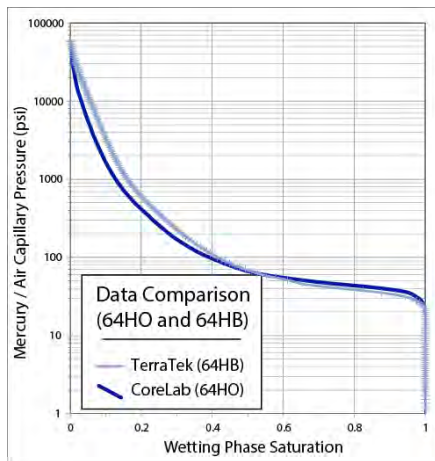


Figure 6.9. Data comparison of Capillary Pressure curves between TerraTek and CoreLab for plug 64H.

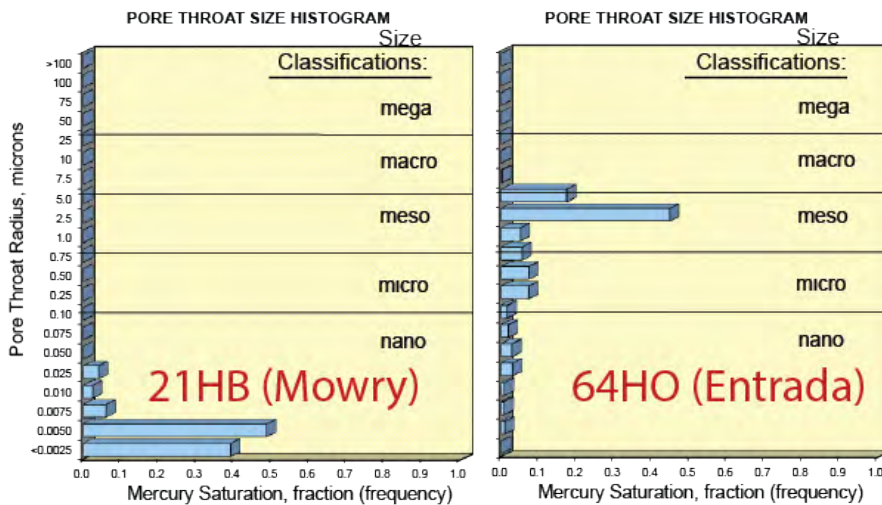


Figure 6.10. Typical pore throat size distribution for RMCCS shales (left) and sandstones (right).

Relative Permeability

TerraTek performed unsteady-state relative permeability analyses on plug samples 63°, 63V, 64HB and 79H (

Figure 6.11). The University of Utah performed *steady*-state relative permeability analyses on plug samples 73H (Figure) and 73V. Unsteady-state relative permeability tests were chosen for the TerraTek samples due to the prohibitively high cost and difficulty of obtaining steady-state results.

For the four Entrada samples tested by TerraTek, the relative permeability curves are not exceptionally different, despite all three orientations (45°, horizontal and vertical) being represented. Although a simulation of the relative permeability outcomes are beyond the scope of this section (see the section on model development), this is suggestive that anisotropy will not have a significant impact. The data also indicates that the irreducible water saturation is greater than 50%.

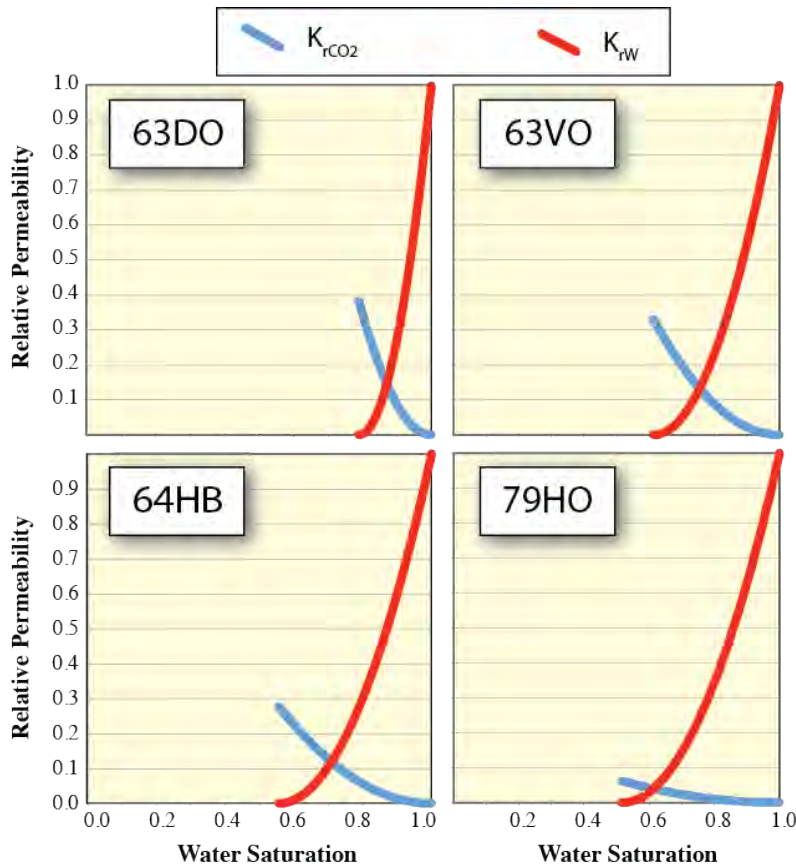


Figure 6.11. Relative Permeability (unsteady state) plots for the 4 Entrada samples analyzed by TerraTek.

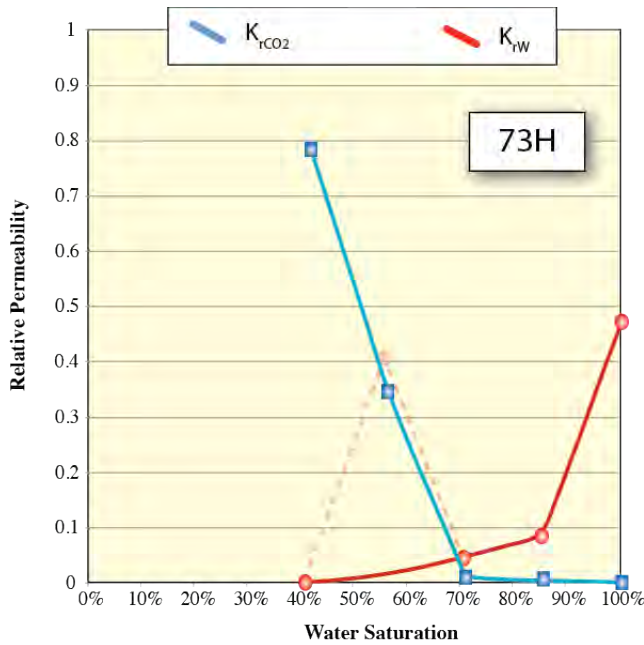


Figure 6.12. Preliminary relative permeability (steady-state) curve for plug 73H analyzed at the University of Utah.

Samples for petrographic thin-sections were obtained by Dr. Dana Ulmer-Scholle of New Mexico Tech. The following are examples from selected formations:

Mowry Formation petrographic results

Depositional Environment:

Most of the thin sections are dominated by silty shales and shaley siltstones.

One of the reasons that the water depth is interpreted to be great (deep) is due to the lack of an overall diverse or abundant fauna within these units. For the most part, siliceous, pelagic radiolarians are a dominant microfossil in this section of the core. The shales in the section are composed of illite and mixed layered clays (I/S). X-ray diffraction was not done on these units, so the identification of these clays is based on petrographic observations. Many of the shale zones also appear to have been partially silicified, resulting in hardening (more brittle) of some of the shale zones. Others also contain carbonate (both calcite and dolomite).

Diagenesis:

An idealized diagenetic sequence was developed for the rocks of the Mowry formation. Compaction was not a single event, but rather shows a progression during burial. The following are the diagenetic events in order of their occurrence based on cross cutting relationships:

- Pyrite replacement of organics, grains and groundmass;
- Minor illite and chlorite cements (rare);
- Phosphate cements and phosphate-replaced feldspars and other grains (sedimentary bioclasts and rock fragments);

- Quartz and plagioclase overgrowths. Also minor euhedral megaquartz replacements;
- Poikilotopic calcite cements filling interparticle porosity in sandy laminae and burrow fills;
- Silicification and phosphatization of shales;
- Calcite replacing radiolarians, VRFs and feldspars;
- Plagioclase alteration to sericite;
- Compaction (due to overburden):
 - Wispy pressure solution, horizontal stylolites, flattened grains and compactional drape,
 - Fractures (partially to completely filled with calcite, minor gypsum and matrix). These fractures commonly show multiple generations of opening and filling;
- Euhedral to subhedral dolomite cements and oil migration;
- Leaching of feldspars and radiolarians;
- Anhydrite and gypsum cements;
 - Compaction (due to compressional tectonics): Horizontal, shear fractures filled with calcite cement,
 - Vertical stylolites.

Dakota Formation petrographic results

Based on one thin section, the conglomeratic nature of the sediments and the composition (quartz, quartzite, feldspars and chert/chalcedony), indicate that these deposits were formed most likely in a fluvial or alluvial channel deposit feeding from highlands to the west of the Craig well site. The distance is moderately far because of the dominance of quartz grains and the scarcity of feldspars and other grains.

Diagenesis:

The diagenetic sequence for the one thin section made from Dakota Formation was:

- Early feldspar (both K-spar and plagioclase) overgrowths
- Quartz overgrowths
- Leaching of K-spar and chert/chalcedony grains
- Kaolinite and illite cements
- Pyrite replacement (very minor)

Because of the early quartz cementation, the sands were well cemented prior to significant burial, and few compactional fabrics were found. Porosity makes up about 12% of the thin section with most of the porosity being secondary intraparticle, vuggy and intercrystalline (10%) and primary interparticle (2%).

Morrison Formation petrographic results

The plug was probably taken from the Salt Wash member of the Morrison Formation (but the Brushy Basin member is possible). The thin section is dominated by pebble-sized chert clasts and quartz sand. A probable depositional environment was a high-energy fluvial channel or braided stream environment. All of the less durable clasts were removed both mechanically and chemically.

Diagenesis:

Like the Dakota Formation, we only had one sample from the Morrison Formation to characterize its diagenesis. The observed diagenetic sequence was:

- Quartz overgrowths on monocrystalline quartz grains
- Leaching of unstable grains and minerals like dolomite and microcrystalline quartz
- Kaolinite and illitic (minor) clays are found in both primary and secondary porosity
- Fracturing
- Calcite fracture fills
- Oil migration

Porosity is made up of both primary interparticle and secondary fracture, dolomoldic, biomoldic and intraparticle. Primary porosity dominates over the secondary porosity.

Curtis Formation petrographic results

Depositional Environment:

Burrows and abundant fauna indicate well-oxygenated conditions and normal salinity. Scattered grains like ooids indicate a nearby high-energy shallow water environment. Mud clasts and coarsely crystalline dolomite clasts were ripped up from a intertidal to supratidal environment during storms. Fauna includes: brachiopods, crinoids, echinoids, pelecypods, ostracods, rare foraminifera, calcispheres, and sponges. Glauconite is very common in these sediments and is indicative of slow sediment accumulation rates in marine shelf settings.

Diagenesis:

A generalized paragenetic sequence for the Curtis slides is:

- Isopachous, fibrous marine calcite cements,
- Glauconite, chert/chalcedony and phosphate replacement pellets, bioclasts and grains and filling porosity within bioclasts on the sea floor,
- Syntaxial overgrowths and blocky cements on echinoid and crinoid debris,
- Pyrite replacement,
- Soft-sediment deformation,
- Dolomite cements,
- Leaching of grains and matrix,
- Gypsum/anhydrite and chalcedony replacement of matrix and grains,
- Compaction associated with fractures, horizontal stylolites and wispy pressure solution,
- Calcite filling of fractures,
- Dolomite cements and hydrocarbon migration
- Horizontal compression producing vertical stylolites

Porosity within this unit is very limited due to the lack of early quartz cementation and extensive compaction. The porosity that is in this slide is minor primary intercrystalline and intergranular and secondary microfracturing, fracturing and intraparticle porosity.

Entrada Formation petrographic results

Overall, the Entrada Formation in the core is dominated by large cross-bed sets interbedded with a few planar-laminated sections. The cross bedding are the dunes and planar units are probably the playa deposits.

Diagenesis:

The diagenetic sequence developed for the thin section from the Entrada Formation varied very little within the thin sections. The sequence was:

- Minor quartz overgrowths on grains
- Minor pyrite replacement of organics and matrix
- Illite cements incompletely coat grains
- Quartz and feldspar (less common) overgrowths fill primary porosity and provide support to the sediments
- Kaolinite cements
- Euhedral, zoned dolomite and anhydrite cementation
- Minor titanite (sphene) cementation and replacements of dolomite
- Leaching of unstable grains like feldspars and rock fragments (volcanic and sedimentary)
- Overburden compactional fabrics include fractures, wispy pressure solution seams and stylolites. Fractures are filled:
 - First with euhedral, baroque dolomites and
 - Followed by dogtooth calcite spars
- Leaching associated with fracturing. Both the dolomite and calcite fracture fills are stained by hydrocarbons
- Hydrocarbon migration and filling of late formed pores
- Overburden compaction. Unlike the other units, there are few fabrics indicating compressional shortening of the region. It may be due to the extensive silicification of the unit.

Porosity ranges from less than 1% to over 15% of the thin sections. Both primary and secondary porosity are common. Of the primary porosity types, intergranular and intercrystalline, the most important factors controlling porosity preservation was the relationship between the amount of quartz cementation and the timing of compaction. The key to porosity in this unit was to have enough quartz overgrowths to support the rock during compaction, but not enough to fill all the pore spaces. Porosity in the upper parts of the core was significantly higher than the lower sections of the core where compaction had larger impacts. Intercrystalline porosity is formed within kaolinite books. While this doesn't have a large impact on the overall porosity, the kaolinite does impact the permeability of the unit by possibly blocking pore throats. Secondary porosity types include moldic, fracture and intraparticle. While fracture porosity enhances permeability and porosity, moldic and intraparticle can improve the porosity, but depending on the interconnectivity of the molds, the impact on the permeability may be minimal.

Chinle Formation petrographic results

The plug the thin section was made from may be from the Chinle Formation, but there is some uncertainty about it.

Diagenesis:

The diagenetic sequence in the one plug from the Chinle(?) Formation is:

- Minor illite cements with iron staining
- Quartz overgrowths
- Leaching of feldspar grains
- Kaolinite and dickite (similar to kaolinite compositional, but usually larger, coarser vermicular books)
- Quartz overgrowths continued
- Compaction produced microstylolites and compromised crystal boundaries
- Hydrocarbon staining.

The porosity within this sample is good, and it consists of a combination primary and secondary pores. Primary porosity is intergranular and intercrystalline, and secondary porosity is moldic after dissolution of feldspars and sedimentary rock fragments.

Moenkopi(?) Formation petrographic results

Based on previous literature, a sample from the Moenkopi Formation in the area around the Craig well site should be a terrestrial siltstone, sandstone to conglomerate, but the sample provided for thin section is none of those. It is a marine shale that was deposited on a distal platform or in a basin due to the grain size and fauna.

The slide appears to have Inoceramid fragments/prisms in it in addition to siliceous radiolarians, foraminifera and ostracods. If the prisms are from Inoceramid sp., then this slide has to be Cretaceous in age and probably from the Mowry Formation. Could there be a fault between the previous sample and this one? It is something that should be investigated geophysically.

Diagenesis:

The diagenetic sequence for the Moenkopi(?) sample is:

- Minor quartz replacements;
- Pyrite replaces matrix and bioclasts
- Kaolinite infills of foraminifera chambers
- Calcite fills the remaining tests of the foraminifera tests
- Compaction associated with wispy pressure solution and possible fracturing

The only visible porosity in this sample is secondary fracture porosity. It may result from plugging or it may be natural.

7. Database assembly and static model development

Schlumberger Carbon Services and the Colorado Geologic Survey (CGS) worked together to develop a static geologic model in Petrel of the Sandwash Basin and Piceance Basin in northwestern Colorado (Figure 4.1). The model was developed to properly assess the geologic structure, CO₂ storage capacity, CO₂ injectivity, and CO₂ confinement of the Sandwash Basin and Piceance Basin. In order to develop this geologic model, geologic and geophysical data was integrated and ultimately used to characterize potential repositories, traps, and sealing mechanisms that would be needed to design and implement a CO₂ storage project.

Like many geologic models, this model was developed in stages and was updated when new data became available. Phase 1 of the model was constructed prior to the drilling of the stratigraphic test well RMCCS State #1 (Craig Project Site) and was used, from a CO₂ storage perspective, as a tool to understand the geological characteristics of the Sandwash Basin and Piceance Basin. This geologic understanding was used to shortlist suitable locations to drill RMCCS State #1 which ultimately provide valuable geologic information specific to a CO₂ injection scheme. This model was also used for a well prognosis of RMCCS State # 1 to estimate likely conditions (formation tops and associated geological characteristics) to be encountered while drilling at the location. Once RMCCS State # 1 was drilled, new well data and 2D seismic survey data became available, which allowed for subsequent more detailed site specific Phase 2 modeling.

Figure 4.1 displays the Regional Model area and the two subareas (Geostatistical Model and Simulation Model) which were utilized to meet the RMCCS modeling project objectives. The below points and Table 7.1 summarize the three model areas. For structural consistency across multiple scales, the structural control for Geostatistical Model grid and Simulation Model grid was extracted from the Regional Model grid. The Regional Model was built first than scaled down into the Geostatistical Model and then to the Simulation model to meet project objectives that required a finer scale around RMCCS State # 1.

- **Regional Model** - A 3D structural framework model was generated for this model area with the main structural control surfaces being provided by CGS. This area covers an aerial extent greater than the available petrophysical data. This model area is 108 miles x 83.5 miles.
- **Geostatistical Model** – This local subarea of the Regional Model covered by the available petrophysical data is roughly 40 mile x 40 mile centered on the stratigraphic test well (RMCCS State # 1). This model was used for geostatistical analysis of petrophysical properties.
- **Simulation Model** - This subarea of the Geostatistical Model was the area used for simulation work and porosity and permeability stochastic modeling. Simulation engineers at the University of Utah (UU) specified a 20 mile x 20 mile area centered on RMCCS State # 1 to be appropriate for the project objectives.

Table 7.1: Geocellular Model Area Grid Summary

| Model Area | Model Size (mile) | X-Y Cell Size (feet) | Total Cells (Dakota, Entrada, Weber) (Y, X) | Vertical Cell Thickness (Z) |
|----------------------|-------------------|----------------------|---|--|
| Regional Model | 108 x 83.5 | 1000 x 1000 | 570 x 441 | Selected for each zone based on geophysical logs |
| Geostatistical Model | 40 x 40 | 500 x 500 | 216 x 211 | |
| Simulation Model | 20 x 20 | 100 x 100 | 1056 x 1056 | |

During the development of the Regional Model, 15 formation surfaces were modeled. These formation surfaces were the structural framework for subsequent stochastic property modeling (porosity and permeability) of 7 formations in all three model areas (Table 7.2). Of these 7 formations, the Dakota, Entrada and Weber were the primary formations of interest because they are the Potential CO₂ injection Reservoirs.

Table 7.2: Modeled Formation Surfaces and Formations with Property Modeling Results

| Modeled Formation Surface | Formation with Property Model Results | | | Formation Notes |
|---------------------------|---------------------------------------|----------------------|------------------|---|
| | Regional Model | Geostatistical Model | Simulation Model | |
| Mesa Verde (Surface DEM) | | | | Digital Elevation Model |
| Mancos | | | | |
| Marapos | | | | |
| Niobrara | | | | |
| Carlisle | | | | |
| Frontier | | | | |
| Mowry | | | | |
| Dakota | x | x | x | Potential CO ₂ injection Reservoir |
| Morrison | x | x | x | |
| Curtis | x | x | x | |
| Entrada | x | x | x | Potential CO ₂ injection Reservoir |
| Chinle | x | x | x | |

| | | | | |
|------------|---|---|---|---|
| Phosphoria | x | x | x | |
| Weber | x | x | x | Potential CO ₂ injection Reservoir |
| Maroon | | | | |

Property modeling results (porosity and permeability) from all three modeled areas were utilized to provide the site specific foundation for subsequent RMCCS project objectives. The Regional Model was built first, then scaled down into the Geostatistical Model and then to the Simulation model to meet project objectives that required a finer scale around RMCCS State # 1. The subsequent RMCCS project objectives are listed below:

- Capacity assessment (Pore Volume Distribution) in the Sandwash Basin (Section 8 of this report) (Utilized Regional Model)
- Uncertainty assessment workflow (Section 9 of this report) (Utilized Geostatistical Model)
- Simulation and risk assessment (Section 10 of this report)(Utilized Simulation Model)
- To support regulatory and permitting requirements (Utilized all model areas).

Phase 1 Static Model Development (Before Drilling RMCCS State # 1)

The RMCCS Petrel static model development began with acquiring the data types listed below from various sources such as IHS and from the State Geologic surveys. Before this data was imported into Petrel, it underwent a QA\QC process to ensure its reliability and relevance to the project.

RMCCS Phase 1 Model: Database Assembly

The data types below were incorporated into the Petrel model (Figure 4.6):

- Well names, type and coordinates (X, Y, Z, TD, TVD) (4202 wells)
- Well deviation surveys
- Well formation tops (Table 3)

Table 7.3: Formation Tops Used in the Model

| Modeled Formation Surface | Number of Well Tops used in Regional Model |
|----------------------------------|---|
| Mancos | 319 |
| Marapos | 346 |
| Niobrara | 553 |
| Carlisle | 504 |
| Frontier | 506 |
| Mowry | 488 |
| Dakota | 523 |
| Morrison | 479 |
| Curtis | 381 |
| Entrada | 387 |
| Chinle | 253 |
| Phosphoria | 198 |
| Weber | 201 |

- Selected Applicable Well logs – Within a 40 mile proximity to RMCCS State # 1 (Geostatistical Model area), a well log search focus was for porosity, resistivity, and gamma ray logs because they are required for petrophysical analysis which computes permeability. Based on the available data from this search, 20 wells were selected for petrophysical analysis. Additional logs selected for incorporation to the model included density, neutron, sonic, SP and caliper.
- Cultural Data
 - Oil and gas activity
 - Sandwash basin fault locations
 - Dakota, Entrada and Weber Outcrop locations
 - Digital elevation model (DEM)
 - Power plant locations (3 within the Regional Model Area)
 - Local roads and highways

RMCCS Phase 1 Model: Model Development

Phase 1 of the model was constructed prior to the drilling of RMCCS State # 1 and was used as a tool to understand the local and regional geological characteristics (porosity, permeability and pore volume) of the Sandwash Basin and Piceance Basin from a CO₂ storage perspective. This geologic understand was used to shortlist suitable locations to drill RMCCS State #1 which ultimately provide valuable geologic information specific to a CO₂ injection scheme. This model was also used for a well prognosis of RMCCS State # 1 to estimate likely conditions (formation tops and associated geological characteristics) to be encountered while drilling at the location. A summary of the Phase 1 model development steps are presented below:

1. After a rigorous QA\QC process, relevant data was uploaded into Petrel.
2. The Regional Model area was defined.
3. With the guidance of CGS, who has unique geological expertise in the area, formation surfaces were generated to fit the known local geology characteristics and surface outcrop locations.
4. The generated formation surfaces were the foundation for a structural framework geocellular model.
5. Available log data (porosity, resistivity, and gamma ray logs) were utilized for petrophysical analysis, which calculated a permeability log. Much of the available log data was of early vintage, limited and unreliable. Based on the proximity to RMCCS State # 1 and the available budget, 20 wells with appropriate log data, in a 40 mile proximity to RMCCS State # 1, were selected for advanced petrophysical analysis (Figure 4). At these wells, available data varied but several wells had density and sonic data available for porosity computation. Before drilling RMCCS State # 1, these 20 wells represented the best information as to porosity and the derived permeability in the area around RMCCS State # 1. The spatial extent of these wells defined the extent of the Geostatistical Model area and an associated finer scale geocellular model was generated.
6. The porosity and permeability data at these 20 wells were upscaled into the Geostatistical Model cells (Dakota, Entrada and Weber Formations).
7. Using these 20 selected wells, variogram analysis was conducted to understand the variation in porosity as a function of separation distance between wells. It was also used as means of determining directions/degree of anisotropy. The results of this analysis are presented in Table 7.4.

Table 7.4: Log Porosity Statistical Summary

| Formation | Porosity Mean | Porosity Standard Deviation | Variogram Analysis | | |
|-----------|---------------|-----------------------------|--------------------|-------------|---------|
| | | | Major Range | Minor Range | Azimuth |
| Dakota | 0.102 | 0.046 | 30,979 | 23,595 | 141 |
| Entrada | 0.085 | 0.036 | 29,177 | 29,144 | 160 |
| Weber | 0.053 | 0.022 | 31,182 | 29,729 | 160 |

1. Using the variogram parameters, Sequential Gaussian Simulation (SGS) was then used to populate the porosity values to each grid cell

within the Dakota, Entrada and Weber throughout the Geostatistical Model and Regional Model areas.

2. Formation Pore Volume (PV) (ft³) was calculated individually for the Dakota, Entrada and Weber Formations via the below simple calculation:

- Formation PV=Formation SUM(Cell Pore Volume=Cell Volume*Cell Porosity)

3. Formation Permeability Thickness (Kh) (mD-ft) was calculated individually for the Dakota, Entrada and Weber Formations as a proxy for well injectivity. While KH serves as a good proxy for injectivity on a localized basis, long term injectivity is highly dependent on lateral connectivity of pore space. Therefore, long term injectivity estimates should be verified with numerical simulation. Formation Kh, localized at the planned RMCCS State # 1 well location was calculated via the below simple calculation:

- Formation Kh (RMCCS State # 1)= At RMCCS State # 1, Formation Vertical SUM (Cell Height*Cell Permeability)

Phase 2 Static Model Development (After Drilling RMCCS State # 1)

RMCCS Phase 2 Model: Database Assembly

The data types below were appended to the already existing Petrel model:

- RMCCS State # 1 coordinates (X, Y, Z, TD, TVD)
- RMCCS State # 1 Wireline logs and associated Elemental Analysis (ELAN) data provided excellent porosity and permeability data.
- RMCCS State # 1 Core Analysis results
- RMCCS State # 1 Well Tops
- 12 recently depth converted 2D seismic surveys within the Simulation model area. These lines were converted from time to depth by Schlumberger WesternGeco. Two of these lines were newly acquired and cross directly at RMCCS State # 1.

RMCCS Phase 2 Model: Model Development

Once RMCCS State # 1 was drilled, new well data and 2D seismic survey data became available. The new data collected from RMCCS State # 1 was more specific to a CO₂ injection project than previous data that had already been incorporated into the model. RMCCS State # 1 also provided excellent porosity and permeability data, which when benchmarked to the petrophysical analysis of the 20 wells in the Geostatistical model area, showed that the initial petrophysical analysis was accurate. With this new data, Phase 2 of modeling was now able to move forward and the model was updated with this valuable data. A summary of the Phase 2 model development steps are presented below:

1. After a rigorous QA\QC process, relevant data acquired from RMCCS State # 1, was uploaded into Petrel.

2. CGS, who has unique geological expertise in the area, regenerated the formation surfaces with the new well tops from RMCCS State # 1 and from interpreted horizons interpreted from the recently converted 2D seismic survey lines. These generated formation surfaces were the new foundation for a structural framework geocellular model.
3. A new geocellular model was regenerated for the Regional Model area and the finer scale Geostatistical Model area.
4. The 20 wells with porosity and permeability data in the Geostatistical Model area were compared to results from RMCCS State # 1 and showed the initial petrophysical analysis was accurate.
5. From these 20 wells and RMCCS State # 1, porosity data were upscaled into the new Geostatistical Model cells (Dakota, Entrada and Weber Formations).
6. Given the addition of spatial porosity data from RMCCS State #1 to the 20 selected wells, the previous variogram analysis was reviewed. This review concluded that the addition of RMCCS State # 1 did not significantly impact the previous variogram analysis.
7. When conducting property modeling within the Geostatistical Model area there is a great deal of uncertainty between known data points because there are only 20 wells and RMCCS State # 1, with porosity and permeability data available in this large area (40 mile x 40 mile). Because these wells are spaced so far apart, correlation ranges for porosity extracted from experimental variograms were very long and not felt to be representative of actual heterogeneity. Because of this poor spatial sampling an uncertainty analysis was conducted to understand how changes in variogram parameters ultimately affect the porosity and permeability results of SGS within the geocellular model areas. The results showed this to be a useful proxy to understand the spatial geologic uncertainty and how it impacts understanding of porosity distributions.
8. A finer scale geocellular model was generated for the Simulation Model area.
9. Using the results from the above described variogram uncertainty analysis, the P50 set of variogram parameters were selected. Using these parameters, SGS was then used to populate the porosity values to each grid cell within the Dakota, Entrada and Weber Formations of the Simulation Model area, the Geostatistical Model area and the Regional Model area.
10. Pore Volume (PV) ft³ for the Dakota, Entrada and Weber Formations were recalculated.
11. Permeability-Height (KH) mD-ft, at the RMCCS State # 1 location was calculated with the newly acquired data from RMCCS State #1 for the Dakota, Entrada and Weber Formations.

12. These results were used to support subsequent RMCCS modeling objectives as described previously.

8. Capacity assessment

The Geological Surveys of the four states in which the Colorado Plateau Region is located, AZ, CO, NM and UT, were tasked to improve the regional geologic assessment of the listed formations. That was accomplished by generating structure and thickness contour maps for each of the formations. These maps were not just based on interpolating well-derived data but also incorporated additional available information and studies. In addition, each of the partnering geologists contributed in-depth, sedimentary basin expertise during the compilation of the regional geology. Besides digital contour maps, the surveys also provided regional porosity data and geothermal gradient values.

Methodology and Workflow

Storage capacity was estimated through the volumetric method (Atlas III; U.S. DOE 2010) using the following formula: $G_{CO_2} = A_{thg} \Phi_{tot} \rho E_{saline}$. This formula generates the CO₂ storage-resource, mass estimates (G_{CO_2}); based on combining data for the total area (A_t), gross formation thickness (h_g), total porosity (Φ_{tot}), CO₂ density (ρ) and the storage efficiency factor (E_{saline}). The first two input parameters account for the total bulk volume; the CO₂ density converts the reservoir volume of CO₂ to mass while the storage-efficiency factor reflects the fraction of the total pore volume that will be occupied by the injected CO₂.

The University of Utah, in cooperation with the State Geological Surveys, developed a five-step workflow method for processing the regional data. This workflow combined GIS procedures and spreadsheet calculations, to generate storage capacity estimates and convert the input data into the by NETL predefined NATCARB Atlas format (Table 8.1). The regional capacity estimates describe the numbers derived for the saline formations of interest occurring in the northern UT and CO sedimentary basins (Uinta, Piceance and Sand Wash Basins) and those occurring in the in the basins of the Four Corners area of AZ, UT, CO and NM (San Juan, Black Mesa, Paradox basins). The local storage capacity estimates refer to those derived from the geocellular model that was created for the specific Sand Wash Basin site characterization study.

The first step for the regional workflow consisted of extracting depth and thickness values from the contour maps by converting the data to 1-km² gridded data using GIS tools. After the grid attribute values were converted to point data, they were further manipulated in a spreadsheet. This spreadsheet – the EGI capacity calculation spreadsheet – contained a macro that generated CO₂ density values based on temperature and pressure data derived from the depth values. The CO₂ capacity numbers, at three different efficiency factors (0.51%, 2% and 5.4%), were derived by combining the CO₂-mass values and the available pore volume derived from thickness, grid cell area and porosity for each record. These capacity estimates were further manipulated in GIS to resolve data problems that occurred along State Boundaries and to integrate the points for each formation into a single feature class across State Boundaries. Finally the data were aggregated into the 10km² predefined NATCARB polygons and all the data, including outlines of the area representing the spatial extent of the formations, were integrated into a single GIS geodatabase.

Table 8.1: Major methodology workflow steps:

| Workflow step | Processing environment | Data Scale | Responsibility |
|---|------------------------|--------------------|--------------------------------------|
| 1. Regional Data Preparation | GIS | Regional | AZ, CO, NM & UT Geological Surveys |
| 2. CO ₂ storage capacity calculations | Spreadsheet | 1 km ² | State Surveys and University of Utah |
| 3. Creation of GIS CO ₂ storage capacity point database | GIS | 1 km ² | University of Utah |
| 4. Edge matching formation data across state boundaries | GIS & spreadsheet | 1 km ² | University of Utah & State Surveys |
| 5. Integration of the regional 1-km-spaced Rocky Mountain CO ₂ capacity GIS database | GIS | 1 km ² | University of Utah |
| 6. Aggregating (upscaling) the data into 10 km ² NATCARB predefined polygons | GIS | 10 km ² | University of Utah |

The storage capacity calculations for the local Sand Wash basin model were generated based on the static geocellular petrel model properties. This required a few modifications to the workflow designed to process the regional data (Laes et al., 2013b). The petrel geocellular model is a corner-point-defined grid. The height of the cells (= thickness of the formation) in such a grid is not constant. Thickness, a required NATCARB Atlas database field, was also not a parameter stored specifically in the model as a property but the volume for each cell was. The area of each cell was constant for all cells so an average thickness was derived from the cell volume. Another difference between the regional and the local capacity calculations was how the porosity was handled. The regional model was based on a single porosity value for each formation that was assigned a single value in each state. The local model assigned variable porosity values derived by sequential Gaussian simulation (sGs) based on variogram models. Porosity data from 20 deep wells in the basin were the input data for the variography. After the values were extracted from the geocellular model and the data, which were originally processed in ArcGIS using the projection parameters of the Petrel model (UTM, zone 13, NAD 83 with units in feet), the data were projected to the projection required for the NATCARB Atlas (Lambert Azimuthal Equal Area, WGS 1984 with the units in meters). The cell size was scaled up from 1000ft originally, to 1000m so the data would conform to the regional data.

Storage capacity estimate input parameters

The input parameters used to estimate the carbon storage are listed in Table 8.2. The parameters differ by formation and by state. The minimum values represent a minimum depth of 3000’ below the surface. This is a conservative cut-off value, also

used for the existing carbon storage capacity numbers in the southwest region of the US. Generally, under average conditions CO₂ stays in the supercritical state at around 800m (approximate 2650’).

For all the formations in all four states, except Colorado, a constant geothermal gradient was used to calculate the temperature at the top of the formation. Due to buoyancy effects the CO₂ will migrate to the top of the formation where it will be trapped assuming there is a suitable seal to cap the saline formations in place. If the center of the formation had been taken to calculate the CO₂ density, the temperature would have been higher resulting in a slightly lower density and a corresponding lesser amount of CO₂ that could be stored. The geothermal gradients are listed in Table 8.3. Colorado used a geothermal gradient that is location dependent. The gradients were calculated based on data from deep wells that were interpolated across the sedimentary basins.

Table 8.2: Input parameters for the carbon storage capacity estimates for the deep saline formations in the Colorado Plateau.

| Formation | Unit | Statistic | Dakota | | | | Entrada | | | | Weber | | Hermosa | De Chelly | | | Cedar Mesa | Leadville |
|-------------------------|-------------------|-----------|-------------------|----------|----------|--------|------------------|----------|----------|--------|------------------|--------|----------|------------|---------|---------|------------|-----------|
| | | | CO | CO | NM | UT | CO | CO | NM | UT | CO | UT | NM | AZ | CO | UT | AZ | NM |
| Basin | | | Piceance Sandwash | San Juan | San Juan | Uinta | Piceance Sandwas | San Juan | San Juan | Uinta | Piceance Sandwas | Uinta | San Juan | Black Mesa | Paradox | Paradox | Black Mesa | San Juan |
| Area | km ² | total | 28522 | 3214 | 19599 | 28834 | 30052 | 4595 | 16511 | 29989 | 15577 | 27789 | 9444 | 10053 | 1934 | 1579 | 17139 | 12247 |
| | | min | 60 | 149 | 89 | 14 | 6 | 90 | 167 | 431 | 0 | 0 | 965 | 731 | 2 | 43 | 0 | 67 |
| Thickness | ft | mean | 185 | 245 | 236 | 131 | 332 | 215 | 299 | 905 | 434 | 499 | 1,577 | 1,286 | 99 | 160 | 195 | 125 |
| | | max | 522 | 373 | 413 | 373 | 957 | 379 | 661 | 2,317 | 1,452 | 1,600 | 2,133 | 1,661 | 238 | 373 | 705 | 257 |
| | | min | 3,000 | 3,002 | 3,010 | 3,003 | 3,000 | 3,002 | 3,345 | 3,000 | 3,000 | 3,000 | 3,001 | 4,693 | 3,000 | 3,003 | 3,000 | 3,000 |
| Depth | ft | mean | 10,635 | 6,375 | 5,858 | 12,031 | 10,950 | 6,362 | 6,993 | 11,925 | 13,000 | 13,201 | 9,233 | 3,820 | 4,528 | 3,971 | 4,349 | 10,145 |
| | | max | 22,142 | 10,325 | 8,796 | 27,045 | 22,794 | 11,400 | 9,678 | 29,227 | 24,377 | 35,550 | 12,051 | 4,754 | 6,627 | 8,218 | 5,906 | 13,810 |
| | | min | 91 | 95 | 139 | 93 | 91 | 101 | 148 | 93 | 95 | 90 | 183 | 97 | 89 | 101 | 97 | 156 |
| Temp | F | mean | 238 | 162 | 213 | 222 | 245 | 162 | 243 | 220 | 250 | 207 | 301 | 103 | 134 | 113 | 107 | 325 |
| | | max | 523 | 279 | 290 | 436 | 541 | 292 | 313 | 467 | 556 | 464 | 374 | 110 | 190 | 159 | 119 | 420 |
| | | min | 1,299 | 1,300 | 1,303 | 1,351 | 1,299 | 1,300 | 1,449 | 1,350 | 1,299 | 1,711 | 2,032 | 1,299 | 1,300 | 3,180 | 1,299 | 1,576 |
| Pressure | psi | mean | 4,605 | 2,760 | 2,537 | 5,414 | 4,741 | 2,755 | 3,028 | 5,366 | 5,629 | 15,039 | 3,998 | 1,654 | 1,960 | 4,210 | 1,883 | 4,393 |
| | | max | 9,587 | 4,471 | 3,809 | 12,170 | 9,870 | 4,936 | 4,191 | 13,152 | 10,555 | 40,527 | 5,218 | 2,059 | 2,869 | 8,711 | 2,557 | 5,980 |
| | | min | | | | | | | | | | 1.12 | | | | | | |
| Porosity | % | mean | 10 | 10 | 6.34 | 12 | 15 | 15 | 10 | 16 | 8 | 6.22 | 9.87 | 14.3 | 10 | 20 | 4.62 | 4 |
| | | max | | | | | | | | | | 22.45 | | | | | | |
| | | min | 259 | 264 | 262 | 711 | 258 | 286 | 283 | 712 | 249 | 746 | 442 | 386 | 335 | 371 | 386 | 300 |
| CO ₂ density | kg/m ³ | mean | 587 | 556 | 378 | 720 | 586 | 551 | 410 | 720 | 648 | 989 | 733 | 636 | 484 | 481 | 691 | 453 |
| | | max | 935 | 651 | 444 | 722 | 937 | 702 | 454 | 723 | 940 | 1,040 | 830 | 748 | 741 | 925 | 774 | 482 |
| | | min | | | | | | | | | | | | | | | | |

Table 8.3: Rocky Mountain Carbon Sequestration Project geothermal gradients used to derive temperatures at top of formation depth for deep saline CO₂ storage formations

| State | Basin | Formation(s) | Gradient* | Temp @ depth Formula = Surface temp (F) + gradient |
|-------|---------------------|----------------------|-------------------|--|
| AZ | Black Mesa | Cedar Mesa | 13.5°C/km | 75 + (0.0074 * D ^{**}) |
| CO | Piceance/S and Wash | Dakota | Spatial dependent | 55 + (gradient in the 1km ² cell * D) |
| | | Entrada | | |
| | | Weber | | |
| UT | Paradox San Juan | Dakota | 25°C/km | 55 + (0.0138 * D) |
| | | Entrada | 20°C/km | 55 + (0.0115 * D) |
| | | Weber | 20°C/km | 55 + (0.0115 * D) |
| NM | San Juan | Dakota | 47°C/km | 61 + (0.026 * D) |
| | | Entrada | | |
| | | Hermosa Leadville | | |

* Geothermal conversion factor from °C/100m to °F/100ft: 0.549 (Klett 2005)
 D^{**} = depth in feet

Salinity and Permeability data are not required input parameters to calculate the carbon storage capacity. Only NM provided those data as mean values for each formation within the San Juan Basin (Table 8.4).

Table 8.4: Salinity and Permeability data from the NM deep saline formations

| State | Formation | Salinity (TDS) | Permeability (mD) |
|-------|-----------|----------------|-------------------|
| NM* | Dakota | 25000 | 0.83 |
| | Entrada | 35000 | 0.09 |
| | Hermosa | 85000 | 0.2 |
| | Leadville | 35000 | - |

*Only NM provided salinity data

Sand Wash Basin storage capacity input parameters

The carbon storage capacity estimates were generated based directly from the exported geocellular model properties. For these estimates the original cell size of 1000’ was used and a geothermal gradient was extracted from the spatial dependent grid created for Colorado based on measured regional deep well temperatures.

The input parameters to calculate the storage capacity data for the Sand Wash Basin model for the geocellular model in UTM are listed in table 8.5. They represent a cut-off of the data at 3000’ depth and a geothermal gradient of 31°C/km. A combination of these two parameters generates the most conservative estimate for the Sand Wash Basin.

Table 8.5. Sand Wash Basin geocellular model parameter ranges for the Dakota, Entrada and Weber at the 3000' depth constraint and a geothermal gradient of 31°C/km)

| | | Min | mean | Max |
|---------|--|-------|--------|--------|
| Dakota | Thickness (ft) | 52 | 177 | 243 |
| | Depth (ft) | 3,001 | 13,345 | 22,248 |
| | Porosity (%) | 1.65 | 6.37 | 14.34 |
| | Temperature (F) | 107 | 286 | 440 |
| | Pressure (psi) | 1299 | 5778 | 9633 |
| | CO ₂ Density (kg/m ³) | 340 | 618 | 641 |
| Entrada | Thickness (ft) | 1 | 321 | 804 |
| | Depth (ft) | 3050 | 14089 | 23120 |
| | Porosity (%) | 1.63 | 4.68 | 13.64 |
| | Temperature (F) | 108 | 299 | 455 |
| | Pressure (psi) | 1320 | 6101 | 10011 |
| | CO ₂ Density (kg/m ³) | 346 | 623 | 642 |
| Weber | Thickness (ft) | 1 | 316 | 836 |
| | Depth (ft) | 3006 | 15392 | 24765 |
| | Porosity (%) | 1.50 | 2.98 | 7.22 |
| | Temperature (F) | 107 | 321 | 483 |
| | Pressure (psi) | 1301 | 6665 | 10723 |
| | CO ₂ Density (kg/m ³) | 341 | 628 | 643 |

Storage capacity estimates

Rocky Mountain Region estimates

CO₂ capacity numbers grouped by formation but separated by state and sedimentary basin are listed in Table 8.6. Figure 8.2 shows the spatial distribution of the total cumulatively capacity numbers summed over all of the formations at the 1-km² data-distribution scale. The total, calculated CO₂-storage-capacity for all seven formations (using the average porosity for most data) varies between 13.6 and 143.7 billion metric tonnes depending on the efficiency factor (Table 8.7). For the three major, deep-saline formations the values vary between 9.8 and 104.0 billion metric tonnes. The regional storage capacity numbers for the Dakota, Entrada and Weber formations, represent an approximate 8% decrease in capacity when compared to the 2012 NATCARB Atlas IV numbers (Laes et al 2013a). This decrease is attributed to better characterization of the geologic formations.

Table 8.6: Rocky Mountain Carbon Sequestration Project deep-saline, CO₂-capacity numbers derived from the 1 km² scaled points:

| State | Basin | Formation | Area (km ²) | CO ₂ Storage Volume (metric Tonnes) | | |
|----------------|-------------------|----------------|-------------------------|--|------------------------|-------------------------|
| | | | | Low Efficiency (0.51%) | Medium Efficiency (2%) | High Efficiency (5.4 %) |
| CO | Piceance_Sandwash | Dakota | 28,522 | 482,624,867 | 1,892,646,535 | 5,110,145,645 |
| CO | San Juan | | 3,214 | 68,252,705 | 267,657,665 | 722,675,695 |
| NM | San Juan | | 19,599 | 172,502,878 | 676,481,873 | 1,826,501,060 |
| UT | Uinta | | 28,834 | 507,104,513 | 1,988,645,149 | 5,369,341,904 |
| CO | Piceance_Sandwash | Entrada | 30,052 | 1,393,361,516 | 5,464,162,810 | 14,753,239,586 |
| CO | San Juan | | 4,595 | 127,397,634 | 499,598,566 | 1,348,916,127 |
| NM | San Juan | | 16,511 | 300,019,280 | 1,176,546,181 | 3,176,674,688 |
| UT | Uinta | Entrada-Navajo | 29,989 | 4,857,039,869 | 19,047,215,174 | 51,427,480,970 |
| CO | Piceance_Sandwash | Weber | 15,577 | 549,361,376 | 2,154,358,336 | 5,816,767,507 |
| UT | Uinta | | 27,789 | 1,361,192,180 | 5,338,008,549 | 14,412,623,083 |
| NM | San Juan | Hermosa | 9,444 | 1,672,530,703 | 6,558,943,933 | 17,709,148,619 |
| AZ | Black Mesa | De Chelly | 10,053 | 1,820,718,060 | 7,140,070,822 | 19,278,191,219 |
| CO | Paradox | | 1,934 | 13,715,122 | 53,784,794 | 145,218,943 |
| UT | Paradox | | 1,579 | 35,650,148 | 139,804,502 | 377,472,155 |
| AZ | Black Mesa | Cedar Mesa | 17,139 | 168,097,713 | 659,206,719 | 1,779,858,142 |
| NM | San Juan | Leadville | 12,247 | 42,728,636 | 167,563,275 | 452,420,844 |
| Totals: | | | | 13,572,297,199 | 53,224,694,882 | 143,706,676,188 |

Table 8.7: Rocky Mountain Carbon Sequestration Project deep-saline, CO₂-capacity numbers summarized by formation

| Formation | CO ₂ Storage Volume (metric Giga Tonnes) | | |
|-----------------------|---|------------------------|------------------------|
| | Low Efficiency (0.51%) | Medium Efficiency (2%) | High Efficiency (5.4%) |
| Dakota | 1.23 | 4.83 | 13.03 |
| Entrada | 6.68 | 26.19 | 70.71 |
| Weber | 1.91 | 7.49 | 20.23 |
| Partial Total: | 9.82 | 38.51 | 103.96 |
| Hermosa | 1.67 | 6.56 | 17.71 |
| Cedar Mesa | 0.17 | 0.66 | 1.78 |
| De Chelly | 1.87 | 7.33 | 19.80 |
| Leadville | 0.04 | 0.17 | 0.45 |
| Total: | 13.57 | 53.22 | 143.71 |

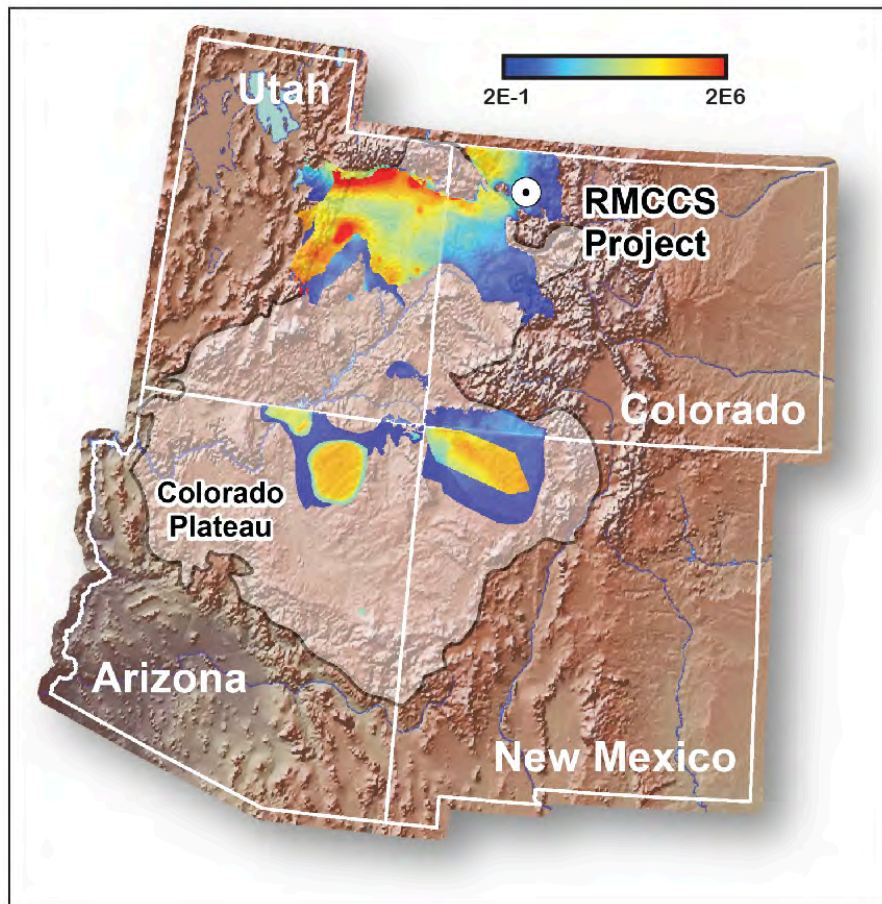


Figure 8.2: Spatial distribution of the CO₂ storage capacity summed over all 7 formations using a 1-km² cell size. The legend represents the medium efficiency CO₂ capacity data in metric tons.

Sand Wash Basin Estimates

The site-specific storage capacity estimates for the Dakota, Entrada and Weber Formations, the only formations assessed for the Sand Wash Basin, are listed in Table 8.8. The capacity numbers derived from the parameters as extracted from the geocellular model based on a constant geothermal gradient throughout the Sand Wash Basin area resulted in a 10% higher estimate using the lower geothermal gradient (Laes et al. 2013b). Applying the spatial determined gradient, which varied between 10°C/km and 50°C/km, provided the largest storage capacity numbers (Table 8.8). The differences in the estimates were approximately 5% and 16% when compared to the 27°C/km and to the 31°C/km gradient respectively. The spatial cumulative storage capacity distribution summed for the three formations shows that the northwestern section of the basin could accommodate more CO₂ than eastern part of the basin (Figure 8.3).

Table 8.8. Sand Wash Basin CO₂ storage capacity estimates calculated for records below 3000' deep after converting the geocellular model derived data to the required NATCARB atlas required Lambert Azimuthal Equal area projection using a spatial dependent geothermal gradient.

| | | | CO ₂ Storage Capacity Estimates (million metric Tonnes) | | | |
|-----------|-----------------|-------------------|---|------------------------|------------------------|----------------------------------|
| Formation | # of 1 km cells | # of 250 m points | Low Efficiency (0.51%) | Medium Efficiency (2%) | High Efficiency (5.4%) | Adjusted area (km ²) |
| Dakota | 8446 | 131860 | 102.093 | 400.363 | 1,080.980 | 8,241 |
| Entrada | 8420 | 131528 | 144.380 | 566.196 | 1,528.730 | 8,221 |
| Weber | 8462 | 131865 | 86.810 | 340.431 | 919.163 | 8,242 |
| | | Total Σ: | 333.282 | 1,306.990 | 3,528.873 | |

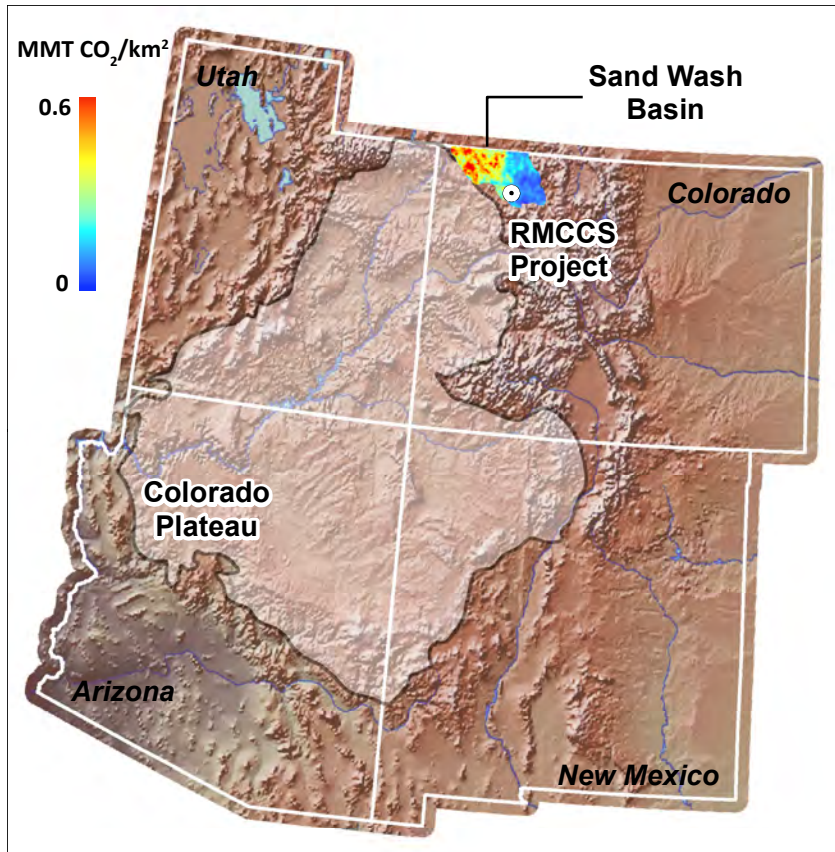


Figure 8.3: Spatial distribution of the CO₂ storage capacity summed over all 3 saline formations in the Sand Wash Basin using a 1-km² cell size. The legend represents the medium efficiency CO₂ capacity data in million metric tonnes (MMT). The distribution pattern for other efficiency levels is the same but the numbers will vary according to the efficiency level.

Significance

The 2010 CO₂ emission rate for the coal- and gas-fired power plants in the region is listed as about 320 million tonnes per year (EPA 2010). Based on the medium efficiency storage capacity of 38.5 GT for the three main formations characterized in this study (Table 8.8), this corresponds to 120 years of capacity. When the other formations characterized in this study are included, the storage capacity potential climbs to 166 years. These numbers are based on near constant CO₂-emission numbers and assuming all of the calculated storage volume is available for CO₂ sequestration.

This study estimated a carbon storage capacity ranging between 0.33 and 3.53 metric GT for the Sand Wash Basin. The storage capacity at the medium efficiency factor is 1.3 metric GT. The two coal-fired power plants located within Sand Wash Basin in Craig and Hayden emitted a combined total of 13.5 and 12.2 million metric tonnes of CO₂ during 2010 (U.S. EPA, 2010) and 2011 (U.S. EPA 2011). Using the highest geothermal gradient and a cut-off storage depth of 3000', the saline formations within the Sand Wash basin have the capacity of storing CO₂ for approximately 97 years at the medium storage efficiency level of 2%.

There are 3 coal-fired power plants within a distance of 60 to 80 miles to the west and northwest of the Woodside Dome site. Their combined 2010 CO₂ emissions summed to 15.9 million metric tonnes. The storage capacity estimate of 12.6 million metric tonnes at the 2% efficiency levels derived using conservative geologic constraints would provide storage for less than a year. Because the listed storage capacity numbers are conservative estimates the site would benefit from additional study to characterize the extent of the geologic structure better.

According to the UGS research, the Bonanza site is the best potential Utah commercial CO₂ storage site in the Colorado Plateau. At a combined estimated storage capacity of 116 million metric tonnes (2% efficiency), the Dakota, Entrada and Weber Formations could handle the 2010 reported CO₂ Bonanza plant emissions of 3.4 million metric tonnes for 34 years.

Conclusions

The newest capacity data reported here are markedly different when compared to the regional data reported to DOE/NETL for the NATCARB Atlas IV version (DOE 2012). The primary explanations for the contrast in results include more data, better quality data, and more-robust geological analysis of those data. The data improvement can be attributed to the cooperation with the state geological surveys providing a partnership that gave the project access to expert knowledge of the sedimentary basins. Because the data and interpretations are better, the regional capacity estimates may be considered to be more significant in the context of reliability and usefulness. The upshot is that regional capacity estimates will be better and more significant as more resources are invested in the analysis.

Some of the saline formations occur in very deep parts of the studied sedimentary basins. Because of limited well information in the deeper parts, the stratigraphic boundaries of the formations are not as well constrained there. Of the wells that do penetrate to top of the oldest and deepest formations, few penetrate the entire formation leading to a higher level of uncertainty of the thickness and thus the storage capacity numbers, of the older formations at greater depth.

Although the cooperation required between groups of geologist from the states involved resulted in improved data, it did however also create problems that would not have occurred if the same person had generated all data. Notably were geological continuity problems across administrative state boundaries. Those problems were solved in cooperation with the different groups using GIS techniques. Another continuity problem across state boundaries was related to different states using different cut-offs for bounding basal and top of formation layers leading to differences in thickness occurring at the state boundaries. There were a few data structural problems because it took a while before the group had a system worked out that was workable for all the participating geologists. Despite all the problems that needed to be solved, the quality improvement of resulting dataset is an indication that the system of using partnering experts and the data streamlining method developed by this project could serve as an example for the other carbon sequestration data compilation efforts, not just in the southwest but most likely for other regional carbon sequestration partnerships as well.

9. Simulation and uncertainty assessment

During the characterization activity, potential of a site/reservoir for CO₂ storage is generally examined by three criteria: capacity, injectivity, and seal integrity.

- Capacity defines how much CO₂ can be stored within a target formation in terms of available pore space (e.g., porosity, thickness, and areal extent) for the storage.
- Injectivity is dependent on permeability, fracture pressure; geometry and connectivity, and CO₂-water-rock interactions, which determines the relative mobility of CO₂ within the pore space.
- Caprock or seal integrity is the ability to contain CO₂ within the injection zone determined by seal extent, fault stability and maximum sustainable fluid pressure.

Due to the lack of economic interest, CCS target formations (especially saline aquifer) typically have relatively low, well penetration compared to hydrocarbon production reservoirs. Therefore, the available subsurface data sets within the potential CCS target formations are often sparse and suffer from a relatively higher level of uncertainty. In order to understand this uncertainty, we focused on the uncertainty in the storage capacity estimation and demonstrated how the local data (e.g., well data, number of wells, and location of wells) affect the storage capacity estimates and what the degree of well density (number of wells) is required to appropriately estimate the capacity within a specified degree of confidence. In other words, this study is not intended to provide specifics as to the true storage capacity of a reservoir/basin, but is intended to provide an understanding how much information is required in the characterization process to adequately estimate the storage capacity in practice. To do this, we developed a new workflow accommodating the addition of random pseudo wells to represent the virtual characterization wells.

Geocellular Model

Within the Sand Wash Basin, the stratigraphic formation top picks, well information, and well log images available from the project site were gathered to establish the geocellular model. Porosity values were assigned to the grid cells of the Dakota, Entrada and Weber Formations. This process began by taking porosity data from 20 existing wells within the Sand Wash Basin model boundary. Variogram analysis was conducted to understand the variation in porosity as a function of separation distance between existing wells. It was also used as means of determining directions/degree of anisotropy. Using the sample variogram results, Sequential Gaussian Simulation (SGS) was used to assign porosity values to each cell within the Dakota, Entrada and Weber Formations of the Sandwash Basin.

In this study, the geocellular model (porosity) within the basin boundary shown in Figure 9.1 serves as a “true” geology, or basis for comparison. The constructed 3D model contains 6 formations starting with the Cretaceous Dakota formation to the Weber formation from top to bottom. The static model domain covers 107.7 miles by 58 miles in the x and y direction. The grid configuration is 569x306x26 cells in x, y, and z direction, respectively, with a cell dimension of 1,000 ft by 1,000 ft.

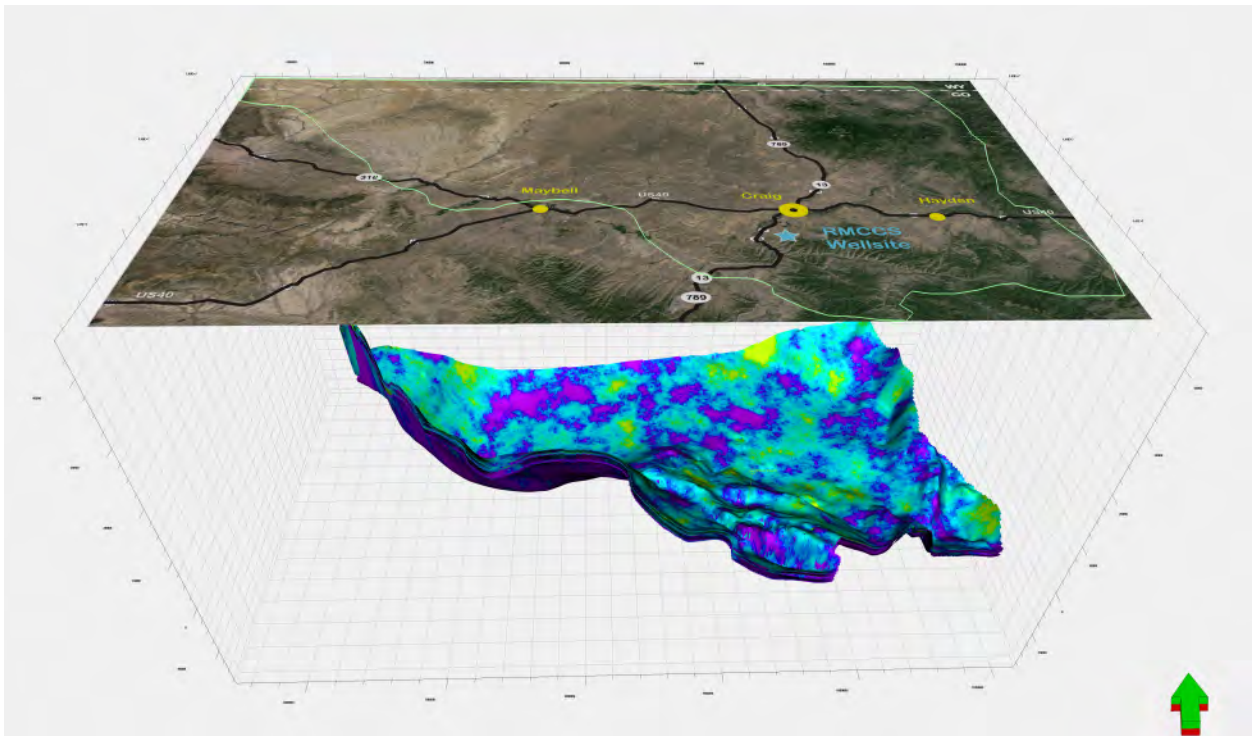


Figure 9.1. The Sand Wash Basin boundary and simulated porosity field within the boundary. Vertical exaggeration is 2x.

Methods

One newly drilled characterization well will provide good additional information on storage capacity; however, how close this new well progresses the project to understanding the true storage capacity estimate within the Sand Wash Basin is uncertain. It is also uncertain as to how many additional wells would be required to approach the true pore volume within the Basin. To understand this uncertainty a methodology was developed focusing on randomly placing “pseudo-wells” in a basin-scale model. Therefore, each randomly placed pseudo-well was assumed to provide new well data and additional geologic information. The recently developed geocellular model of Sand Wash Basin was considered to be “true” or best estimate of real geology. We evaluated how the degrees of data density (well density) represented by the pseudo-wells affects the capacity estimates of target formations within the Sand Wash Basin. Note that we considered the estimated pore volume as a proxy to the capacity estimate in this work.

Figure 9.2 shows the general workflow we followed in this study. Based on the geocellular model of Sand Wash Basin, for 25 individual cases, we randomly sampled the location of pseudo-wells (or new characterization well) up to 25 within the model. As each well was placed, porosity and formation thickness information within each well was extracted from the Sand Wash Basin geocellular model which is considered to be “true” or best estimate of real geology. Starting from a first randomly sampled point, we sequentially added a new pseudo-well into the previous well(s) and calculated the estimated pore volume at each step to see how the new information affects the capacity estimates. That is, addition of pseudo-well(s) is supposed to provide additional information within the Sand Wash Basin.

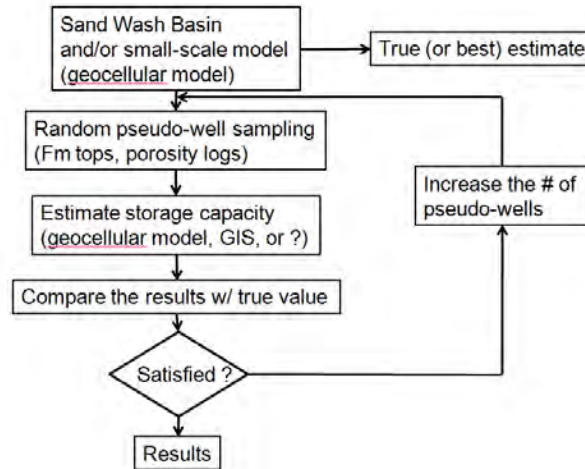


Figure 9.2. Workflow for the pore volume estimation with the incremental addition of pseudo-well.

Average porosity value and thickness of a target formation were determined from each pseudo-well and assigned uniformly to the subarea corresponding to the pseudo-well. The estimated pore volume of a subarea was simply computed by the product of average porosity value, thickness, and size of the subarea. For example, Figure 9.3 shows 25 subareas of Dakota formation corresponding to the randomly selected 25 pseudo wells for case 1. The boundary of each subarea was determined by the closest distance from each pseudo-well. Total estimated pore volume of the basin is the sum of each subarea’s estimated pore volume. We repeated the same process for a total of 25 cases with a different starting pseudo-well location for statistical analysis.

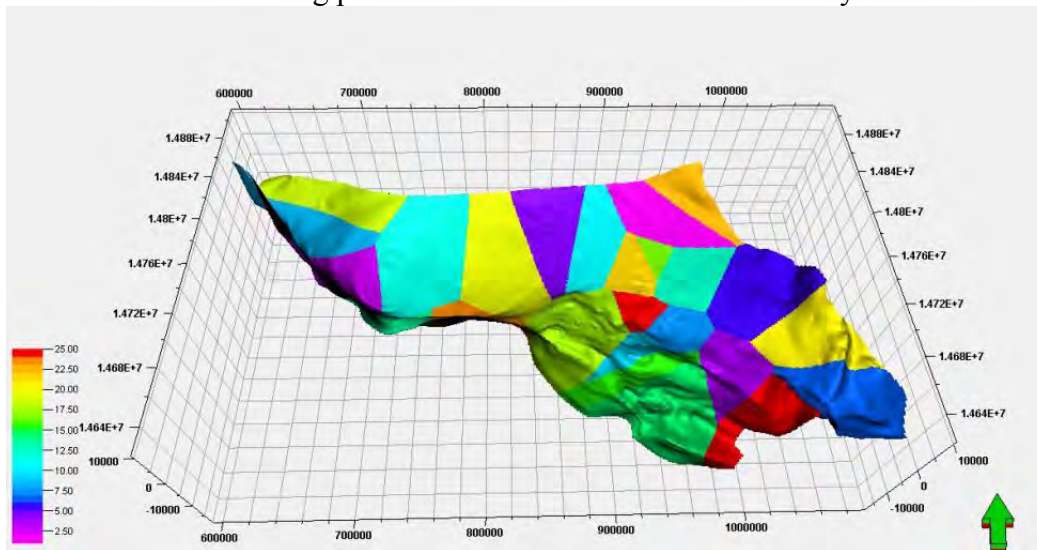


Figure 9.3. Case 1, 25 subareas applied in the Dakota formation based on the closest point from corresponding pseudo wells within the Sand Wash Basin. For this method, 24 other cases like the above were run and produced alternate data sets. Vertical exaggeration is 2x.

Results and Discussion

Figures 9.4-9.6 show the obtained relative differences of the capacity estimates from the true value of geocellular model for Dakota, Entrada, and Weber formation, respectively for cases 1-25. The relative difference is defined by $\frac{V_{est}-V_{true}}{(V_{est}+V_{true})/2}$ where V_{est} is the estimate of total pore volume and V_{true} is the true capacity value from the geocellular model. That is, if the relative difference reaches zero, the pore volume (or storage capacity) estimate is close to the true value. Positive relative difference represents the overestimation and negative value is underestimation to the true value.

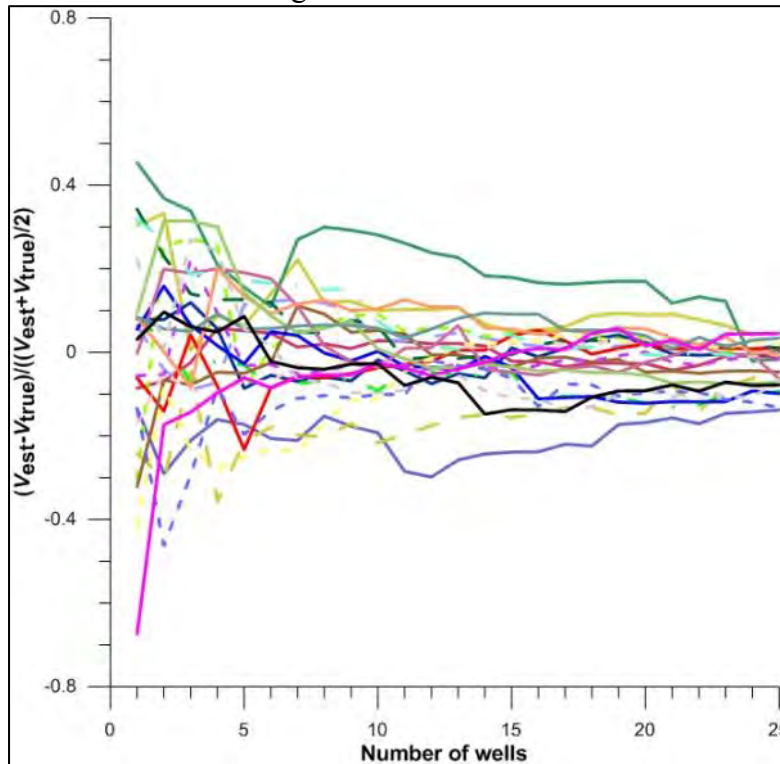


Figure 9.4. Case 1-25 combined data set, relative differences of the capacity estimates from the true value of geocellular model for Dakota formation. Each line represents 1 of the 25 cases.

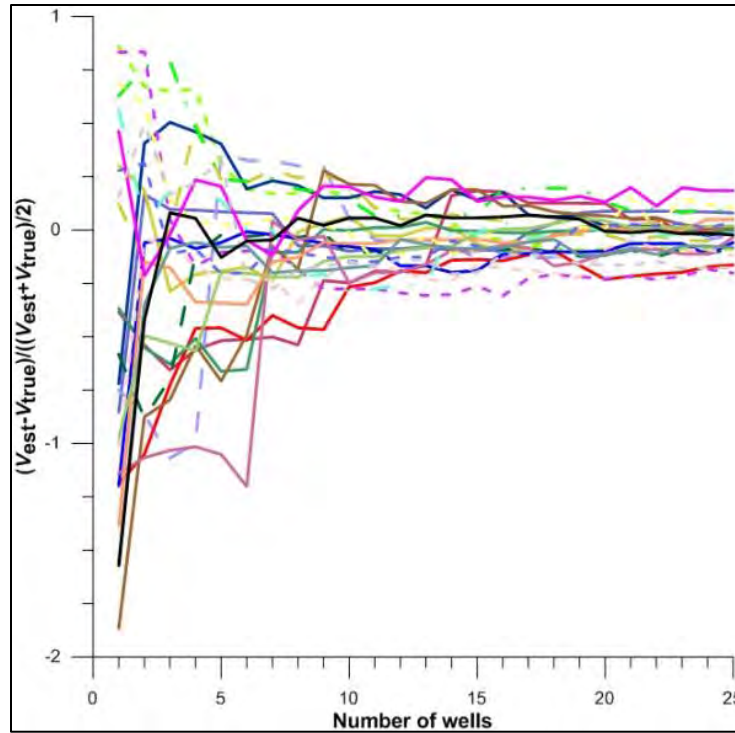


Figure 9.5. Case 1-25 combined data set, relative differences of the capacity estimates from the true value of geocellular model for Entrada formation. Each line represents 1 of the 25 cases.

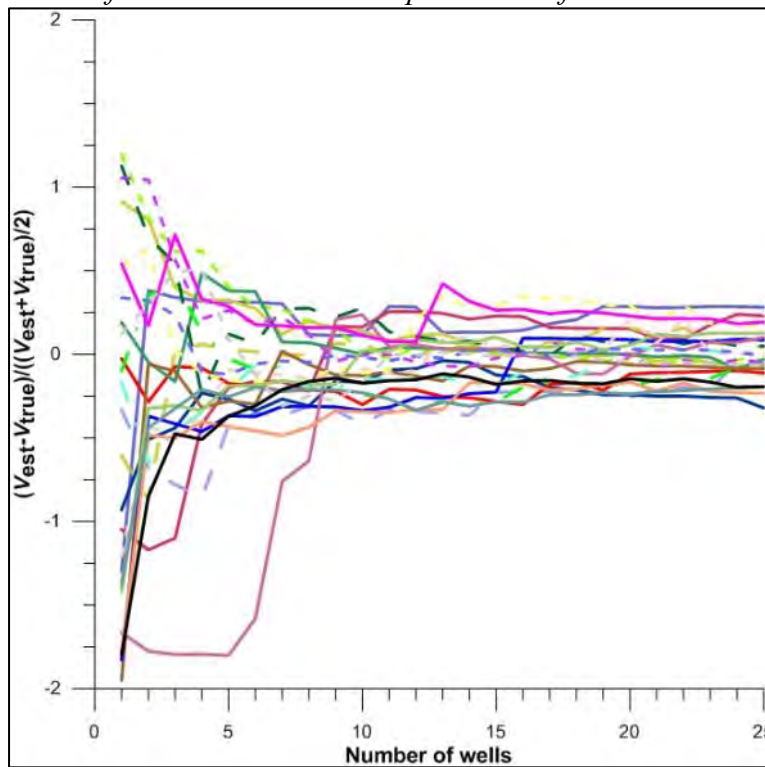


Figure 9.6. Case 1-25 combined data set, relative differences of the capacity estimates from the true value of geocellular model for Weber formation. Each line represents 1 of the 25 cases.

As expected, our results show that the difference between the estimated pore volume and true value is decreasing with the addition of new data (pseudo-wells) (Figures 9.4 – 9.6). However, pore volume estimation for the Dakota (Figure 9.4) shows better fit especially with less number of pseudo-wells compared to Entrada and Weber formation (Figures 9.5 and 9.6). Since the estimated pore volume of a subarea is computed with the single porosity and thickness value given by the corresponding pseudo-well, the difference will increase if there is a large spatial variation in the porosity and thickness within a subarea. In other words, our results indicate that Dakota formation has relatively less spatial variation in the porosity and thickness. Targeting $\pm 30\%$ relative difference as a tolerable error range, our results show that we would need at least 5 characterization wells for the Dakota and 9 wells for Entrada and Weber formations, respectively. Note that appropriate density of characterization data/well is dependent on the geologic formations even within the same basin.

With the minimum, lower quartile, median, upper quartile, and maximum, Box-Whisker plots shown in Figures 9.7 – 9.9 graphically summarize the results for cases 1-25 of the pore volume estimates (relative difference) at different number of pseudo-wells for the Dakota, Entrada, and Weber, respectively. The bottom of the box is the 25th percentile and the top is 75th percentile. The horizontal line within the box shows the median value and the end of whiskers are the minimum and maximum. The range/distribution of relative difference value for the small number of wells is significantly larger for the Entrada and Weber formation compared to the Dakota. Even with the single characterization well, median of relative difference out of 25 cases is close to zero. Whereas, the Entrada and Weber formation exhibited large negative median (underestimation) with a single characterization well and gradually decreased the difference as the number of wells increased.

As our relative difference measurement shows the deviation from the true value, we also analyzed which factor is more significant in terms of pore volume estimation. Note that our pore volume estimates in this work involves the uncertainties only in porosity and cell volume (geometry of geologic structures). To adequately quantify the degree of variation in the geologic structures and its effect on the capacity estimation, we calculated volume-weighted average dip angle of each target formation. Being consistent with our relative difference measurements, the volume-weighted dip angle for the Dakota is the smallest (4.95 degrees) among three target formations (Table 9.2). Entrada and Weber are characterized by higher volume-weighted dip angle of 11.32 and 9.49 degrees, respectively. That is, a formation with a large dip angle is likely to have more uncertainty and greater error in the capacity estimation with the limited characterization data. However, unlike the volume-weighted average dip angle, the degree of heterogeneity in the porosity was not consistent with our relative difference results. Table 9.2 summarizes the general statistics of the porosity from the original well logs and simulated true porosity field.

Although our results did not consider the cost analysis in this study, greater characterization efforts and cost should be accounted for the reliable capacity estimates in the Entrada and Weber due to their more complicated spatial variation in geology and/or petrophysical properties. Our findings demonstrate with confidence that spatial geologic variation strongly affects the capacity estimation and associated uncertainty.

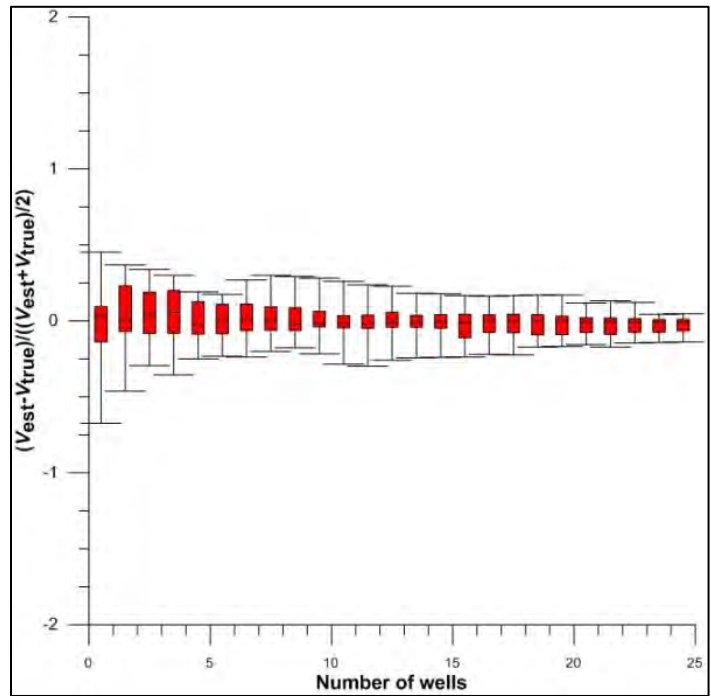


Figure 9.7. Case 1-25 combined data set, Box-Whisker plot of the relative difference of the capacity estimates for Dakota formation from the true value of geocellular model.

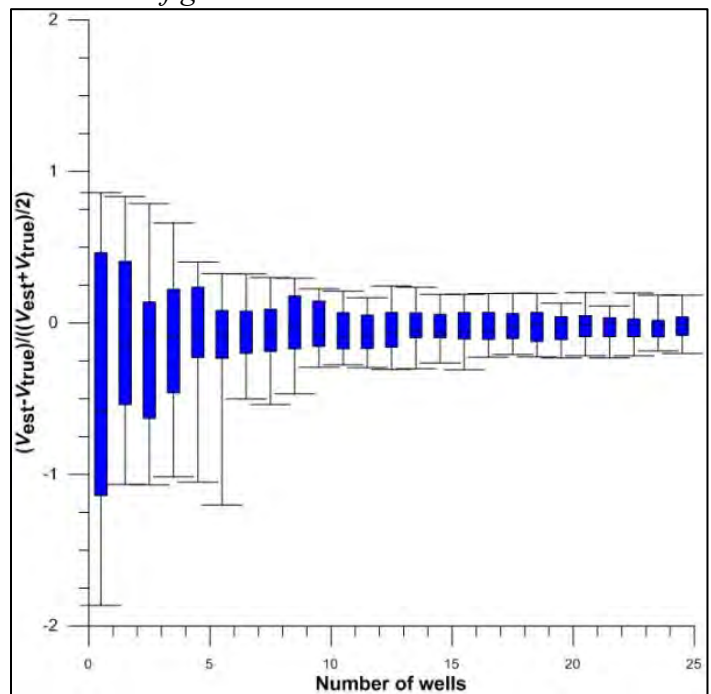


Figure 9.8. Case 1-25 combined data set, Box-Whisker plot of the relative difference of the capacity estimates for Entrada formation from the true value of geocellular model.

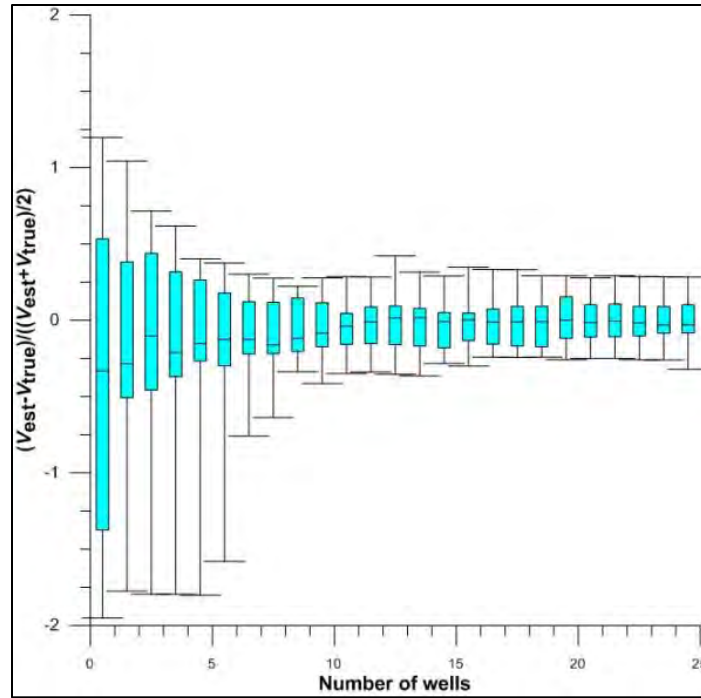


Figure 9.9. Case 1-25 combined data set, Box-Whisker plot of the relative difference of the capacity estimates for Weber formation from the true value of geocellular model.

Table 9.2. Volume-weighted average dip angle and general statistics of porosity field.

| | | <i>Dakota</i> | <i>Entrada</i> | <i>Weber</i> |
|--|-----------|---------------|----------------|--------------|
| Volume-weighted average dip angle | | 4.95 | 11.32 | 9.49 |
| Minimum | Property | 0.0165 | 0.0163 | 0.015 |
| | Well Logs | 0.015 | 0.015 | 0.015 |
| Maximum | Property | 0.1434 | 0.1364 | 0.0722 |
| | Well Logs | 0.3706 | 0.1558 | 0.1168 |
| N | Property | 89173 | 88549 | 88862 |
| | Well Logs | 2886 | 2366 | 840 |
| Mean | Property | 0.0637 | 0.0468 | 0.0297 |
| | Well Logs | 0.0667 | 0.0517 | 0.0342 |
| Std. Dev. | Property | 0.0172 | 0.02 | 0.0136 |
| | Well Logs | 0.0365 | 0.0247 | 0.021 |

10. Final risk assessment

Introduction

Carbon dioxide (CO₂) storage in the deep subsurface has been considered a potential option combined with CO₂ capture for the mitigation of global climate change [IPCC, 2007]. For reliable and successful project performance, predictive tools integrated with site characterization, Monitoring, Verification, & Assessment (MVA), and risk assessment need to be routinely applied and updated as more scientific and operational data are collected throughout the life of a project. However, due to the incomplete knowledge of subsurface environment with CO₂ injection and storage, a commercial-scale geologic CO₂ storage project requires the predictive tools that account for the uncertainties, and subsequently can help build confidence that a system will meet its design targets as well as regulatory requirement within the probabilistic framework [Mathias *et al.*, 2013; Sato, 2011; Walter *et al.*, 2012].

Recent work by EPA's Underground Injection Control (UIC) Program for geologic CO₂ sequestration (Class VI) provides an example of federal requirement imposed on the geologic CO₂ storage in the US [EPA, 2010]. The Class VI rule is under the authority of the Safe Drinking Water Act's UIC program designed to protect Underground Sources of Drinking Water (USDW). This rule specifies the use of computational modeling to predict the migration of CO₂ plume and formation fluids. The definition of an Area of Review (AoR) for a Class VI well is the region surrounding the geologic sequestration project where USDW may be endangered by CO₂ injection activities. However, given the uncertainty of the deep subsurface environment, prediction on the environmental impacts such as AoR, CO₂ leakage, or groundwater vulnerability always includes specific uncertainties in the outcome.

In order to quantify the uncertainty, Monte Carlo-based method is traditionally used to estimate a system's output response (e.g., probability density function) from known or estimated statistical distributions of input parameters. While Monte Carlo simulation method is simple, it typically requires a large number of probability-weighted samplings of inputs and subsequently high computational cost to yield a probability distribution of an output metric. Furthermore, numerical simulation of geologic CO₂ sequestration involves computationally intensive multi-phase simulation efforts [Deng *et al.*, 2012; Han *et al.*, 2010]. Thus, new efficient and readily-applicable methodology within the probabilistic framework is necessary for better compliance with the project goals and regulatory requirement in timely manner.

Monte Carlo methods are commonly used for forecasting uncertainty associated with reservoir simulations. However, Monte Carlo methods typically require tremendous computational power (or time), and thus we elected to use a response surface methodology (RSM) instead. In comparison to traditional Monte Carlo methods, application of RSM with appropriate experimental design is relatively efficient for a variety of reservoir engineering analyses including performance prediction, upscaling, history-matching, and optimization (design) studies [Bu and Damsleth, 1996; Chu, 1990; Willis and White, 2000]. RSM with a statistically linear model uses only a small

number of runs at specified input points. Recently, RSM has also been introduced for assessing geologic CO₂ storage [Ghomian *et al.*, 2010; Liu and Zhang, 2011; Rohmer and Bouc, 2010; Wood *et al.*, 2008]. Using a first-order model with a two-level Plackett-Burman design of experiment, [Liu and Zhang, 2011] focused on a parameter sensitivity analysis of upscaled aquifer models including seven 7 parameters (vertical gradient of background aquifer flow, geothermal gradient, degree of heterogeneity (variance), maximum residual gas saturation, salinity of formation water, injection rate, and caprock permeability). They found that residual gas saturation, degree of heterogeneity (variance), and salinity are critical parameters for a heterogeneous model. However, the first-order Plackett-Burman design of experiment does not include the interaction among the parameters and the effect of higher order terms. [Ghomian *et al.*, 2010] used the design of experiment (DoE) and RSM to investigate the uncertainties in CO₂ flooding design parameters for EOR and CO₂ sequestration. They used a fractional factorial design for sandstone and a D-optimal design for carbonate reservoirs. [Wood *et al.*, 2008] applied the Box-Behnken design (BBD) to screen CO₂ flooding in Gulf Coast reservoirs based on dimensionless groups. [Rohmer and Bouc, 2010] applied a first-order polynomial approximation with Latin hypercube sampling for cap rock failure assessment due to the CO₂ storage. In addition to the RSM approach, this study proposes the integration of Monte Carlo samplings combined with the obtained RSM to achieve the uncertainty quantification within the probabilistic framework.

The project team caucused regarding the most significant risk features, events and processes, or “FEPs,” for the RMCCS project site, and elected to focus risk analyses on the top two (most significant) FEPs, (1) plume size or Area of Review (AoR), and (2) injection-induced pressure buildup. Specifically, we probabilistically delineated the spatiotemporal responses (e.g. AoR and injection-induced pressure buildup) resulting from CO₂ injection into the subsurface. In the RMCCS project, we applied RSM, but combined it with Monte Carlo sampling (Kalla, 2005) to facilitate a probabilistic assessment of potential CO₂ storage in the candidate formations within the Sand Wash basin near Craig, Colorado.

Saline Aquifer Description

The Craig site is located in Moffat County, northwestern part of Colorado (Figure 10.1). The three potential storage formations (Dakota, Entrada, and Weber) are deep saline aquifer targets. The Weber and Entrada formations consist of mostly aeolian deposits and the Dakota is comprised of fluvial and marginal marine deposits. The Weber Sandstone, target formation of this study, is one of the major saline reservoirs that are present throughout the Colorado Plateau and Rocky Mountain basins, including the adjacent Piceance and Green River basins. The Weber Sandstone is estimated to have a storage potential of nearly 5 billion tons of CO₂ in Colorado, and potentially an equal amount from the same reservoirs in Utah, northeast Arizona, and northwest New Mexico [DOE, 2010; NATCARB, 2010]. Local and regional sources of CO₂ include the Craig coal-fired power plant and the Hayden coal-fired power plant approximately 35 km to the east of Craig, Colorado. The Craig and Hayden plants output at least 9.5 and 3.5 MMT of CO₂ per year, respectively [NATCARB, 2010].

The proposed injection site is geologically situated on northerly dipping beds that plunge into the Sand Wash Basin. Regional dips are typically between 5 and 13 degrees north into the basin. South of the proposed injection site, dips become steeper (~10 to 15 degrees or more). Superimposed on the regional north dip, asymmetrical anticlines plunge northwest into the basin. The southwestern limbs of these anticlines are typically steeply dipping forced folds and possibly faulted. Structural closure is created by the Axial Basin Uplift to the south.

Uncertainties associated with the geology of the region are limiting the accuracy of both total CO₂ capacity and CO₂ injectivity [Bradshaw *et al.*, 2007]. Sparse data from the 233 oil and gas wells within the 50 km radius (7,854 km²) around the proposed injection site results in large areas where basic petrophysical data is lacking. Extrapolation/interpolation of down-hole geophysical data attempts to reduce the uncertainty where data is lacking, but the geophysical logs are also incomplete, or not available, especially for the deep saline aquifers.

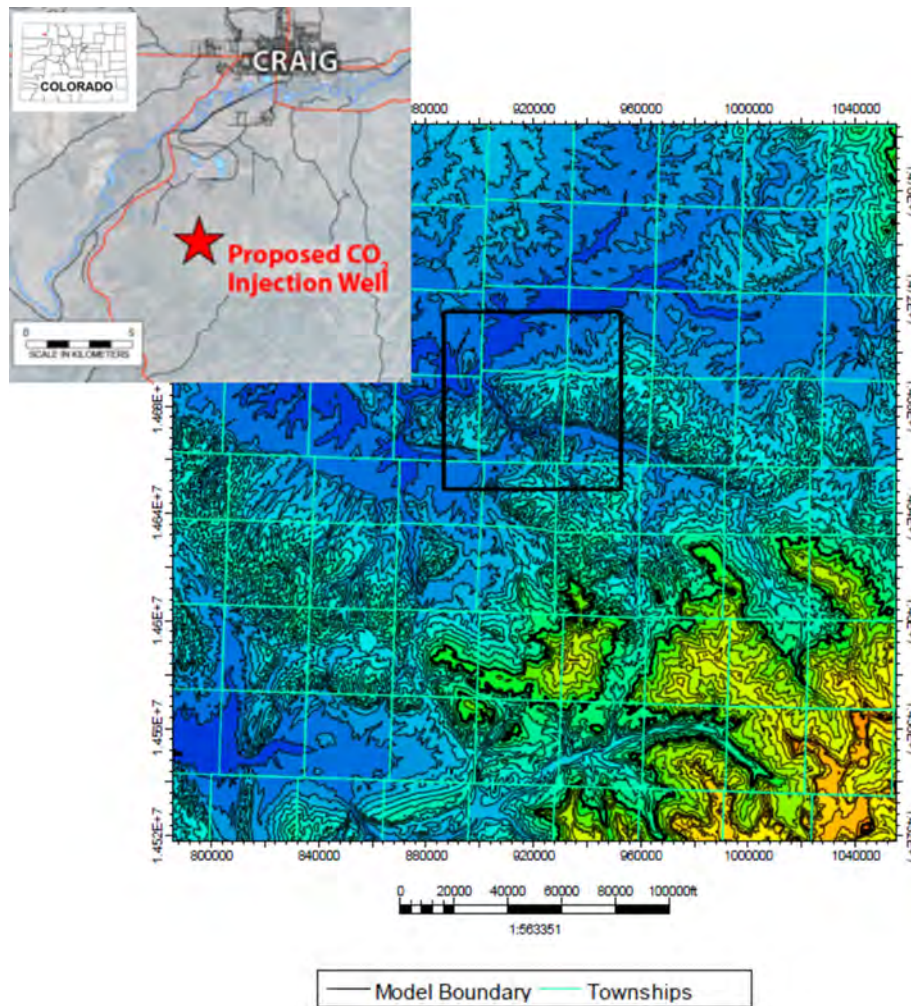


Figure 10.1. Location map of Craig site in Moffat County, Colorado.

Geologic Model

The stratigraphic-formation, top picks, well information, and well log images available from the project site were gathered to establish the numerical model grid. We built a site-specific aquifer model for the numerical simulation based on the regional geologic model developed and provided by Colorado Geological Survey and Schlumberger. The site-specific static model within the model boundary is shown in Figure 10.2. The constructed 3D model contains 6 formations starting with the Cretaceous Dakota formation to the Weber formation from top to bottom. Among them, we only considered a single well injection into the deepest target formation (Weber) interval for our study. The assumption was made that the overlying Chinle formation works as a perfect seal and thus no flow at the top of Weber. The static model domain covers 20.1 km (66,000 ft) by 20.1 km (66,000 ft) in the x and y direction. The grid configuration is 200x200x20 cells in x, y, and z direction, respectively, with a cell dimension of 100.6 m (330 ft) by 100.6 m (330 ft). Twenty cells were equally spaced vertically in the target formation.

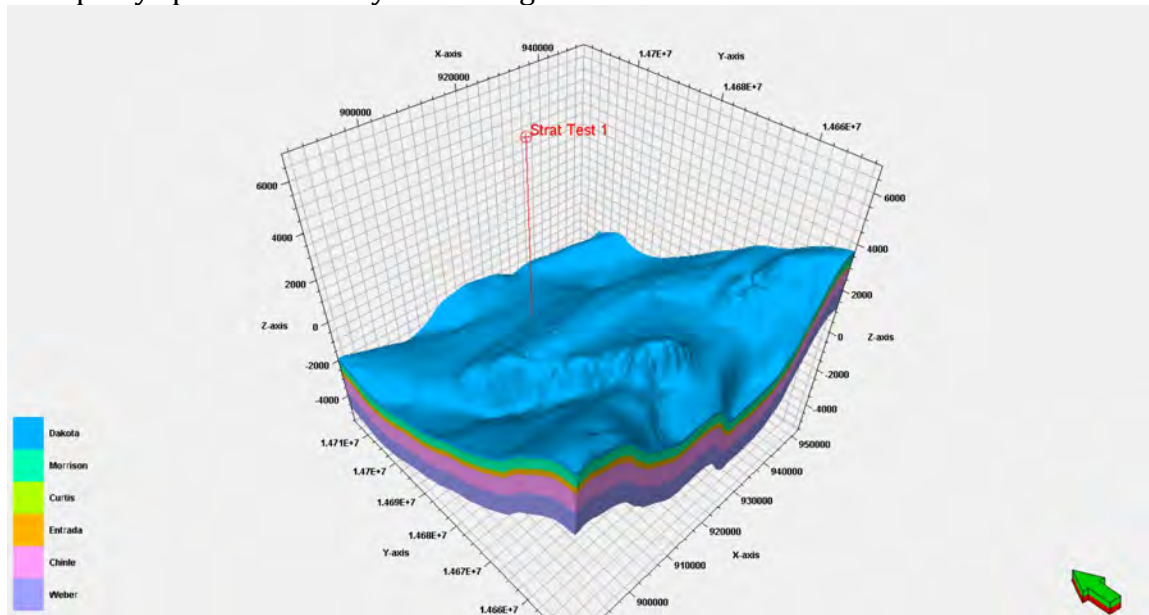


Figure 10.2. Stratigraphic distribution of geologic formations starting from Dakota formation within the Craig site model boundary. Vertical exaggeration is 5x.

Methods

Figure 10.3 summarizes the workflow we followed in this study. We first determined independent variables/factors to construct the DoE based on the BBD followed by the numerical experiments. Then, the spatiotemporal evolution of CO₂ migration and pressure build-up was delineated by constructing the response surface (or proxy model) for each different time. We utilized stepwise regression technique to eliminate insignificant factors from the regression equation. Then, several goodness-of-fit measurements examined the performance of the regression model. Lastly, Monte Carlo samplings of mutually independent, input parameters

through the obtained, response-surface models for each time-generated, temporal evolution in the CDFs of output responses from the given input distributions.

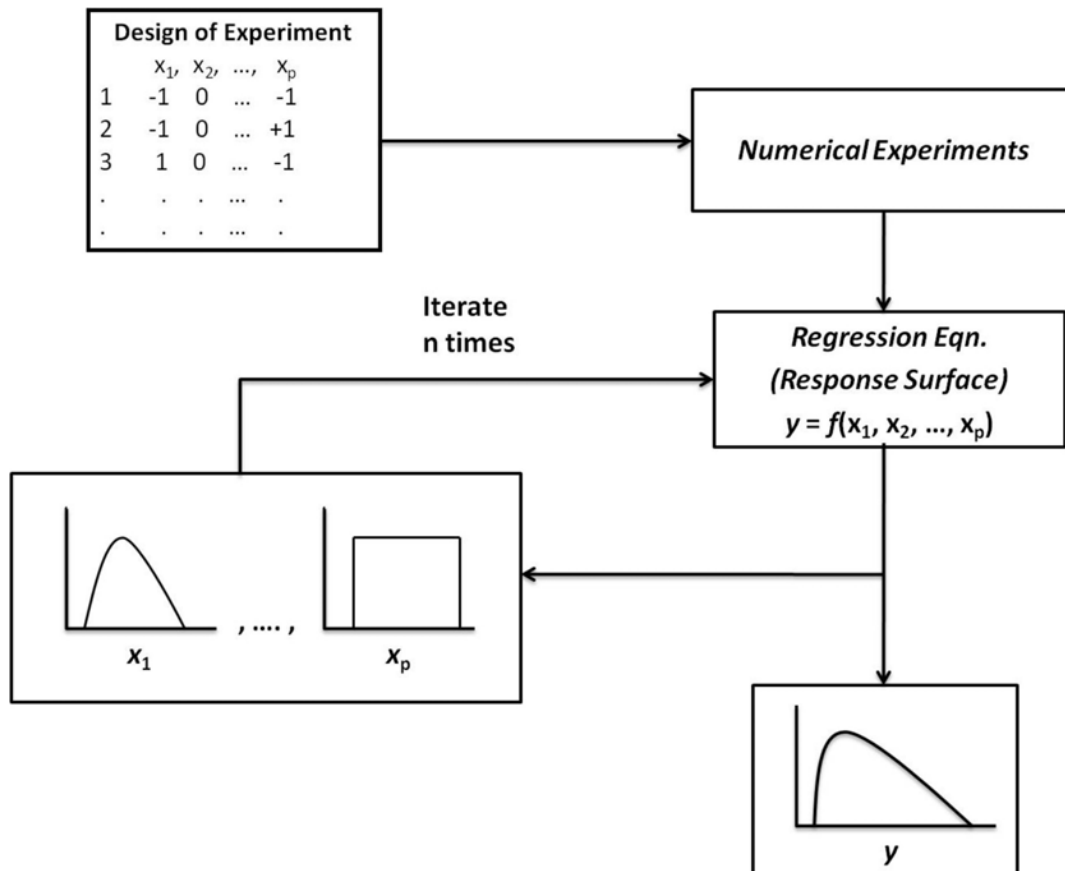


Figure 10.3. Workflow of the response surface method combined with the Monte Carlo simulations.

Design of Experiment (DoE)

RSM estimates a statistically linear model that fits to the responses from the DoE, which initially involves the identification of appropriate factors or design variables to be varied in the prediction of responses or outcome. Major goal of DoE techniques is to represent sampling space as much as possible given a limited set of laboratory or numerical experiments. Design space of factors should represent possible values and usually follows linear scaling of factor into the range of -1 (min) and 1 (max). Note that the invalid selection of the design space range in the input factors will lead to poor predictability beyond the range of -1 and 1.

In this study, BBD was used for the experimental design. The BBD is a particular subset of the factorial combinations from the 3^k factorial design, which consists of three levels (-1, 0, 1) for each factor. Each factor is placed at one of the three equally spaced values. The BBD has been widely used because of its economical design (less number of runs) compared to the full factorial designs

[Montgomery, 2008]. Full factorial design with 2-level (-1, 1) or 3-level (-1, 0, 1) is fully crossed design requires 2^k and 3^k runs, respectively. For example, for 5 factors BBD requires 41 runs while 3-level full factorial design requires 243 experiments. In addition, BBD contains not only the interaction terms of factors but also the higher-order quadratic effects. BBD includes the midpoint in the design and is nearly orthogonal and rotatable mathematically.

We selected 4 independent variables to be considered key factors for the BBD; thickness and permeability of Weber formation, permeability anisotropy ratio, and formation temperature. Likely variations in each factor are scaled to -1 and 1 for minimum and maximum of the range, respectively. Table 1 summarizes the three levels for each factor. Log-normal distribution is assumed for the permeability of Weber formation with mean ($\mu=100$ mD) and standard deviation ($\sigma=1$). Minimum, midpoint, and maximum of Weber formation’s permeability in Table 1 correspond to $\mu-2\sigma$, μ , and $\mu+2\sigma$ in the log-normally distributed permeability, respectively. Uniform distribution is assumed for the remaining factors with each lower endpoint, midpoint, and upper endpoint given in Table 1. The thickness of Weber formation ranges from 61 to 244 m (200 to 800 ft) based on the initial geologic interpretation. The anisotropy ratio (k_v/k_h) is assumed to be constant but ranges from 0.1 to 1. Reservoir temperature is assumed to be isothermal and its variation among the numerical experiments is from 150 to 198 °F. Total 25 runs specified by BBD provide the corresponding output variables from the numerical experiments.

Table 10.1. Independent variables used in the design of experiment.

| Independent variables (Xi) | Low (-1) | Mid (0) | High (+1) | Statistical distribution |
|--------------------------------------|---------------|---------------|---------------|--------------------------|
| X1 Thickness of Weber (m) | 61.0 | 152.4 | 243.8 | Uniform |
| X2 Permeability of Weber (mD) | 13.5 | 100 | 738.9 | Log-normal |
| X3 Anisotropy ratio | 0.1 | 0.55 | 1 | Uniform |
| X4 Reservoir Temperature (°C) | 65.6 (150) | 78.9 (174) | 92.2 (198) | Uniform |

Numerical Simulation

Given the design of experiment specified with the BBD, we performed numerical modeling work for the 25 cases. For initial conditions of the model, we assumed that the model is fully saturated with brine. A hydrostatic pressure ($P=\rho_wgh$) ranging from 1,872 psi to 4,948 psi was initially assigned according to the formation depth. Reservoir temperature was assumed to be isothermal and its variation among the numerical experiments is given in Table 1 as a dependent variable. The assigned pressure field and temperature values maintain the injected CO₂ in its supercritical phase within the model domain.

Both top and bottom layers of this model impose no-flow conditions, imitating the situation where the CO₂ injection formation is present under the regionally extended, low-permeability caprock and above basement rock. For the lateral boundaries representing extended aquifer beyond the simulation grid, we assign a large aquifer block to the lateral boundaries. Under these boundary conditions, the injected brine displaced by the CO₂ is allowed to flow laterally away from the injection region, such that the brine displacement does not exert a downward force on the CO₂ plume and permits buoyancy to act without interference.

In all simulations, supercritical-phase CO₂ was injected into the Weber formation during the initial 2-year period with the rate of 1 MMt/year, totaling 2,000,000 metric tons. We assumed that the injection well is fully perforated through the target formation. Total simulation time for this study is chosen to be 100 years including the injection period. Simulated results were collected and post-processed to obtain the dependent variables for the regression and assessment. Figure 10.4 shows the simulated CO₂ plume distribution of case 1 at 40th year after the CO₂ injection activity ceases. Effect of hysteresis in the relative permeability was separately examined with and without the hysteresis option in the simulation. In this paper, we selected the Killough (1976) hysteresis method for the generation of scanning curves in the relative-permeability, hysteresis model.

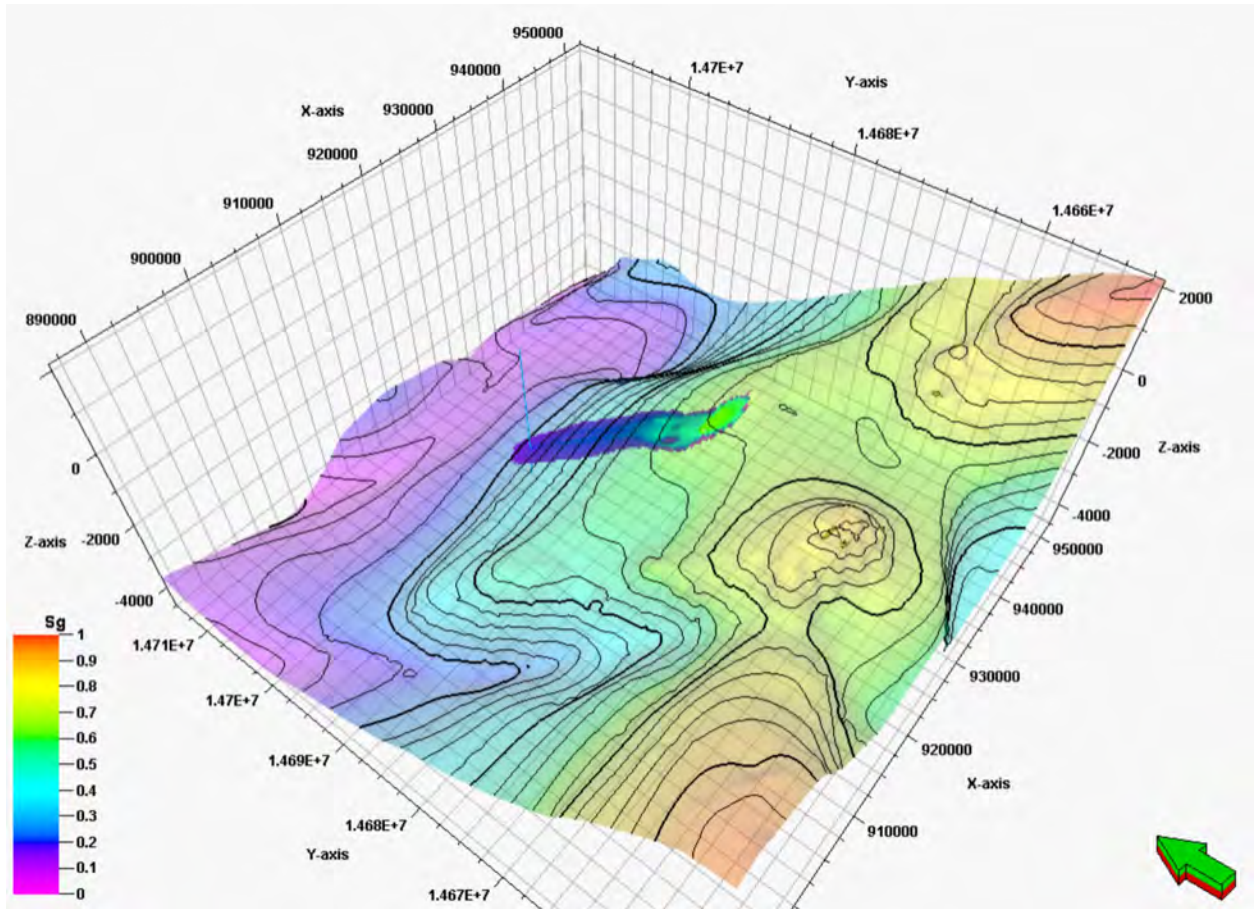


Figure 10.4. Simulated CO₂ plume distribution on top of the Weber at 40th year after the CO₂ injection activity ceases. Horizontal cell dimension is 330ft x 330ft. Vertical exaggeration is 2x.

Response Surface Model

Response surface method (RSM), or regression modeling, consists of mathematical and statistical techniques to develop a functional relationship between a response or dependent variable (y) of interest and associated independent variables or factors (x_1, x_2, \dots, x_k). The RSM typically involves the development of a polynomial approximation to the responses (y) obtained with a linear regression given the input/design variables (X_i) in a chosen DoE. A full second degree RSM for k independent variables is

$$y = \beta_0 + \sum_{i=1}^k \beta_i X_i + \sum_{\substack{i=1, j=2 \\ i < j}}^k \beta_{ij} X_i X_j + \sum_{i=1}^k \beta_{ii} X_i^2 + \varepsilon \quad \text{Equation (1)}$$

where β_i , β_{ij} , and β_{ii} represent regression coefficients and ε is random error assumed to have a zero mean. “ k ” is four in this study. Unlike the laboratory experiment, the random error due to the non-repeatability does not exist in a deterministic numerical experiment and is ignored in this study. Eqn. (1) contains linear, two-way interactions, as well as quadratic terms. We used least square method to

determine the coefficients of the polynomial equation at each time. Least squares estimator of beta is:

$$\hat{\beta} = (\mathbf{X}'\mathbf{X})^{-1} \mathbf{X}'\mathbf{y} \quad \text{Equation (2)}$$

Only significant variables and interaction terms (at the 95% significance level) were included in the RSM after application of stepwise regression procedure. The stepwise procedure is a multi-linear regression of the response values with iterative stepping based on their statistical significance in a regression. That is, it is repeatedly altering the model at the previous step by adding or removing a predictor variable in accordance with the entry and removal criteria, respectively until the stepping or altering is no longer possible given the stepping criteria or the maximum number of steps is reached.

We post-processed the numerical results for AoR (the areal CO₂ plume extent), x- and y-directional 1st moment of CO₂ plume, and pressure buildup as dependent variables. To quantify AoR, we evaluated the areal extent of CO₂ plume in the top layer and first spatial moments of the CO₂ plume with respect to x (M_x) and y (M_y) directions with the following equations [Freyberg, 1986; Han et al., 2010; Tompson and Gelhar, 1990]:

$$M_{ij} = \int_{-\infty}^{\infty} \int_{-\infty}^{\infty} \phi \rho_{CO_2}(x, y) S_{CO_2}(x, y) x^i y^j dx dy \quad \text{Equation (3)}$$

$$M_x = \frac{M_{10}}{M_{00}} \quad \text{Equation (4)}$$

$$M_y = \frac{M_{01}}{M_{00}} \quad \text{Equation (5)}$$

The first spatial moments represent the location of the mass center of the CO₂ plume.

The pressure build-up resulting from the CO₂ injection activity was evaluated at the injection well and three monitoring wells in the top layer. Three monitoring locations at 500 m, 1 km, and 5 km south of the injection well were chosen to investigate the effect on the proximal, middle, and distal region. Simulated pressure values were recorded at the top of each well perforation.

Goodness-of-Fit Measurements

To quantitatively examine and validate the simulated outcome/response fit to the observed values properly, we used two measures including mean absolute error (MAE) and coefficient of determination (R^2). Mean absolute error (MAE) is obtained by

$$MAE = N^{-1} \sum_{i=1}^N |y_i - f_i| \quad \text{(Equation 6)}$$

where y_i and f_i are observed and simulated response, respectively at case i . MAE is given in the units of the variable. Coefficient of determination (R^2) is determined by

$$R^2 = 1 - \frac{\sum_{i=1}^N (y_i - f_i)^2}{\sum_{i=1}^N (y_i - \bar{y})^2} \quad \text{(Equation 7)}$$

where \bar{y} is the mean of the observed data. R^2 measures the degree of variation in the response that can be explained by the model. In addition, we also looked at mean squared error (MSE), normalized MSE (NMSE), normalized root-mean-squared error (NRMSE), mean-absolute-relative error (MARE), coefficient of correlation (R), and coefficient of efficiency (COE) to further investigate whether the response model was statistically acceptable or not. Figure 10.5 showed the cross-plot of the simulated and predicted pressure build-up response at $t=3,650$ days with the goodness-of-fit measure results. We first considered the results with $R^2 > 0.9$ as the acceptable model criteria. Although R^2 is not above the acceptable level, we considered the model as acceptable regardless of the goodness-of-fit measures when the maximum absolute error is less than 0.1% of its corresponding actual value.

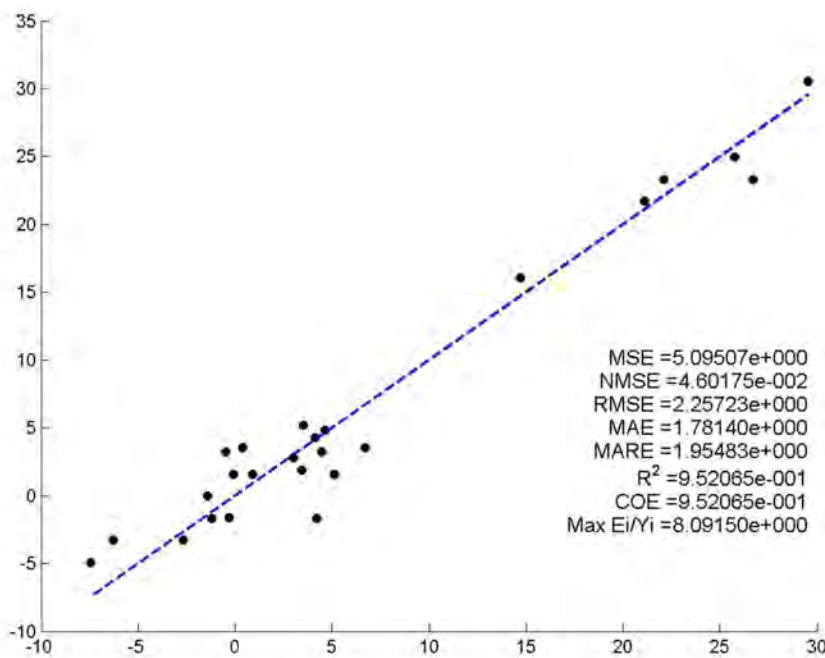


Figure 10.5. Observed vs. predicted pressure build-up (psi) of injection well at $t=3,650$ days.

Monte Carlo simulation through RSM

A series of random combinations drawn from the input distributions of the input factors is applied to the fitted response surface equation and creates a large number of realizations, resulting in a probabilistic distribution function of the output variable. We performed 10,000 iterations of Monte Carlo samplings associated with the identified RSM for each dependent variable and time. Note that dependent variables are statistically mutually independent. Each iteration represents a combination of input variables sampled from the given probability distributions and contributes to the construction of probability distribution in the outcome. Figure 10.6 showed the series of separate, probability-density functions

(PDFs) obtained at each specified time. Smooth change in the PDFs was made possible due to the appropriate adjustment in output interval, leading to the interpolation of probability distribution functions from one to the next time. Because of the rapid change in pressure response during the injection period, it was necessary to reduce the time steps during, and right after, the injection period. Thus, temporal evolution of the probability distribution functions was mapped for each dependent variable as a final result.

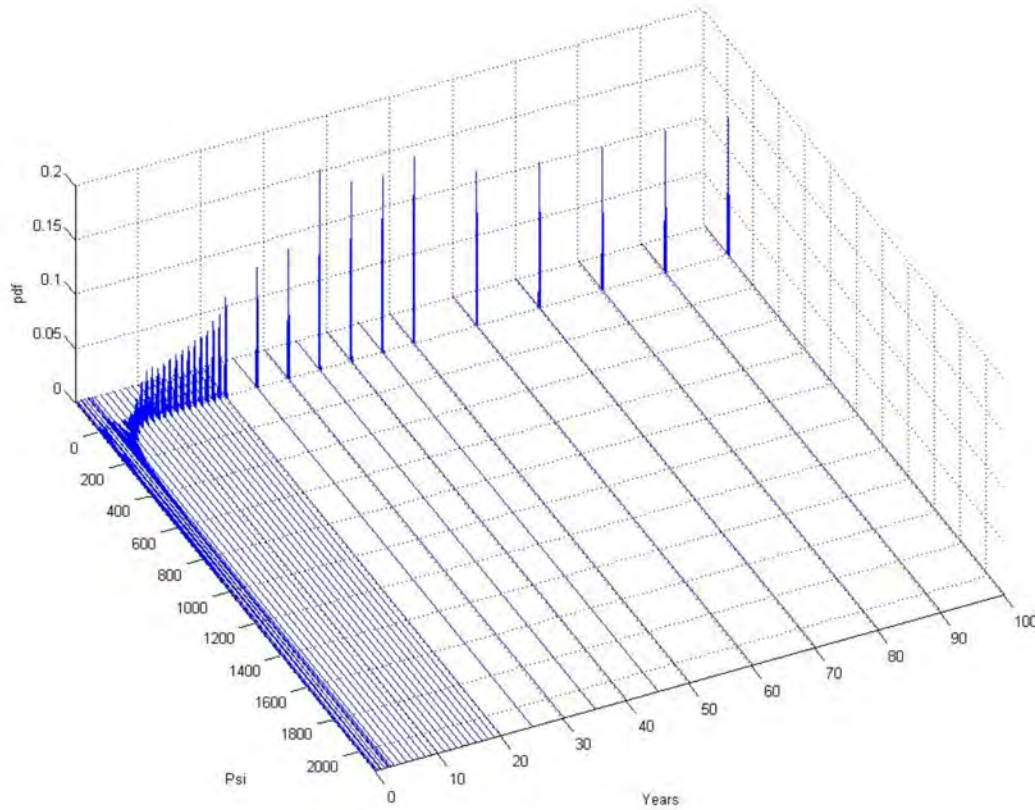


Figure 10.6. Probability density functions for the pressure build-up (psi) at the injection well.

Results

As described in the previous sections, we have constructed a RSM associated with 4-factor BBD experimental design and performed the regression modeling with the stepwise regression method on the outcomes (responses) from the specified numerical runs. After validating the regression model with various goodness-of-fit measures, we applied Monte Carlo simulation with the fitted RSM at each time. Post-processed results include the collection of the dependent variables (y = aerial extent, spatial 1st moments of CO₂ plume, pressure build-up in the injection well and three monitoring wells) for the assessment of geologic CO₂ storage.

Either PDFs or corresponding cumulative distribution functions (CDFs) can display the probability distribution in the outcome. CDFs shows the probability level associated with the dependent variable (e.g., CO₂ plume size) greater than or less than a certain level. In Figure 10.7, the 95th percentile (P95) of projected plume size falls below approximately 6x10⁷ ft² after 20 years. Similarly, the 50th percentile (P50) or median of the projected plume size indicates the plume size is about 2x10⁷ ft². Figure 10.7 also shows the likely range of the projected plume size between lower quartile (P25) and upper quartile (P75) gradually increases and gets stabilized as 2x10⁷ ft² after 20 years. The likelihood, or probability, of being greater than, or less than, a certain plume which can be a design target can also be obtained from this result.

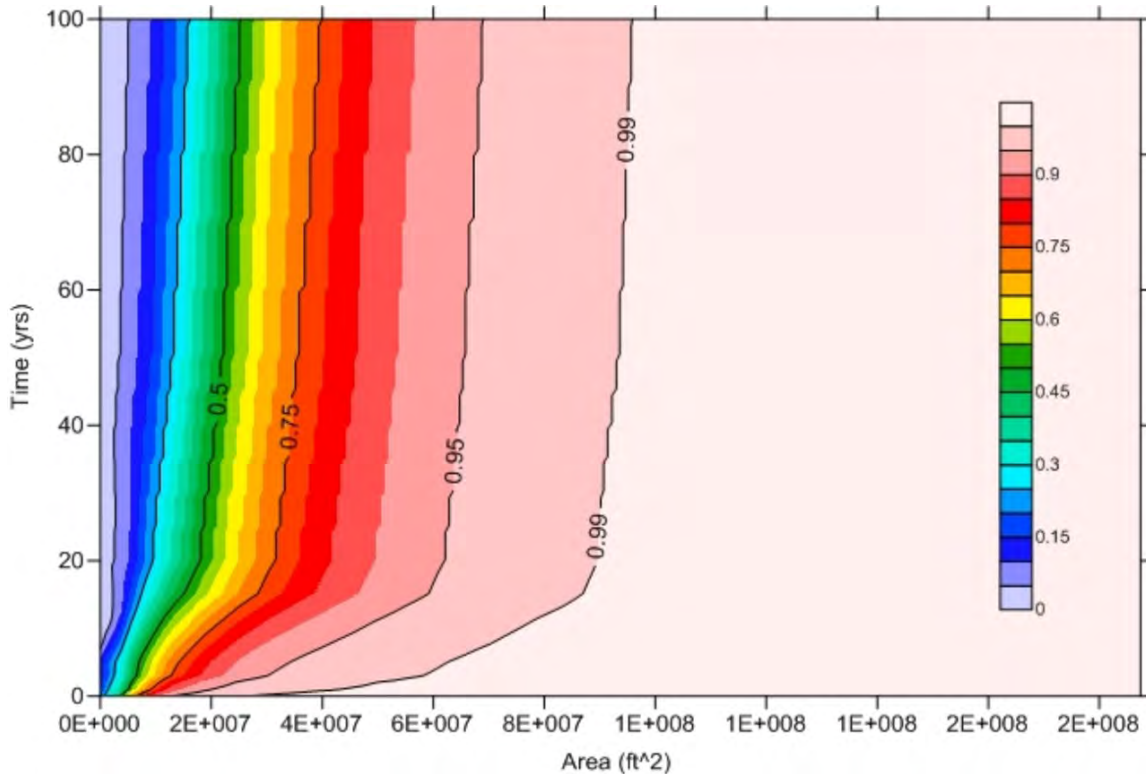


Figure 10.7. Contour map of the CDFs for the CO₂ plume extent in the top layer of the Weber formation.

Given the range/distributions of input variables, the predicted CO₂ plume size tends to increase rapidly for the initial 20 years (Figure 10.7). Our results indicate that the CO₂ plume keeps growing, but slowly, even at the end of the simulation time (year 100). This could be related to the low irreducible gas saturation used in the relative permeability function. Under the conservative perspective, this can provide the maximum CO₂ plume migration, but better prediction can be made from the relative permeability function that will be obtained from the collected core samples.

Since the results of CO₂ plume size do not provide the migration information, x- and y-directional 1st moment results were used to delineate the center of the CO₂ plume (Figures 10.8a and 10.8b). Both x- and y-directional 1st moment results

showed the CO₂ plume tending to migrate toward the east and south, respectively. P95 of x-dir 1st moment is about 875 ft east of the injection well location and 5,000 ft south for the P95 of y-dir 1st moment at the end of the simulation time. Calculated plume migration rate in the up-dip direction (y-dir) after the injection stops is approximately 25 ft/yr in the model with the hysteresis whereas it was about 70 ft/yr without the hysteresis. Our results showed the strong dependency of plume size and migration rate/distance on the hysteresis model especially in the long-term prediction. In addition, the variation/range in the outcomes was reduced notably with the hysteresis model.

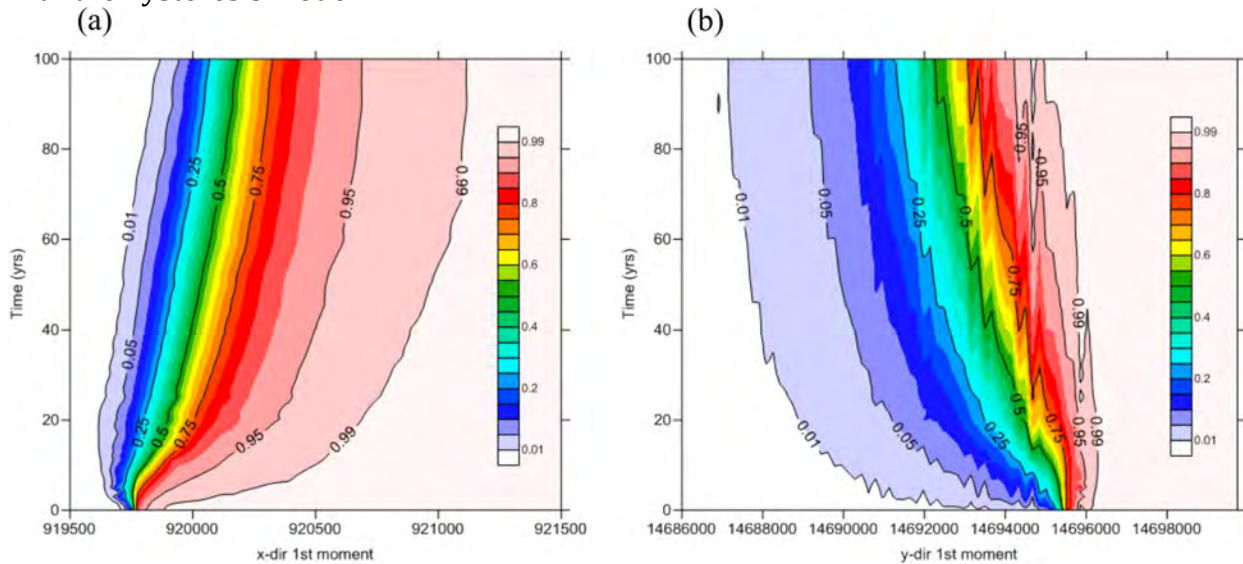


Figure 10.8. Contour map of the CDFs for the x- (a) and y-directional (b) 1st spatial moment of CO₂ plume.

Figure 10.9a showed the predicted pressure build-up at the injection well. The immediate pressure response resulted from the CO₂ injection and reached the peak at about 1 year after the injection starts. After the peak, the pressure build-up decreased and quickly diminished after two years of CO₂ injection. The P95 of the outcome is within the 1,600 psi increase and P50 of the results are less than, or equal to, about 750 psi increase at the peak. It seems it takes about 5 years to return to the original pressure condition after CO₂ injection terminates. At the proximal location (500 m from the injection well), pressure is building up continuously until the injection stops (Figure 10.9b). However, the magnitude of pressure build-up is smaller than the one at the injection well (700 psi within P95 at the peak). In addition, returning to the pre-equilibrated pressure takes a little longer. At the second monitoring well located 1 km south of the injection well, we found the pressure response is very similar to the one at the proximal location. The magnitude of the pressure build-up decreased (about 500 psi within P95 at the peak) and the arrival time of the peak was slightly delayed (Figure 10.9c). Figure 10.9d shows the CDF map of pressure build-up at the distal location (5 km from the injection well). Unlike the pressure build-up at the injection well and proximal well locations, the pressure returns to the original state slowly. The pressure

build-up reached the peak at the end of injection activity ($t = 2$ yrs) for all the monitoring wells and diminished thereafter.

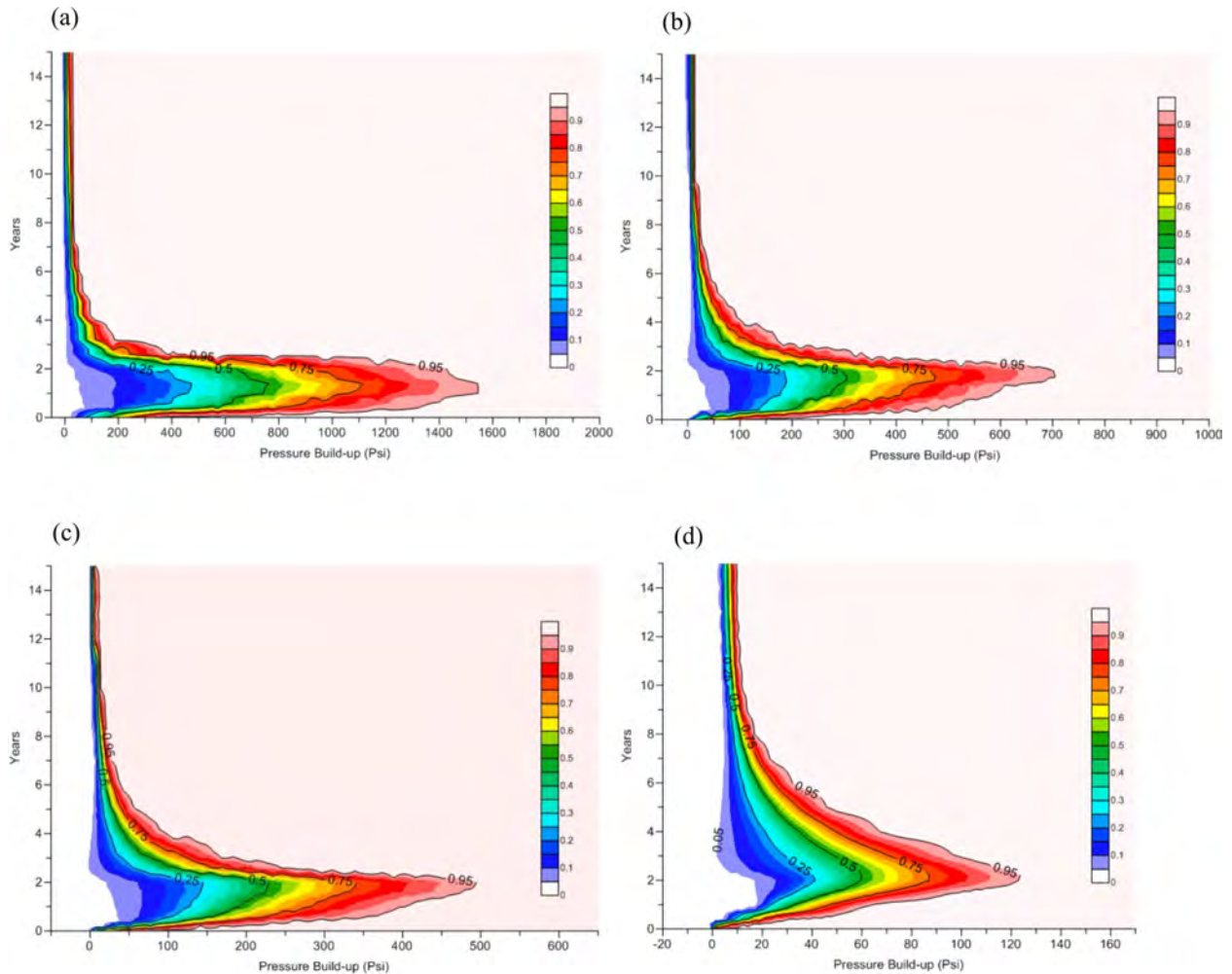


Figure 10.9. Contour map of the CDFs for the pressure build-up at the injection well (a) and three monitoring locations at 500 m (b), 1km (c), and 5 km (d) south of the injection well.

In general, pressure build-up, both in the injection and monitoring wells, exhibited extreme, positively-skewed distribution, which suggests the tendency of low pressure build-up in the mean sense given the range of input parameters. During the injection period, rapid jump in the pressure build-up was well shown both in the injection and monitoring wells. However, its magnitude is smaller in the monitoring well. Likewise, maximum pressure buildup during the injection period was significantly smaller in the monitoring well. In addition, unlike the injection well, the simulated pressure at the monitoring wells exhibited the increase in time lag in the pressure response according to the increase in the distances from the injection well and monitoring wells. Note that the pressure dissipation after injection period took about 6 years to return to the original condition.

Mitigation Strategies

As discussed in detail in the previous sections, estimated PDFs and CDFs for specific risk features, events or processes, or “FEPs,” provide a quantitative measure of the likelihood of that risk FEP. Also essential for comprehensive risk management, is an appropriate mitigation strategy. However, for this, and probably all, geologic carbon storage sites, mitigation plans are predicated on the number and types of wells involved in the project. Thus, for purposes of this topical report, we propose only a generalized Mitigation Strategy that accounts for the most likely permutations of project design and setting.

Figure 10.10 exhibits a generalized geologic carbon storage site under normal conditions, including an injection well and at least two observation wells.

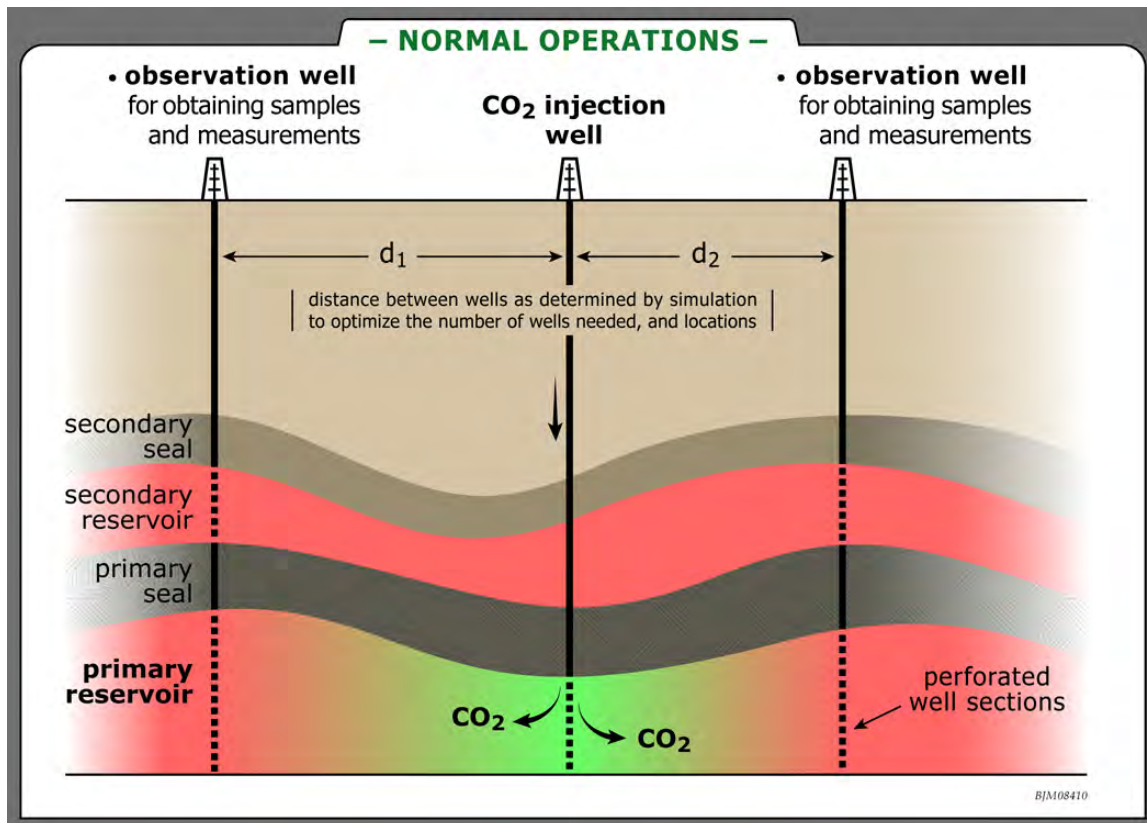


Figure 10.10. Schematic of “normal” operations of a geologic storage site. Adapted after McPherson (2009).

Figure 10.11 expresses how leakage from the primary reservoir (into a secondary reservoir above) may be managed by injection of water into the secondary reservoir, thus imposing a “fluid pressure seal” in that secondary reservoir. Such an approach assumes that observation wells can be used for injection, or that separate injection wells are ready.

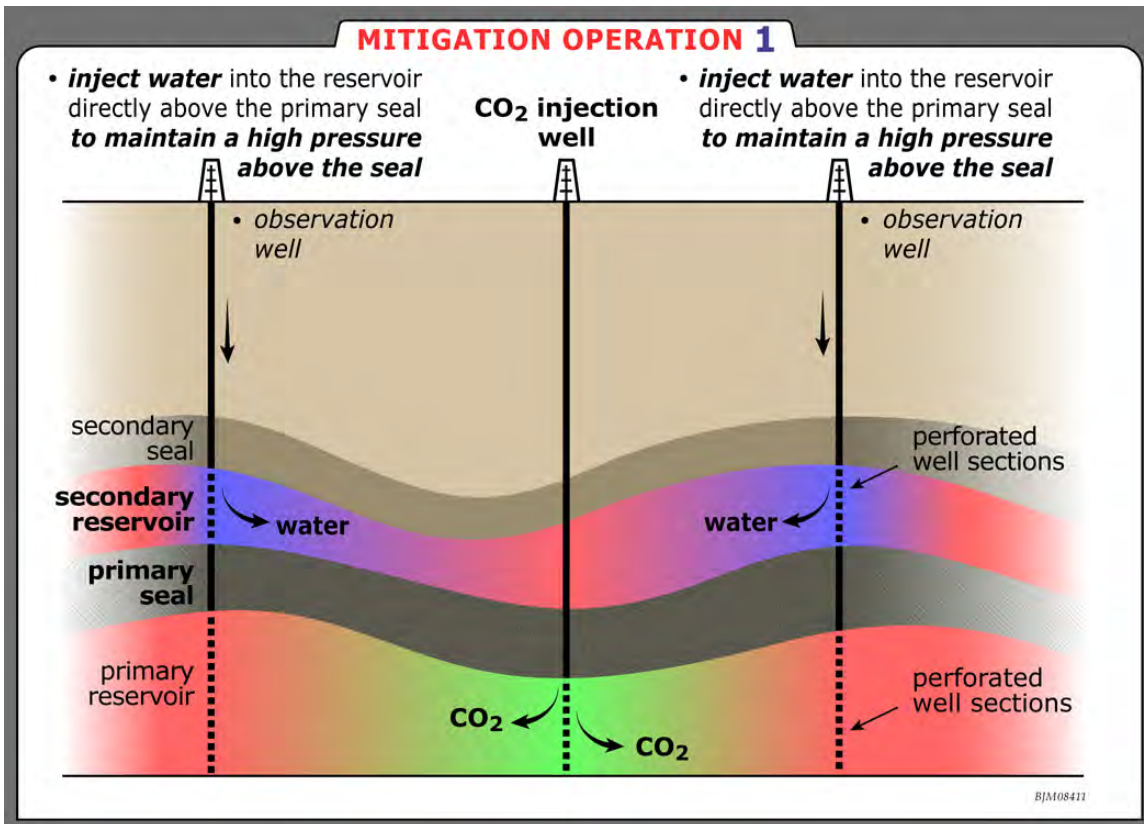


Figure 10.11. Schematic showing injection for inducing a “fluid pressure seal” in the secondary reservoir, to minimize leakage from the primary reservoir into that secondary reservoir. Adapted from McPherson (2009).

Figure 10.12 expresses a mitigation approach with respect to containing a CO₂ plume and reducing AoR. Specifically, injection of water into the primary reservoir could be used to create a pressure “wall” to contain the plume. Such an approach is predicated on sufficient injection well availability.

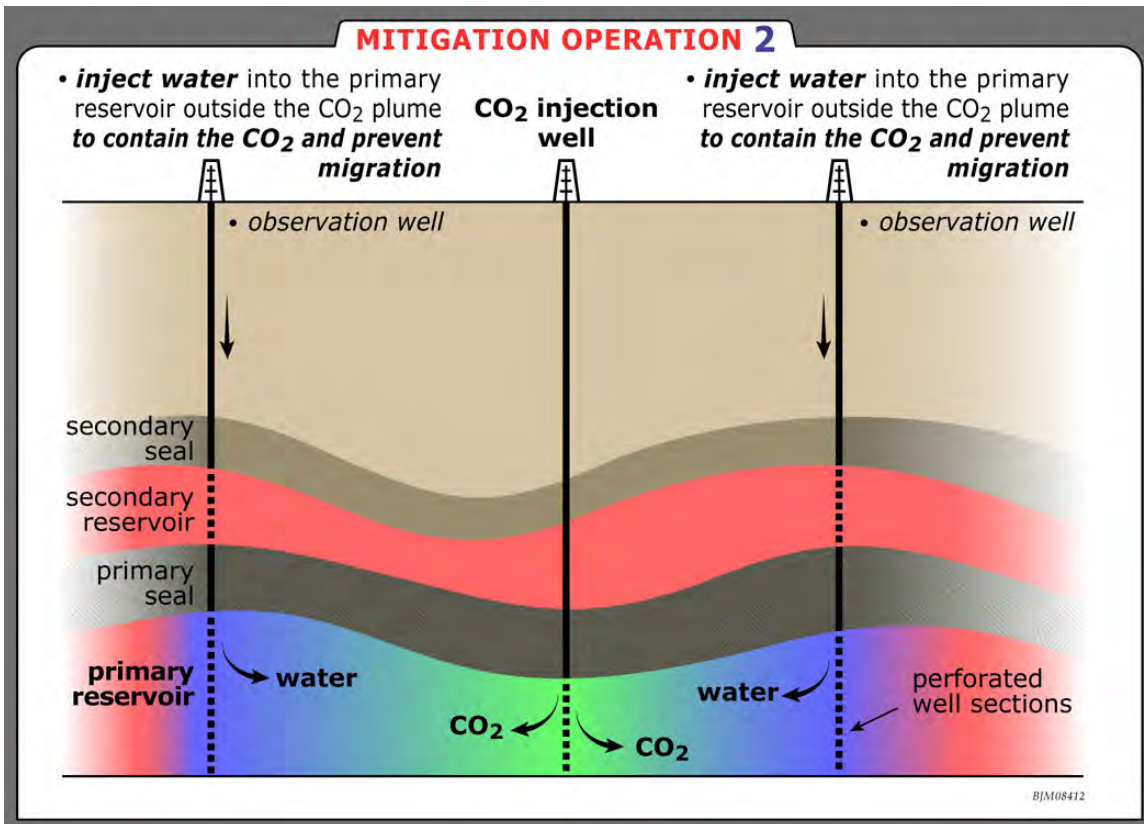


Figure 10.12. Schematic of how injection wells may be used to create a “pressure wall” that contains a CO₂ plume and limits AoR. Adapted from McPherson (2009).

Regarding effective reservoir pressure reduction, or relief, from excessive pressure buildup associated with injection, Figure 10.13 expresses the simplest of concepts: vent CO₂ to the atmosphere. Of course, hydraulic diffusivity may be such that the time for pressure to decay is too long, in which case either water/brine production from the secondary reservoir (Figure 10.14a) and/or CO₂ production from the primary reservoir (Figure 10.14b) may be necessary to facilitate faster pressure reduction. Other permutations are possible, depending on the FEP in question and the project design, specifically, the number of production/injection wells available for mitigation operations.

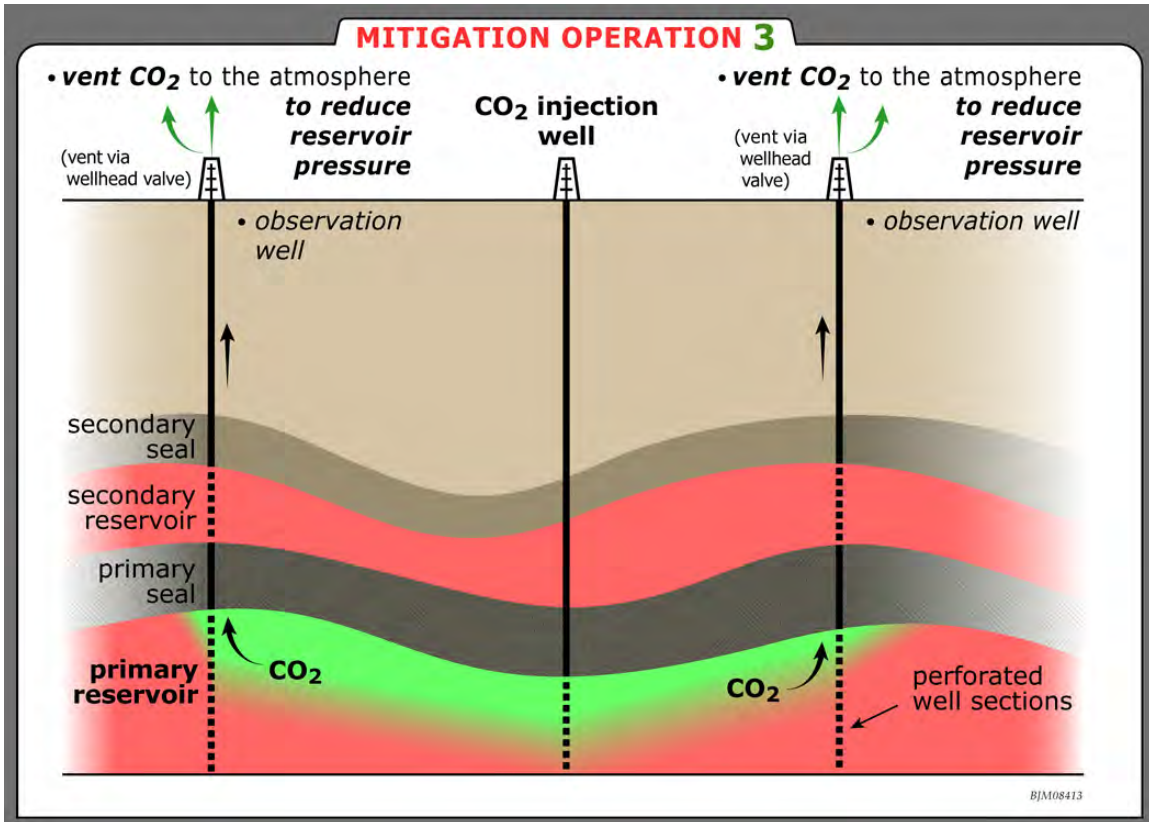


Figure 13. The simplest mitigation approach for excessive pressure buildup is CO₂ venting. Adapted from McPherson (2009).

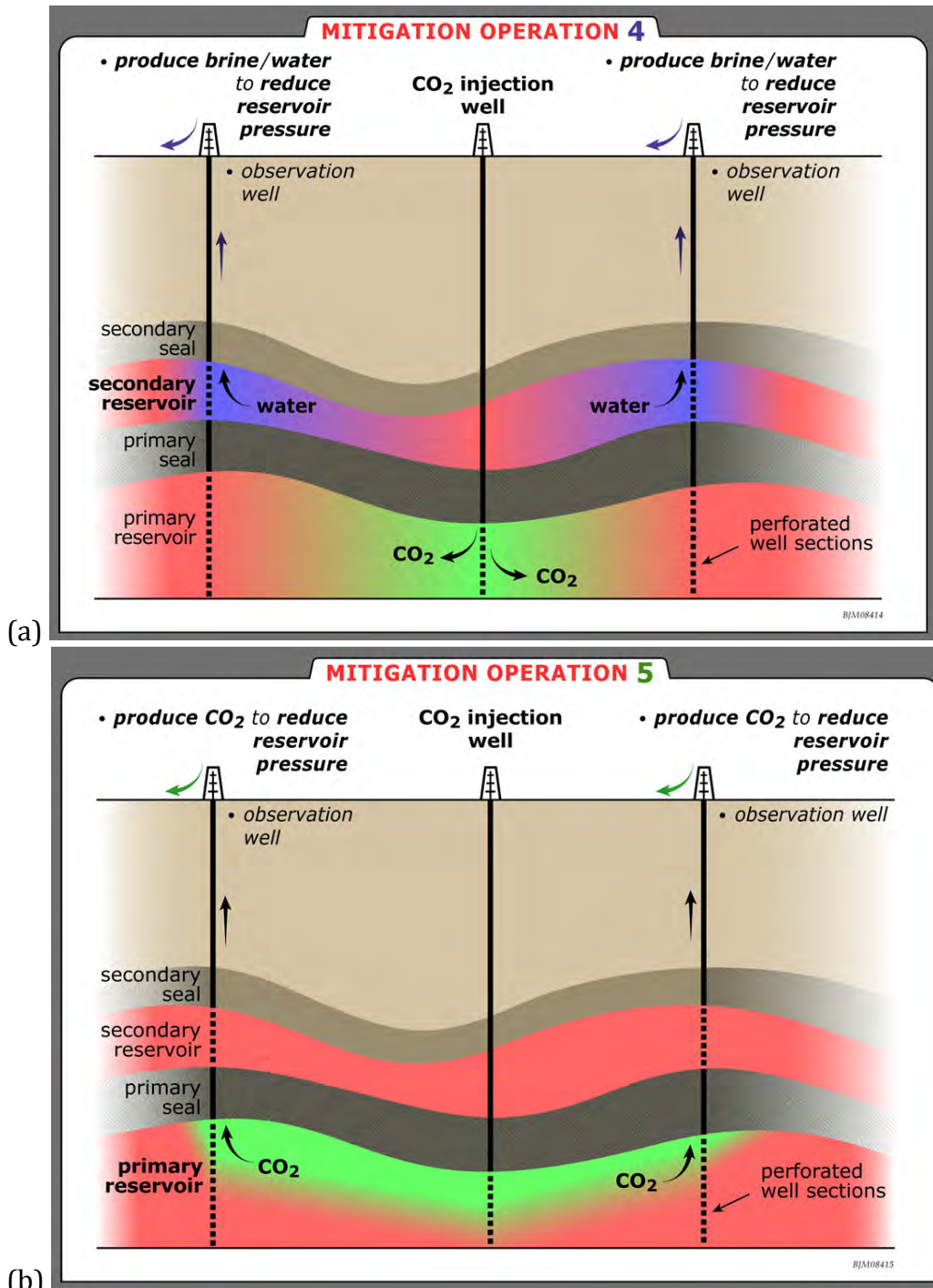


Figure 14 (a) Water production from the secondary or primary reservoir may be a means of pressure management; (b) CO₂ production from the primary reservoir is also a means of pressure reduction. Adapted from McPherson (2009).

Risk Assessment Summary

We presented the probabilistic evaluation of growth and migration of injected CO₂ plume and pressure build-up in the proposed injection well and monitoring wells, in Craig site, Colorado. Our approach includes the development of

response surface model (RSM) associated with the Box-Behnken design (BBD), corresponding numerical modeling experiments, and Monte Carlo simulations. Our approach accounted for the probability distributions to characterize variability or uncertainty in prediction estimates for the probabilistic evaluation of geologic CO₂ storage and allows us to effectively analyze the risk or uncertainty in the site selection (pre-injection) stage and easily update the results upon the availability of additional data throughout a project (during- and post-injection stage). Furthermore, it can also be applied to the site screening and project management, monitoring plan, optimization, and risk mitigation plan given the uncertainty in the input parameters.

Conclusions

This report expresses a Ten-Point Protocol for CO₂ Storage Site Characterization, the final outcome of an extensive Site Characterization analysis of the Rocky Mountain region, USA. While the results detailed here are primarily germane to the Rocky Mountain region, the intent of this protocol is to be portable or generally applicable for CO₂ storage site characterization.

References